Cisplatin-induced DNA damage in normal and malignant cells: Mechanisms of drug resistance and side effects and strategies for their prevention

Inaugural-Dissertation

zur

Erlangung des Doktorgrades

Dr. rer. nat.

der Fakultät

Biologie und Geographie

an der

Universität Duisburg-Essen

vorgelegt von

Diana Mendus

aus Dzenzelivka (Ukraine)

November 2010

Die der vorliegenden Arbeit zugrunde liegenden Experimente wurden am Institut für Zellbiologie, in der Abteilung DNA-Reparatur am Universitätsklinikum Essen der Universität Duisburg-Essen durchgeführt.

1. Gutachter: PD Dr. rer. nat. Jürgen Thomale

2. Gutachter: Prof. Dr. Elke Winterhager

3. Gutachter:

Vorsitzender des Prüfungsausschusses: Prof. Dr. Peter Bayer

Tag der mündlichen Prüfung:

17. Februar 2011

Table of Contents

Abbreviations and Units

Abbreviations

(-/-)	Homozygote knockout
(+/-)	Heterozygote
(+/+)	Homozygote wild type
8-oxoG	8-Oxoguanine
αMEM	α-Modified Eagle's medium
A	Adenine
ABR	Auditory brainstem response
AdCre	Cre recombinase
ADP	Adenosine diphosphate
ADPR	ADP-ribose moieties
AT	Ataxia telangiectasia
ATM	Ataxia telangiectasia mutated
ATP	Adenosine-5'-triphosphate
ATPB7	ATPase, Cu++ transporting, beta polypeptide (or Wilson disease protein)
ATR	Ataxia-telangiectasia and Rad3-related protein
BAER	Brainstem auditory evoked responses
BER	Base excision repair
BALB/c	Albino strain of the mouse
BRCA	Breast cancer protein
BSA	Bovine serum albumin
C	Cytosine
C57BL/6	C57 black 6 (mouse strain)
CDK	Cyclin-dependent kinase
CNS	Central nervous system
Cre	Cyclization recombination
cis-DDP	cis-Dichlorodiammineplatinum(II) or cisplatin
CSA	Cockayne syndrom protein A
CSB	Cockayne syndrom protein B
CTR1	Copper transport protein 1
Cy3	Cyanine 3
DAPI	4',6-Diamidino-2-phenylindole
DDB	Damaged DNA binding protein
DIPH	Diphenylhydramine hydrochloride
DMEM	Dulbecco's modified Eagle's medium
DMSO	Dimethylsulfoxide
DNA	Deoxyribonucleic acid
dNTP	Desoxyribosenucleotide triphosphate
DRG	Dorsal root ganglion
DSB	Double strand breaks
EDTA	Ethylendiaminetetraacetic acid
e.g.	*exampli gratia*
EM	Electron microscopy
ERCC	Excision-repair cross-complementing protein
et al.	*et alteri / et alterae*
FACS	Fluorescence-activated cell sorting

FCS	Fetal calf serum
Fig.	Figure
FITC	Fluorescein isothiocyanate
G	Guanine
GADD45	Growth arrest and DNA damage protein 45
GGR	Global genome repair
GSH	Glutathione
GTP	Guanosine triphosphate
H2AX	Histone H2AX
HC	Hair cell
H&E	Haematoxyline and eosin
HHR23	Human homologue of RAD23
HMG	High mobility group
hUBP	Human upstream binding factor
i.e.	*Id est*
IFZ	Institute für Zellbiologie (Institute for Cell Biology)
Ig	Immunoglobulin
IHC	Inner hair cell
i.p.	Intraperitoneal
ICA	Immunocytological assay
K-ras	V-Ki-ras2 Kirsten rat sarcoma viral oncogene homolog
LD_{50}	50% of the lethal dose
MAB	Monoclonal antibody
MC	Marginal cells
MDCK	Madin-Darby canine kidney cells
MRP	Multidrug resistance-related protein
Max.	Maximal
MLH	MutL homolog protein
MMR	Mismatch Repair
M-phase	Mitosis phase
MSH	MutS homolog protein
MT	Mitochondria
MW	Molecular weight
NAD+	Nicotinamide adenine dinucleotide
NER	Nucleotide excision repair
NHEJ	Non-homologous end joining
NSCLC	Non-small cell lung cancer
OAT	Organic anion transporter
OATP	Organic anion transporting polypeptides
OCT	Organic cation transporter
OCTN	Organic cation ergothioneine/carnitine transporter
OHC	Outer hair cell
PARP	Poly-(ADPribose)-polymerase
PBS	Phosphate-buffered saline
PBST	Phosphate-buffered saline plus Tween20
PCNA	Proliferating cell nuclear antigen
PCR	Polymerase chain reaction
PEPT	Peptide transporter
PFA	Paraformaldehyde
PgP	P-glycoprotein
PS	Phosphatidyl serine
PTC	Proximal tubule cell
Pt-GG	Cisplatin-G:G intrastrand crosslink (Pt-1,2-d(GpG) adducts)

Pt-SH	Inactive glutathione-cisplatin complex
RFC	Replication factor C
RM	Reissner's membrane
RNA	Ribonucleic acid
RNA pol II	RNA polymerase II
ROS	Reactive oxygen species
RPA	Replication protein A
RPMI	Roswell Park Memorial Institute medium
RT	Room temperature
SC	Supporting cell
SD	Standard deviation
SDS	Sodium dodecyl sulfate
S-Phase	DNA synthesis phase
SRY	Sex-determining region Y protein
S-S	Sulfhydryl group
SSC	Saline sodium citrate buffer
T	Thymine
TAE	Tris-acetate-EDTA
TBP	TATA binding protein
TCR	Transcription-coupled repair
TE	Tris-EDTA
TFIIH	Transcription factor IIH
TKPTS	Proximal tubule cell line derived from mouse
Tris	Tris(hydroxymethyl)aminomethane
Tween 20	Polyoxyethylene sorbitan monolaurate
URAT	Urate transporter
WT	Wild type
XAB2	XPA-binding protein 2
XP	Xeroderma pigmentosum
XPA	Xeroderma pigmentosum protein A
XPC	Xeroderma pigmentosum protein C

Units

A	Ampere
AFU	Arbitary fluorescence unit
bp	Base pair(s)
°C	Degrees Celsius
dB	Decibel
g	Gramm(s)
h	Hour(s)
Hz	Hertz
k	Kilo
kb	Kilobase(s)
l	Litre
µ	Mikro (10^{-6})
m	Milli (10^{-3})
ml	Milliliter
µm	Micrometer
min	Minute (s)

M	Molar
n	Nano (10^{-9})
n x g	n x Earth's acceleration
Pa	Pascal
pH	$-\log[H^+]$
rpm	Rotation per minute
s	Seconds
U	Units
V	Volt
v/v	Volume per volume
w/v	Weight per volume
%	Percent

1. Introduction

1.1 Historical perspective of cisplatin discovery

The inorganic platinum complex cisplatin (*cis*-dichlorodiammineplatinum(II) or *cis*-DDP) is a well-known and widely-used antineoplastic drug, and has been used in the clinic for more than 40 years. This compound was first synthesized in 1840 by Peyrone (Peyrone, 1844). However, its antineoplastic activity remained unnoticed for 120 years. The physicist Barnett Rosenberg accidently observed that cisplatin inhibited the proliferation of *Escherichia coli* cells and provoked filamentous growth of bacterial cells (Rosenberg *et al.,* 1965; Rosenberg *et al.,* 1969).

Since its biological properties were first tested on tumors in 1971 (Rossof, *et al.,* 1972; Rosenberg *et al.,* 1977; Hill *et al.,* 1982), cisplatin has become one of the most used drugs in the treatment of solid tumors of epithelial origin. Although cisplatin has been a mainstay for testicular cancer therapy (Oliver *et al.,* 1993; Einhorn, 1997), it is also commonly used to treat ovarian, cervical, bladder, and non small cell lung carcinoma as well as head and neck cancers (Sleijfer, Meijer and Mulder, 1985; Berclaz et al., 2002; Armstrong *et al.,* 2006; Helm and States, 2009; Konstantakou *et al.,* 2009). Cisplatin is also successfully used in the treatment of paediatric malignancies, such as medulloblastoma and osteogenic sarcoma (Saeter *et al.,* 1999; Kortmann *et al.,* 2003). In most recent treatment schedules, the drug is used in combination with other cytotoxic agents such as otoposide, paclitaxel, doxorubicine, 5-fluorouracil, gemcitabine, vinblastine, bleomycin and other (Schiller *et al*., 2002; Lee *et al*., 2006; Armstrong *et al*., 2006; Kang *et al*., 2008; de La Motte Rouge *et al*., 2008; Perilongo *et al*., 2009).

In spite of the clinical success of cisplatin, repetitive treatment often has to be discontinued at a certain stage. The two limiting factors for a successful application of cisplatin are acquired or intrinsic drug resistance of the tumor and severe side effects in normal tissues, mainly in the kidney, in the inner ear and in the peripheral nerves (Siddik, 2003; Kelland, 2007; Pabla and Dong, 2008). New platinum analogs, such as carboplatin and oxaliplatin, were synthesized to avoid these factors. Unfortunately, both of them have severe and dose-limiting side effects as well. Carboplatin and especially oxaliplatin have prominent neurotoxic effects, but do not induce

considerable ototoxicity or nephrotoxicity (Screnci and McKeage, 1999). In contrast to oxaliplatin, carboplatin additionally displays prominent toxicity in the hematopoietic system. The mechanisms of the noted differences in side effects are still not fully understood.

1.2 Chemistry of cisplatin

Cisplatin is a small, uncharged platinum complex (molecular weight: 300 g/mol; Fig. 1) with two chloride ligands. The compound is rather stable and inert as long as it is in a high chloride environment, such as in the blood stream (150 mM). When entering the cell, where chloride concentrations are as low as 5 mM, the ligands of cisplatin are sequentially exchanged by water molecules forming so-called highly reactive positively charged aqua complexes, which can be either monohydrated [Pt(NH)Cl(OH)] or dihydrated [Pt(NH)(OH)] (Fig. 1; Wang and Lippard, 2005).

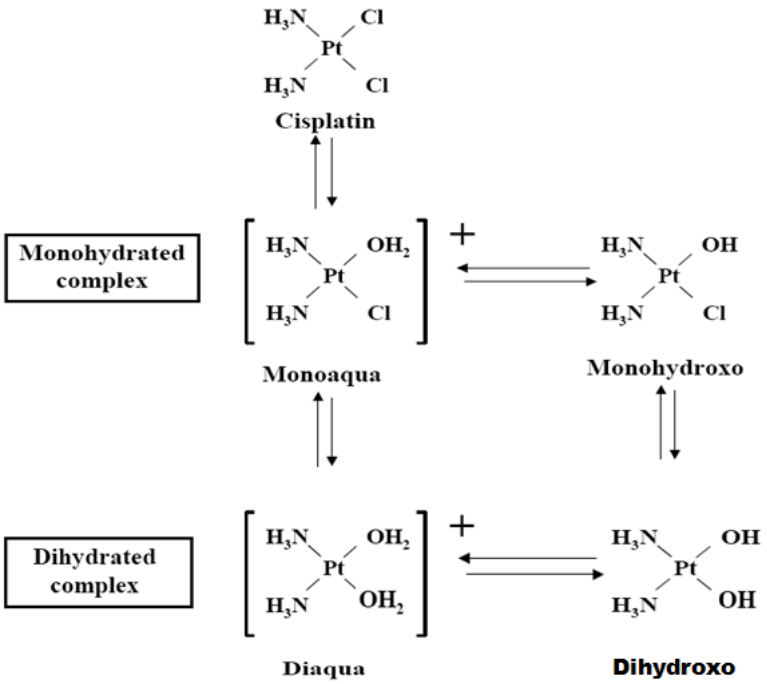

Fig. 1: Cisplatin and its products of hydrolysis. In cisplatin the platinum atom has the oxidation state +2 and its chloride ligands can sequentially be displaced e.g. by water molecules to form aqua complexes.

Both positively charged hydrated forms of cisplatin are electrostatically attracted by negatively charged macromolecules in the cell, such as DNA, and thereby, facilitating the reaction with nucleophilic centers like the N7 atom of guanine (Wang and Lippard, 2005). Due to the presence of two potentially reactive sites, cisplatin is a bifunctional drug enabling the formation of covalent crosslinks between two molecules.

1.3 Mechanisms of cytotoxic action

The exact molecular mechanism of the cytotoxicity induced by cisplatin is still unknown, but it is generally accepted that the primary target for the drug is nuclear DNA. However, a number of other modes of action have also been suggested (Fig. 2).

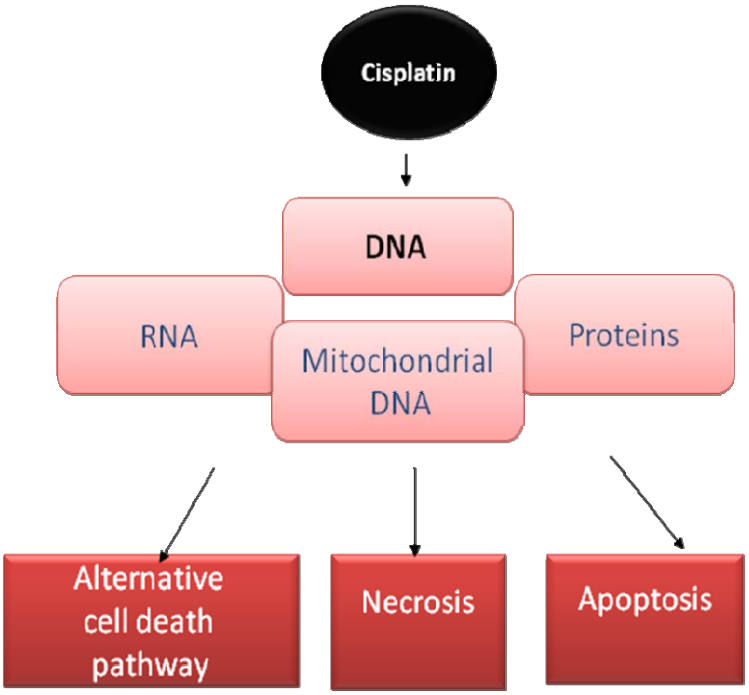

Fig. 2: Cytotoxic mechanisms of cisplatin: possible targets. Once inside the cell, cisplatin has a number of possible targets: DNA, RNA, sulfur-containing enzymes and mitochondria.

There are several reports on the interaction of cisplatin with RNA, proteins involved in antioxidant systems, cell signaling, cell metabolism and mitochondrial DNA. Those

reactions may induce apoptosis, necrosis or autophagy, as cell death pathways (Jordan and Carmo-Fonseca, 1998; Yang *et al.,* 2006; Cullen *et al.,* 2007; Inoue *et al.,* 2009).

However, the induction of apoptosis in tumor cells is believed to be the reason for the antineoplastic effect of cisplatin in cancer chemotherapy (Dive and Hickman, 1991). Binding of cisplatin to mitochondrial DNA leads to necrosis rather than to apoptosis (Troyano *et al.,* 2001).

1.3.1 DNA damage

Upon binding to DNA, cisplatin forms adducts, which are chemical modifications altering the structural integrity of the DNA molecule. Among those adducts, the most frequent structures are intrastrand crosslinks between adjacent guanines (Pt-GG), making up about 65% of all adducts formed after cisplatin exposure (Fig. 3). Crosslinks between neighbouring adenine and guanine bases (Pt-AG) rank second with 25%. In addition, a few other types of adducts have been identified in cisplatin-exposed DNA, but they are formed at rather low frequencies. Among them are (G-X-G) intrastrand crosslinks bridging one unaffected base (X) in between two guanines, and (G-G) interstrand crosslinks that react with the N7 positions of two guanines in opposite strands. At least transiently, cisplatin also induces monoadducts by reacting only at one active site with a nucleophilic position in DNA. Such adducts can lead to DNA-protein crosslinks when the second active position interacts, for example, with a sulfhydryl or disulfide (S-S) groups. When cisplatin is “activated”, the formation of monoadducts is a rather fast process, whereas the secondary formation of crosslinks is comparably slower, taking hours.

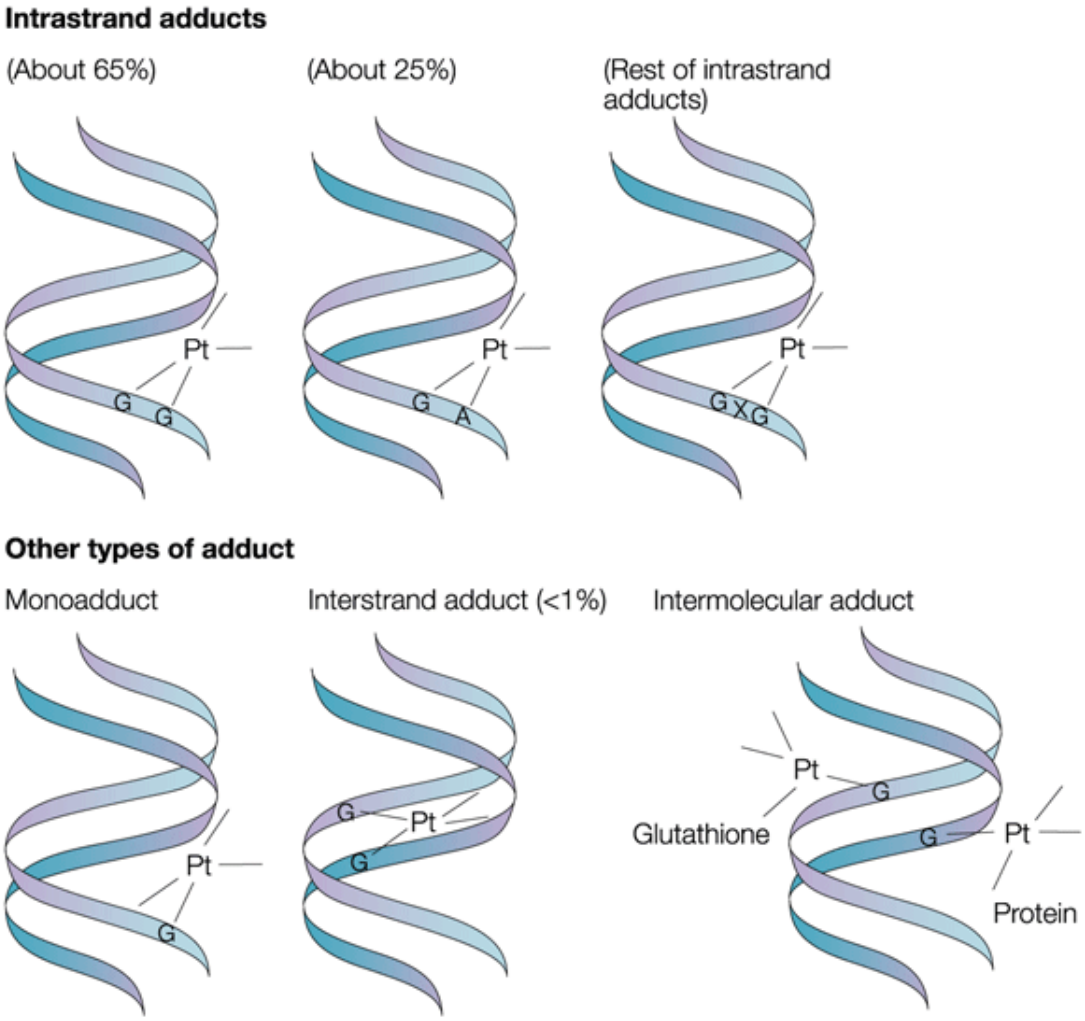

Fig. 3: Schematic overview of cisplatin interactions with DNA. Various types of cisplatin–DNA complexes or adducts can be formed. The most frequently observed adducts are intrastrand links between adjacent guanines (65%) or links between adenine and guanine (25%). Cisplatin can also stretch across a base to join two guanines (GXG) on the same strand of DNA. Cisplatin can also join bases across the two DNA strands (interstrand adducts) or can form monoadducts when only one of the reactive arms is bound to DNA. Such adducts can lead to crosslinks between DNA and proteins or other molecules e.g. glutathione (adopted from Master and Köberle, 2003).

1.3.2 Recognition of cisplatin-DNA adducts

As mentioned above, cisplatin preferentially binds to DNA on adjacent guanines in the major groove of the helix leading to a significant bending towards the major groove and exposing the minor groove to several classes of DNA-binding proteins (Bellon *et al.,* 1991). These include the TATA-binding protein (TBP), the sex-

determining region Y protein (SRY), the human upstream binding factor (hUBP), high mobility group 1 (HMG1) and group 2 (HMG2) proteins, histone H1, a number of DNA repair proteins and transcription factors (Gniazdowski and Czyz, 1999; Kartalou and Essigmann, 2001; Wozniak and Blasiak, 2002). Binding of such proteins to cisplatin-modified sites further enforces the bending of the DNA. The recognition and binding of cellular proteins to cisplatin-damaged sites is not sequence-specific. The "architectural" proteins HMG1/2 recognize the distortions of the DNA helix as natural binding sites (Chow *et al.,* 1995).

1.3.3 DNA repair of cisplatin adducts

All living organisms are able to counteract structural alterations in their genome and nucleotide excision repair (NER) is the main mechanism by which cisplatin-induced damage is removed in mammalian cells (Masters and Köberle, 2003). In sum, 11 proteins from the NER family are involved in recognizing and removing cisplatin adducts. First, a dimeric complex of XPC and HHR23 binds to DNA, altering its structure and allowing access of other repair proteins. In the next step, RPA, XPA, and TFIIH attach to the distorted DNA. Two DNA helicases, XPB and XPD, unwind DNA at the site of damage and several nucleotides further in both directions. Two endonucleases cut out 24-32 base-long oligonucleotides. XPG cuts the 3'-end of the lesion, XPF in complex with excision repair cross-complementing-1 (ERCC1) cuts the 5'-end. The deleted segment is then replaced by DNA polymerase gamma or eta in complex with PCNA and RFC. After the segment is synthesized, the DNA-ligase connects it to the repaired strand of DNA (Masters and Köberle, 2003). Alternatively, platinum adducts can be removed in actively transcribing genes efficiently by a specialized sub-pathway of the NER called transcription-coupled repair (TCR) (Fig.4). The activation of mismatch-repair and recombination repair mechanisms on cisplatin damage have also been reported (Firk *et al.,* 1996; Mello *et al.,* 1996; Zdraveski *et al.,* 2000).

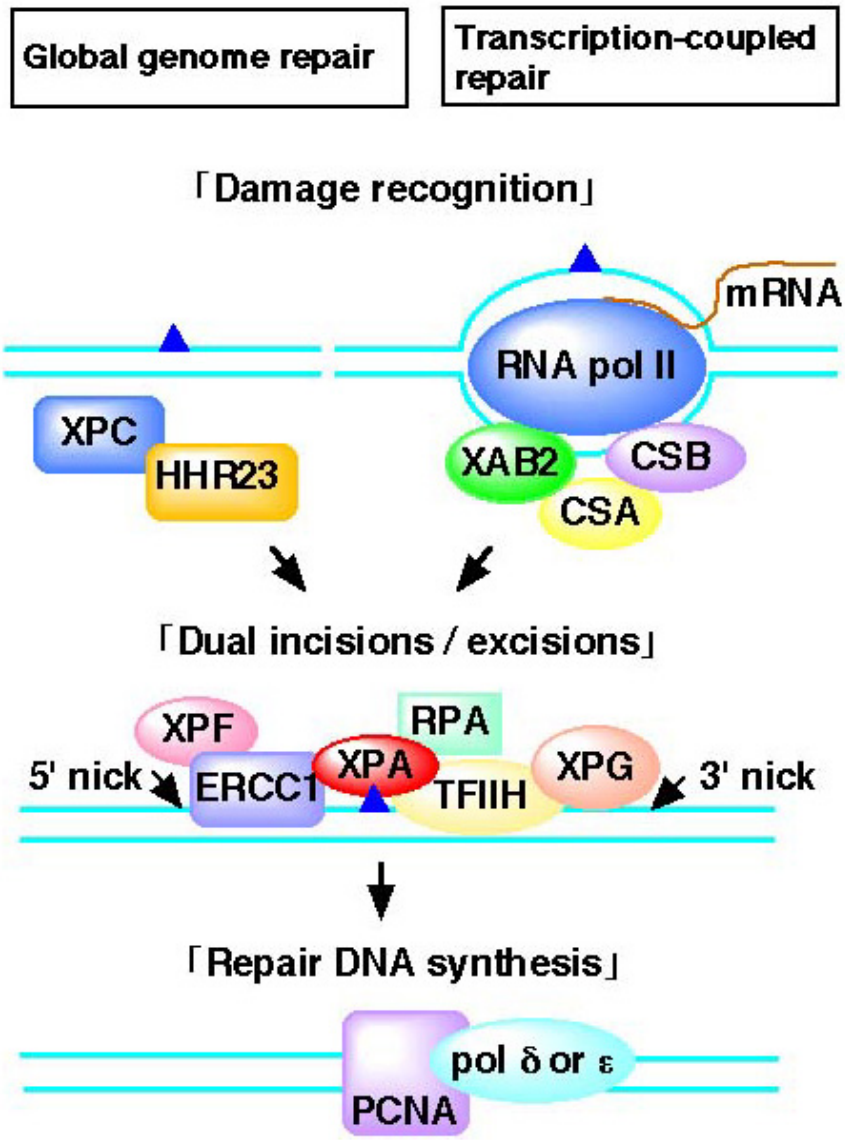

Fig. 4: Schematic model of the two sub pathways of nucleotide excision repair (NER) in mammals. The transcription-coupled repair (TCR) accomplishes fast removal of transcription-blocking lesions in comparison to the slower global genome repair (GGR) pathway. The XPA protein is involved in both sub pathways. After damage recognition by the XPC protein in GGR, or by the RNA polymerase II in TCR, the XPA protein binds to the damaged site and recruits other proteins to build a repair complex. (Figure from www.imcb.osaka-u.ac.jp/en/seminar/03a.html).

1.3.4 Cell cycle arrest and transduction of DNA damage signals

In vitro studies have shown that cisplatin is not a cell cycle phase-specific drug and cancer cells are responsive in different cell cycle phases (Sekiguchi *et al*., 1996). However, cells are more sensitive to the drug in the G2/M-phase than in other

phases. After exposure to cisplatin, most cells pass slower through the S-phase and stop cycling at the G2-M transition. The fate of the cell then depends on the type and level of nuclear DNA adducts remaining unrepaired at this point of the cycle. Cells can either proceed with mitosis or induce apoptotic mechanisms.

Several cellular pathways have been reported to be involved in transducing signals from cisplatin-induced DNA damage to downstream mechanisms like cell cycle arrest, apoptosis or necrosis (Wang and Lippard, 2005). However, most of the studies showed controversial results, and taken together, the main conclusion is that the specific response to the genotoxic stress is strongly related to the origin and the particular nature of the cell line analyzed (Theis and Roemer, 1998; Wang *et al.,* 2000; Cui *et al.,* 2000; Kigawa *et al.,* 2002; Levresse *et al.,* 2002; Fraser *et al.,* 2003; Machuy et al., 2004).

1.3.5 Induction of cell death

There are three main mechanisms of cell death after exposure to cytotoxic agents: programmed cell death (apoptosis), disorder cell death (necrosis) and autophagic cell death (Kroemer *et al.,* 2005; Klionsky and Emr, 2000). Cisplatin has been reported to induce all three types of destruction (Gonzalez *et al.,* 2001; Inoue *et al.,* 2009).

It is widely accepted that cancer chemotherapy with platinum-based drugs predominantly triggers apoptosis in cycling tumor cells via the intrinsic pathway by the release of cytochrome c from mitochondria and a subsequent activation of caspase-9 (Li *et al.,* 1997). There is also evidence that caspase-3 is critical for cisplatin-induced apoptosis (Blanc *et al.,* 2000).

The mechanisms by which cisplatin induces functional loss and structural ruin in differentiated, non-dividing normal cells are much less clear. Most studies in this respect have been performed with kidney proximal tubule cells because these cells are the “target” of the cisplatin-induced nephrotoxicity *in vivo* and they are highly sensitive to the drug *in vitro* and *in vivo* (Lieberthal *et al.,* 1996).

Caspase-9 activation was shown not to be necessary for the induction of apoptosis in these cells (Cummings and Schnellmann, 2002). Instead, Fas and the Fas ligand were found to be upregulated by cisplatin (Fulda *et al.,* 1998). Excessive DNA damage induces hyper-activation of Poly (ADP-ribose) polymerase (PARP). PARP cleaves NAD+ and transfers ADP-ribose moieties (ADPR) to carboxyl groups of

nuclear proteins, thereby causing NAD+/ATP depletion and resulting in necrosis (Herceg and Wang, 2001; Wang and Lippard, 2005).

Autophagy is a mechanism to degrade cellular components such as organelles, protein aggregates and other macromolecules. Under normal conditions, the activity of this mechanism in cells is quite low, but can be strongly upregulated during starvation or other types of cell stress. Treatment with DNA-damaging agents like cisplatin represents such a stress condition. Normally, autophagic processes promote cell survival under unfavorable conditions, but if such a condition persists over time, autophagy can lead to complete cell degradation (Kroemer and Levine, 2008). It is generally assumed that autophagic processes regulate the balance between cell death and survival and that dividing cells actively undergo apoptosis, whereas G0 cells die with signs of necrosis. Several studies have demonstrated autophagy to occur during cisplatin treatment in kidney proximal tubule cells (Periyasamy-Thandavan *et al.,* 2008; Inoue *et al.,* 2009). The relative importance of this process for the distinct nephrotoxicity of the drug, however, is not yet clear. It has to be studied in more detail whether in this context autophagy is a mechanism for mediating cell death or for promoting cell survival (Spano *et al.,* 2008; Lieberthal, 2008).

1.4 Factors limiting the therapeutic efficacy of cisplatin

1.4.1 Drug resistance

The acquired clinical non-responsiveness of tumors to cisplatin chemotherapy can be caused by a wide variety of mechanisms. Basically, such factors can be separated into two groups. In the first group both systemic and cellular mechanisms lead to reduced levels of platinum adducts in the nuclear DNA of malignant cells. Alternatively or concomitantly, drug resistance can also be due to increased cellular tolerance to such adducts by alterations in downstream signaling pathways (Fig. 5).

1.4.2 Resistance through poor DNA platination

Cisplatin is believed to be taken up by cells both via active transport and via passive diffusion. In recent years, active transport of cisplatin has been discussed as the

main entry mechanism of cisplatin into cells. The exact transporter or channel is currently unknown, but the expression of some transporters correlates well with tumor resistance (for example copper transporter CTR1). Decreased expression of CTR1 on the membrane of the cell can reduce the entry of cisplatin and, thereby, help cells to escape being killed (Ishida *et al*., 2002). Another way to increase the cellular resistance to cisplatin is the active export by suitable transporters before its interaction with the nuclear DNA. These transporters are also not known, but some suggest ATP7A and ATP7B for many tumors (Samimi *et al*., 2003; Furukawa *et al*., 2008). It is important to mention here that the reported import and export channels modulate the accumulation of cisplatin as well as carboplatin. The tumors that are resistant to cisplatin via such transport mechanisms are cross-resistant to carboplatin as well. A third possible mechanism for cisplatin resistance is based on the intracellular detoxification and metabolic modification of cisplatin, or on its binding to other molecules, preventing the reaction with DNA. Such binding may occur when cisplatin encounters glutathione or other sulphur-containing peptides (Yang *et al.,* 2006). Cisplatin-glutathione complexes are more anionic and can be more easily exported out of the cell (Ishikawa, 1992).

1.4.3 Resistance through altered processing of platinum-DNA adducts

Once activated by the formation of aqua complexes (see 1.2), cisplatin is able to bind to DNA and form adducts. Resistance of tumor cells to the drug can be mediated by accelerated repair of such adducts (Johnson *et al.,* 1994; Kelland, 2007).
Augmented DNA repair capacity by overexpression of the NER component ERCC1 was suggested to contribute to the clinical resistance of lung and ovarian tumors to cisplatin-based chemotherapy (Reed, 2005). Loss of DNA mismatch repair pathways has been reported in cisplatin resistance as well (Fink *et al.,* 1996; Helleman *et al.,* 2006). Clinical studies with ovarian cancer patients have demonstrated that loss-of-function of the DNA mismatch-repair pathway through hypermethylation of the hMLH1 gene after cisplatin chemotherapy might contribute to the acquired resistance and predicts poor survival (Gifford *et al.,* 2004). The other resistance mechanisms are increasing in tolerance to platinum DNA adducts. Among them is the possibility of replicative bypass, whereby specialized DNA polymerases can override cisplatin-damaged sites via translesion synthesis. The functional inhibition of such

polymerases has been shown to sensitize cancer cells to cisplatin cyctotoxicity *in vitro* (Albertella *et al.,* 2005). Finally, drug resistance can be due to the loss of signaling from DNA damage to cell death pathways caused, for example, by mutation or decreased expression of proapoptotic proteins (Kelland, 2007).

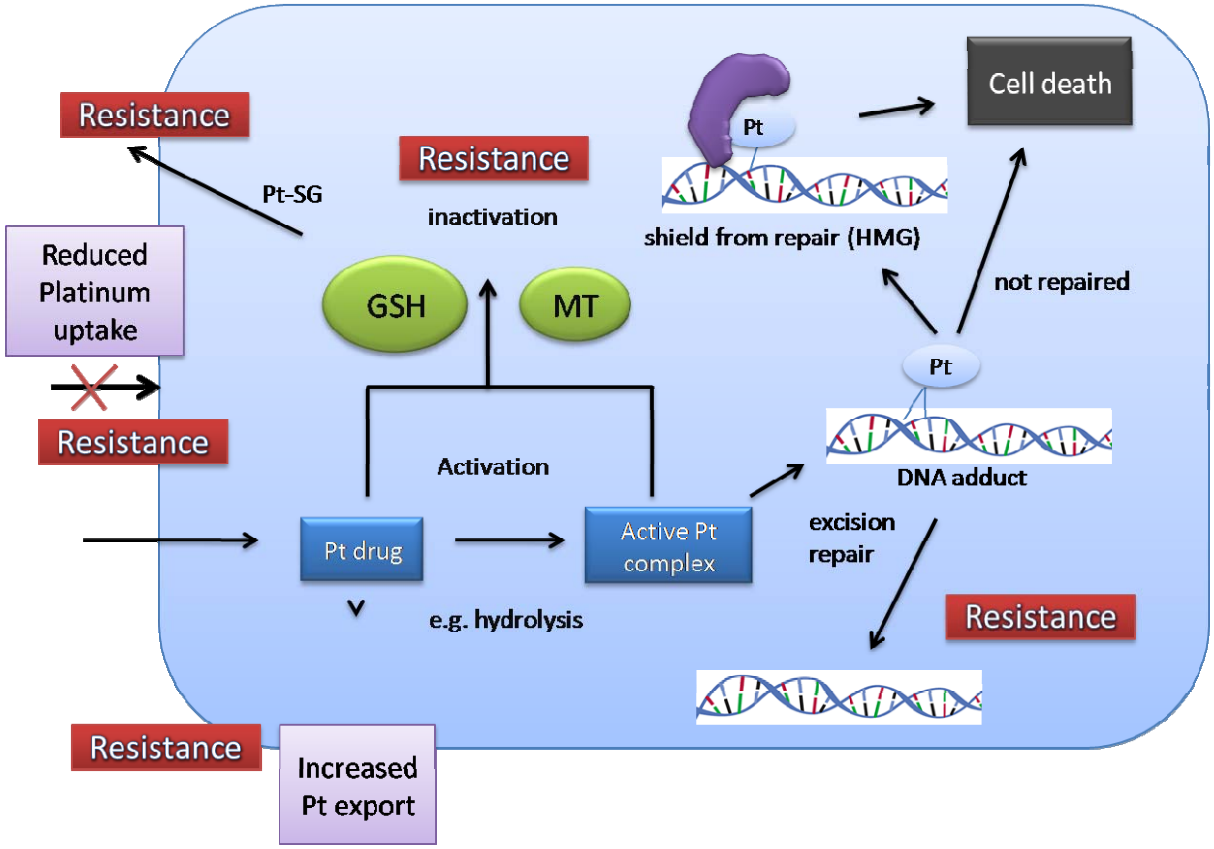

Fig. 5: Possible mechanisms of cisplatin resistance or sensitivity. Given the fact that cisplatin cytotoxicity results from the formation of DNA adducts, anything that decreases the cytoplasmic or nuclear concentration of the drug can be expected to render it less effective and the cell more resistant. GSH: glutathione; MT: mitochondria; Pt-SG: inactive glutathione-cisplatin complex.

1.4.4 Dose-limiting cytotoxic side effects of cisplatin in physiological cells

The second major obstacle limiting successful chemotherapy with platinum-based drugs is their severe systemic toxicity in normal tissues. During the treatment of patients with cisplatin, a typical pattern of side effects that includes nephrotoxicity, neurotoxicity and ototoxicity is frequently observed. Interestingly, in strict contrast to the antineoplastic activity, this type of damage occurs in cells which are assumed to be terminally differentiated and are in the non-proliferative G0 phase.

Neurotoxicity. Cisplatin-induced neurotoxicity commonly manifests as peripheral sensory neuropathy and is irreversible in most cases. The central nervous system is not affected because cisplatin does not readily penetrate the blood-brain-barrier, resulting in low DNA adduct levels (Dzagnidze *et al.,* 2007). In contrast, peripheral neuronal structures, in particular the dorsal root ganglia (DRG) that contain the primary sensory neurons, are highly adducted after systemic application of cisplatin (Windebank *et al.,* 1996; Windebank *et al.,* 2002). Repetitive treatment cycles result in structural impairment of DRG cells as well as in the loss of sensory function, neuropathic pain, severe ataxia and weakness (Umapathi and Chaudhry, 2005; Visovsky, 2003). Although it has been demonstrated in transgenic mouse models that the accumulation of Pt-GG adducts in DRG neurons are the trigger for the onset of cisplatin neurotoxicity (Dzagnidze *et al.,* 2007), and that this process is accompanied by massive mitochondrial damage (Yoon *et al.,* 2009), the exact molecular mechanism and the reason why DRG cells are the main target structures is still not fully understood.

Nephrotoxicity. Urinary excretion is the main route of removing cisplatin from the organism, and severe nephrotoxicity was already described in early clinical studies (Gonzales-Vitale *et al.,* 1977; Dentino *et al.,* 1978; Madias and Harrington, 1978). Unbound cisplatin is freely filtered at the glomerulus and is taken up into proximal tubular cells, which reabsorb filtered physiological ions by active transport. Morphological and biochemical studies revealed structural damage after cisplatin treatment, predominantly in proximal tubular cells, together with increased urinary creatinine values and failed resorption of magnesium, sodium and potassium. Today, this problem is moderated in the clinic by intravenous saline volume expansion and by mannitol-stimulated diuresis (Finley *et al.,* 1985; Bajorin *et al.,* 1986; Cornelison and Reed, 1993).

Ototoxicity. Ototoxicity leads to the functional impairment and cellular degeneration of the tissues of the inner ear, and is caused, among others, by therapeutic agents (Rybak and Ramkumar, 2007). The most common drugs with ototoxic side effects are macrolide and aminoglycoside antibiotics, cisplatin and loop diuretics (Arslan *et al.,* 1999). It is interesting that all these drugs also display a nephrotoxic potential, indicating that the causative mechanisms of oto- and nephrotoxicity might be identical or at least similar. Cisplatin-induced ototoxicity manifests as sensorineural hearing loss beginning in the high frequencies and progressing towards the speech frequency

range (Rybak *et al.,* 2007). Usually, the hearing loss is bilateral and often accompanied by transient or permanent tinnitus, and the degree of hearing loss is roughly correlated to the cumulative dose of the drug (Simon *et al.,* 2002; Bertolini *et al.,* 2004).
Today, cisplatin ototoxicity is the main cause of drug-induced hearing loss in Germany and other countries.

1.4.5 Inter-individual variability

Audiometric studies have disclosed hearing problems in 75-100% of all patients treated with cisplatin and a high inter-individual variability in the severity of the ototoxic effect (Rybak *et al.,* 2007). The sensitivity to cisplatin is more pronounced in elderly and paediatric patients with children under 5 years representing the most susceptible group (Li *et al.,* 2004). The cause of the inter-individual sensitivity is not known, but possible explanations include genetic factors, pharmacokinetic differences and the metabolic status, such as a limited availability of glutathione for the intracellular detoxification of cisplatin (Oldenburg *et al.,* 2007).

1.5 The sense of hearing

The sense of hearing is absolutely important for a human to lead a normal life. Communication skills are very dependent on hearing, as are basic survival skills in the modern world. Children who lose their hearing at an early age cannot speak appropriately. In losing their ability to hear other people, they also lose the ability to control their own voice and to speak in such a manner that would be understandable to other people.

1.5.1 Anatomy and physiology of hearing

The human ear is a mechanoreceptor organ which detects sound signals in a broad range between 20 Hz and 20 kHz and the unit used for expressing the hearing threshold is decibel (dB). Once a sound wave reaches the external ear, it continues through the ear canal to the tympanic membrane, where it transmits the wave to the middle ear ossicular chain and on to the cochlear fluids (Fig. 6).

The inner ear is one of the three parts of the hearing and vestibular system (external ear, middle ear and inner ear, Fig.6). It consists of two parts: the cochlea, which is dedicated to the hearing, and the vestibular portion, which is dedicated to the balance (Dallos *et al*., 1996). The cochlea is responsible for converting sound vibrations into nerve impulses. The inner ear fluids transmit the mechanical waves to the primary sensory cells – the outer and inner hair cells. The movement of the hair bundles on the hair cells leads to the depolarisation of inner hair cells and to the release of neurotransmitters which, in turn, stimulate associated nerve endings (Fig. 7).

The membranous labyrinth in the cochlea of the inner ear forms three compartments: the scala vestibuli, the scala media, and the scala tympani (Fig. 7). The scala tympani and the scala vestibule are filled with perilymph. The composition of this fluid is very similar to the composition of extracellular liquids - low in potassium (3 mM) and high in sodium (154 mM). The concentration of chloride anions is similar to that in plasma (128 mM). In the context of this study this is important because high concentrations of chloride anions prevent the activation of cisplatin. The second important anion in the perilymph of the scala tympani is bicarbonate with a concentration of 20 mM. The composition of the fluid in the scala media, the endolymph, is nearly inverse to the sodium-potassium ratio in the perilymph - low in sodium (1 mM) and high in potassium (161 mM). The chloride concentration is similar to the perilymph (131 mM). The perilymph has a positive potential of about +80 mV, whereas the hair cells and the cells of the stria vascularis carry a negative potential, which is higher than in other surrounding cells (Konishi *et al*., 1978; Offner *et al*., 1987).

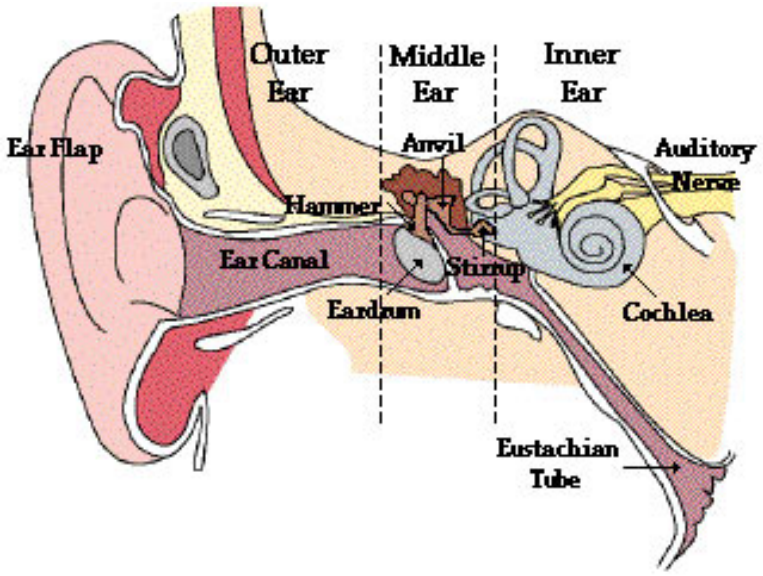

Fig. 6: The structure of the external, middle and inner ear. The ear has three morphological and functional sections: the external ear, the middle ear, and the inner ear. The external ear collects sound waves and funnels them down the ear canal, where they vibrate the eardrum. Within the middle ear, the eardrum is connected to the middle ear bones which mechanically carry the sound waves to the oval window of the inner ear. The cochlea, as part of the inner ear, is a snail-like structure divided into three fluid-filled parts. (Figure from www.topnews.in).

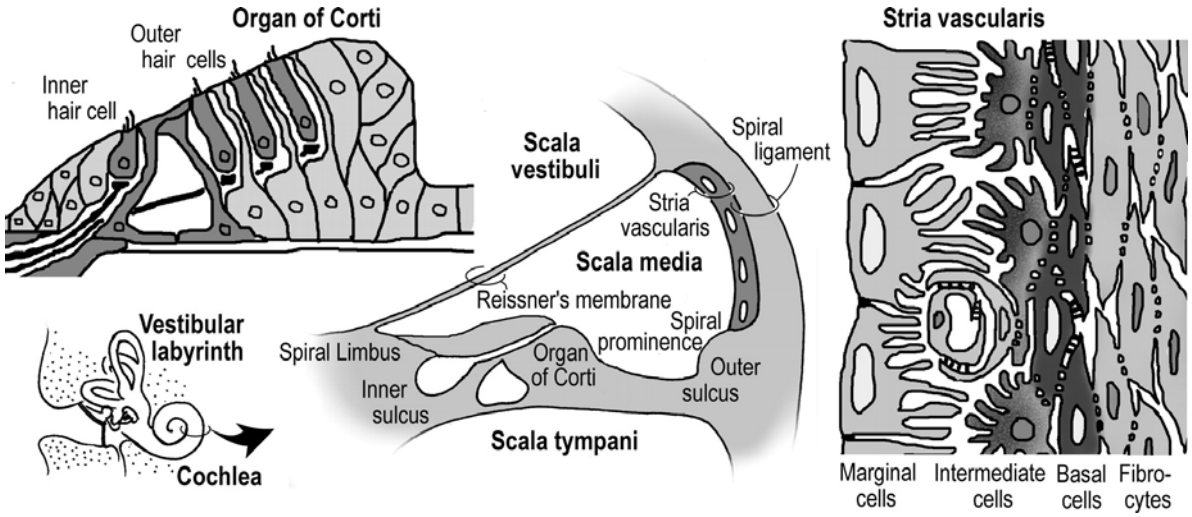

Fig. 7: Schematic diagrams illustrating the anatomy of the cochlea. (Figure from Wangeman, 2006).

The homeostasis of ion concentrations in the inner ear is very important for the appropriate translation of sound waves into neuronal signals (Fig. 8). Therefore, all substructures of the cochlea are equipped with numerous membrane transporters to keep the cells prepared for the next sound stimulus. Chloride and sodium ions have to be recycled quickly within the system during the hearing processes. The difference in cellular and endolymph concentrations creates a potential difference, which transmits signals from outer hair cells to inner hair cells and then as electro-chemical signals to the spiral ganglia. Sound waves, by moving the tectorial membrane connected to the stereocilia, change the microfilament structure of the hair cells, opening apical mechano-sensitive channels on the surface of the outer hair cells, thereby creating electromechanical amplification of the acoustic vibrations. The polarisation that occurs is transmitted to the inner hair cells, which export ions out to the endolymph and to other cells of organ of Corti – mostly to the Deiter's cells (a type of supporting cells). From these cells, the ions are recycled for another round of secretion to the stria vascularis through the next layer of supporting cells and the fibrocytes of the spiral ligament. In turn, potassium is secreted back into the endolymph by the marginal cells of the stria vascularis (Offner *et al*., 1987).

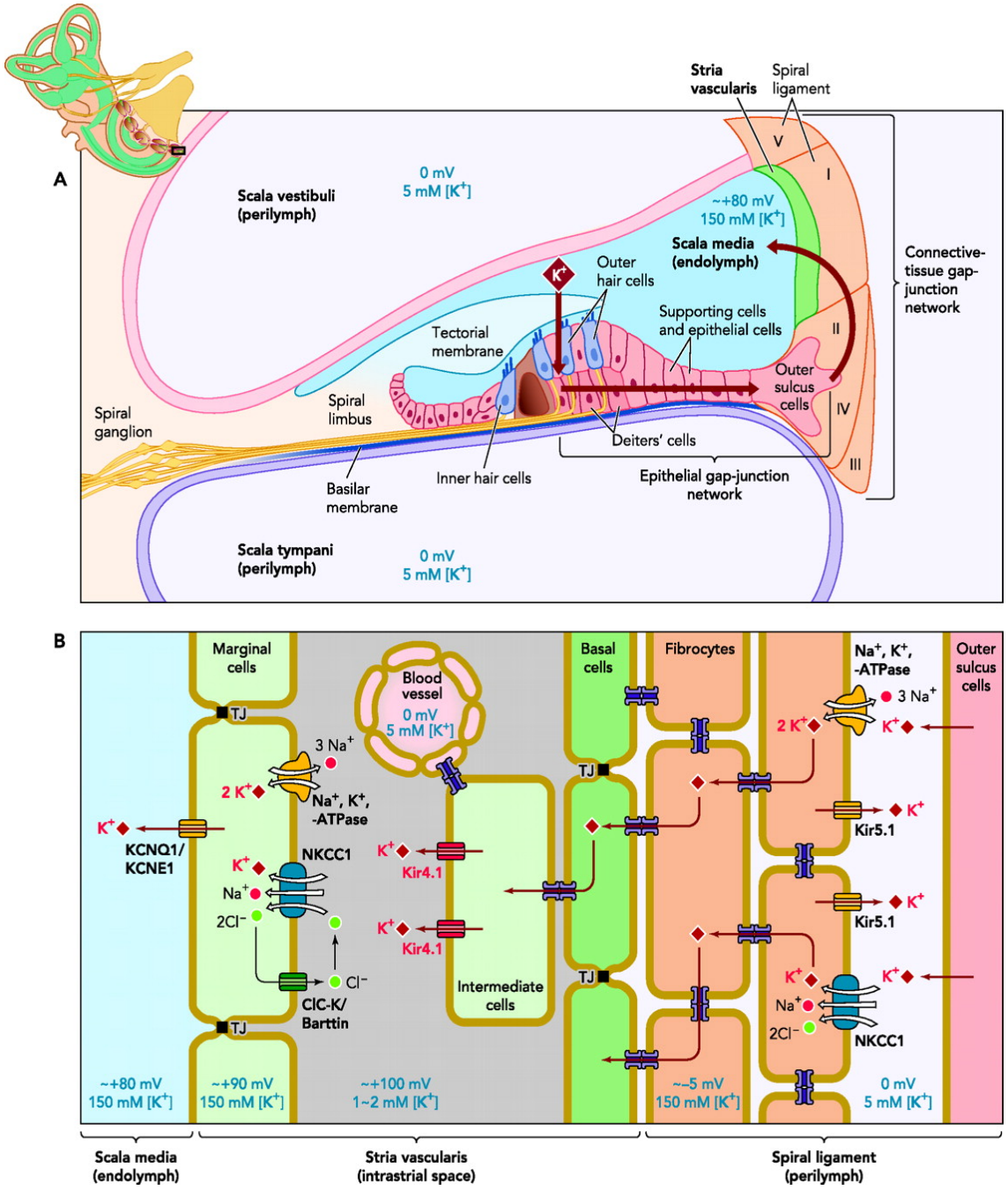

Fig. 8: Potassium recycling in the scala media of the inner ear. (A) K^+ excreted from the hair cells is picked up by Deiters' cells. K^+ is then circulated to the type II and IV fibrocytes in the spiral ligament through the "epithelial gap-junction network," which is composed of the epithelial and supporting cells (purple) on the basilar membrane (dark gray) and the outer sulcus cells (purple) in the ligament. K^+ is taken up by the types II and IV fibrocytes in the spiral ligament and transported to the stria vascularis via the "connective-tissue gap-junction network" comprising the fibrocytes, basal cells, and intermediate cells (see details in B). K^+ is finally released to the endolymph in the scala media across the luminal site of the stria vasuclaris. The concentration of K^+ and the potential of each cochlear fluid are indicated. (B) Ion-transport apparatuses expressed in the stria vascularis and the spiral ligament that participate in cochlear K^+ circulation. The potential and concentration of K^+ in each compartment are indicated. I-V: type I-V fibrocytes; NKCC1: Na^+-K^+-$2Cl^-$ cotransporter; TJ: tight junctions. (Figure adopted from Hibino and Kurachi, 2006).

In drug-induced ototoxicity, this balance of ions is disturbed due to the degradation of hair cells and marginal cells, and the potential of outer hair cells is reduced. These changes lead to a weaker responsiveness to sound pressure.

1.6 Oto- and renoprotective strategies tested so far

Since cisplatin has been used in the clinic for a long time, a plethora of pharmacological protective strategies to counteract the side effects have been attempted. These strategies based on different effects of cisplatin on the cells and tissues such as drug uptake, activation, metabolism, excretion, oxidative stress, cell-cycle arrest, signalling, inflammation (Jones *et al.,* 1992; Santoso *et al.,* 2003; Ludwig *et al.,* 2004; Badary *et al.,* 2005; Durak *et al.,* 2002; Lynch *et al.,* 2005; Karimi *et al.,* 2005; Nagothu *et al.,* 2005; Jo *et al.,* 2005;). However, the rational preventive treatment till now has not been discovered mainly because interaction of such preventive treatment with antineoplastic function of cisplatin.

1.7 Aim of the study

Despite more than 40 000 scientific publications on cisplatin during the last four decades, the precise mechanisms of how primary tumor cells escape *in vivo* from being eradicated by cisplatin-based chemotherapies as well as why particular terminally differentiated normal cells become highly vulnerable targets for the cytotoxic effects of the drug are still obscure. This lack of knowledge is mainly due to the predominant use of cell culture systems and the unavailability of analytical tools to measure structurally defined reaction products of cisplatin in individual cell nuclei. After a monoclonal antibody-based detection system for such DNA adducts was established in our group those two important questions were addressed in this study by employing a panel of mouse models. The experiments should reveal the pharmacodynamic mechanisms underlying the pronounced oto- and nephrotoxicity of cisplatin and the role of DNA platination products as the initial molecular triggers for the induction of cell damage and functional loss in the target tissues.

Based on that knowledge, it was tried to develop a new pharmacological strategy to efficiently suppress the side effects of cisplatin in mice without reducing its antineoplastic efficacy.

A further aim of this study was to elucidate the role of cellular DNA repair for the onset of drug resistance in a mouse model of primary lung cancer.

2. Materials and Methods

2.1 Materials

2.1.1 Equipment

Equipment	Company
ABR recording modified clinical potential system	NeuroScreen Plus
ACAS 6.0 Cytometry Analysis System	Ahrens Electronics
Adhesion slides ImmunoSelect	Squarix Biotech
Agarose Gel Chamber	PEQLab
Axioplan Fluorescence microscope	Zeiss
Centrifuge Rotina 48	Hettich Lab Technology
Charge-coupled device camera C4880	Hamamatsu
CO_2- incubator C200	Labotect
Consort Electrophoresis Power Supply 800	Sigma-Aldrich
Cryostat 2800 Frigocut	Reichert-Jung
Cryostat	Leica
Histochemistry slides	Roth
High-accuracy weighing machine	Bosch
FACSCanto	BD Biosceience
Micro liter centrifuge Mikro200R	Hettich Lab Technology
Microtome	Reichert-Jung
Microwave	Bosch
Nalgene Cryo 1°C Freezing Container	Nalgene
Phase contrast inversion microscope CK2	Zeiss
Photometer Nanodrop	PEQLab
pH-Meter	Mettler-Toledo
Pipettes	Abimed
Pipette-akku, P 900 7001/0294	Hirschmann
Pipette-standard, P990 30 01	Hirschmann

PTC-200 PCR Cycler	BioRad
Stereomicroscope Stemi SV 6	Zeiss
Table centrifuge 5415D, Thermo mixer	Eppendorf
Transmission electron microscope Zeiss EM 902	Zeiss
UV-transilluminator	Bachmann
Vortexer L46	GLW
Water bath TWB 22	Julabo

2.1.2 Chemicals, enzymes and solutions

Reagent	**Company**
Acetic acid	Merck
Agarose	Biozym
Amino acids, non-essential	PAA
Ammonium persulfate	Fluka
BSA (Bovine serum albumin)	Sigma-Aldrich
Cacodylic acid sodium salt trihydrate	Merck
Calcium chloride dihydrate	Merck
Chloroform	Sigma-Aldrich
DAPI (4,6-Diamidino-2-phenylindol)	Roche
Dulbecco's modified eagle medium (DMEM) (High Glucose)	PAA
DMSO (Dimethyl sulfoxide)	Sigma-Aldrich
DNA ladder	Fermentas
EDTA (Ethylendiamintetraacetic acid)	Fluka
Eosin	Sigma-Aldrich
Entellan mounting medium	Merck
Epon 812	Shell Chemical of Houston
Ethanol	Roth
Ethidium bromide	Sigma-Aldrich

Fetal calf serum (FCS)	PAA
Glutaraldehyde	Sigma-Aldrich
Glycine	Merck
Haematoxylin	Sigma-Aldrich
HEPES buffer	Camberex
L-Glutamine	Sigma-Aldrich
Methanol	Fluka
Sodium citrate	Merck
Sodium hydroxide	Merck
Sodium chloride	Merck
PFA (Paraformaldehyde)	Sigma-Aldrich
Penicillin/Streptomycin	PAA
Phosphate buffered saline (PBS)	Lonza
Propylene oxide	Sigma-Aldrich
RPMI-1640	PAA
Skim milk powder	Roth
Sodium dodecyl sulfate (SDS)	Sigma-Aldrich
Sodium pyruvate	Sigma
Sucrose	Sigma
Taq- polymarase	TaKaRa
Tissue-Tek O.C.T. Compound	Sakura Finetek Europe
Tris-base	Sigma-Aldrich
Triton-x-100	Sigma-Aldrich
Trypan blue	Invitrogene
Trypsine/EDTA solution	Sigma
Tween-20	Merck
“VECTASHIELD” mounting medium	Vector

2.1.3 Drugs and inhibitors

Cimetidine	Sigma-Aldrich
Cisplatin	Bristol-Meyers (Platinex)
Diphenhydramine hydrochloride	Sigma-Aldrich
Disloratadine	Sigma-Aldrich
Famotidine	Sigma-Aldrich
Fluoxetine hydrochloride	Sigma-Aldrich
Ketamine	Rotexmedica
Probenecid	Sigma-Aldrich
Ranitidine hydrochloride	Sigma-Aldrich
Scopolamine N-butyl bromide	Sigma-Aldrich
Quinine	Sigma-Aldrich
Xylizine	Loughrea

2.1.4 Primers

PCR was performed according to the modified protocol of Nakane *et al*., 1995.

XPA:

XPA-WT: 5’-GTG GGT GCT GGG CTG TCT AA-3’

XPA-KO/WT: 5’-ATG GCG TGG GTT CTT CTT C-3’

XPA-KO: 5’-ATG GCC GCT TTT CTG GAT TC-3’

2.1.5 Antibodies

Rat anti-(Pt-GG)	Dr. J. Thomale (Uni Duisburg-Essen)
Rabbit anti-(rat OCT1)	Alpha Diagnostic International (Bio Trend)

Rabbit anti-(rat OCT2)	Alpha Diagnostic International (Bio Trend)
Rabbit anti-(rat OCT3)	Alpha Diagnostic International (Bio Trend)
Rabbit anti-(mouse OCTN1)	Alpha Diagnostic International (Bio Trend)
Rabbit anti-(mouse OCTN2)	Alpha Diagnostic International (Bio Trend)
Rabbit anti-(mouse OCTN3)	Alpha Diagnostic International (Bio Trend)
Rabbit anti-(rat Ig) Cy3	Dianova
Goat anti-(rabbit Ig) Cy3	Dianova
Goat anti-(rat Ig) Alexa Fluor488	Molecular Probes

2.1.6 Cell lines

Name	**Origin**	**Obtained from**
GM 00637	Human skin fibroblasts	Dr. Naegeli, University of Zürich
TKPTS	Mouse kidney proximal tubule cells	Dr. Bello-Reuss, University of Texas

2.1.7 Mouse strains

BALB/c	albino	House breeding of the Institute of Cell Biology, University of Essen, Germany
C57BL/6J OlaHsd	Wild type	House breeding of the Institute of Cell Biology, University of Essen, Germany
LSL-K-ras$^{G12D/+}$ mice onto a 129svJae background.	bearing *K-ras* mutation	House breeding of the Koch Institute, MIT, Boston
XPA	C57BL/6J, XPA knockout	House breeding of the Institute of Cell Biology, University of Essen, Germany

2.1.8 Software

ACAS ICM	Ahrens Electronics
Origin 7.0	Origin Lab Corporation
FACSdiva	BD Bioscience
Bioquant	Bioquant Image Analysis Corporation

2.2 Methods

2.2.1 Breeding and treatment of mice

All animals were kept under specific pathogen free conditions at 12 hours light/dark cycle with free access to water and standard laboratory mouse food "Zuchthaltungsfutter Maus-Ratte 10 H 10" (Eggersmann) and water ad libitum.
All experiments have been approved by the state animal welfare board. Mice were weighed and checked for signs of drug toxicity before each application of cisplatin.
Wild type mice. All experiments were performed when animals were aged 12-14 weeks. Male C57BL/6J mice (or BALB/c mice for electron microscopy studies) were from the in-house breeding stock. All drugs were administrated by i.p. injections and treatment regimens were as follows: 10 mg/kg of cisplatin (acute, single treatment) or 5 mg/kg of cisplatin (plus 500 µl of saline solution) every second day for 8 days (cumulative dose: 20 mg/kg of cisplatin; chronic treatment). In the case of inhibitor treatment: the inhibitors wer administered 1 hour before cisplatin treatment. In all following studies after first check, diphenhydramine (DIPH) was administered 30 minutes before cisplatin.
Mice bearing lung tumors. 8 weeks old mice were infected with AdCre (University of Iowa) by nasal inhalation as described previously (Jackson *et al.,* 2001; Oliver *et al.,* 2010) and were further kept for 12–16 weeks to allow the development of lung tumors.
Treatment of mice was done by i.p. injections in three schedules.
Acute treatment: 10 mg/kg of cisplatin with or without inhibitor DIPH 57 mg/kg.
Chronic treatment: 5 mg/kg of cisplatin with or without DIPH plus saline buffer.
Long-term treatment to study tumor regression: mice were treated onece per week with 7 mg/kg of cisplatin, 4 times a month.
Long term treatment to study drug response of tumors: 4 consecutive treatments once per week (7 mg/kg of cisplatin).
XPA-/- mice. 10 -16 week old males validated by PCR genotyping were used. Mice were treated with cisplatin twice (1mg/kg on the first day and 2.5 mg/kg after one week). After each cisplatin treatment an i.p. injection of saline (500 µl) was given to prevent kidney toxicity.

2.2.2 Tissue preparation and frozen tissue section

The sacrificed animals were immediately dissected. Kidneys and lungs were submerged in the embedding medium (Tissue-Tek O.C.T. Compound) and frozen in liquid nitrogen. Cochleae were dissected and fixed by intralabyrinthine perfusion with Carnoy´s solution (3 hours; for DNA adduct staining) or with formaldehyde (4 % in PBS; 1 hour; for OCT protein staining). Cochleae were decalcified in EDTA solution (10 % w/v in PBS) for 3 days and then placed in sucrose solutions (5 % in PBS for 12 hours and 15 % in PBS for 5 hours). After that samples were imbedded in special freezing blocks with Tissue-Tek medium and were frozen in liquid nitrogen. Frozen tissue blocks were stored in sealed freezing vials at -80°C.

Frozen tissue blocks were placed into the chamber of the cryostat, allowed to equilibrate to the chamber temperature (-25°C) for 30 minutes, bound with the embedding medium to the specimen block and mounted on the stub. The stub temperature was kept at –26°C while cutting. Cryosections (10 µm) from all tissue samples were placed onto specific adhesion slides (ImmunoSelect, Squarix Biotech) for optimal preservation of structures during the immunostaining procedure. Slides were air-dried at 24°C for at least 16 hours and stored at -20°C until further processing.

Carnoy´s fixator:
60 % Ethanol
30 % Chloroform
10 % Acetic acid

2.2.3 Morphological examination of haematoxylin-eosin stained tissue sections

Frozen tissue sections were warmed up to room temperature and fixed in an acetone bath at 25°C for 10 minutes. Subsequently the slides were immersed in the haematoxylin solution for 5 minutes at 25°C. The slides were then rehydrated for 10 minutes and stained in 1 % ethanol/eosin solution for 5 minutes. Following washing, the slides were dehydrated stepwise in 70 %, in 96 %, and in 100 % ethanol and then in xylene by immersing in each solution twice and after that embedded in mounting

medium Entellan (Merck). Morphological examination of the samples was performed by light microscopy.

Haematoxyline solution (ingredients were solved in 1000 ml dH_2O):

2 g haematoxyline

0.2 g $NaIO_3$

17.6 g $KAl(SO_4)_2$

2.2.4 Immunocytological assay (ICA): visualization and measurement of DNA adducts

Frozen tissue sections of inner ear or kidneys on the ImmunoSelect slides were fixed in methanol at -20^{0}C for at least 2 hours or overnight and then rehydrated for 10 minutes in PBS, at room temperature. To provide better antibody penetration in the tissue structures the samples underwent alkaline permeabilisation of cytoplasmic and nuclear membranes for 5 minutes at 0°C, followed by washing in PBS at room temperature for 5 minutes. The proteolytic cleavage of cytoplasmic and nuclear proteins was performed in two steps. At first, pre-warmed pepsin solution (60 µg /ml for cell culture or 100 µg/ml for tissue sections in PBS/HCl) was applied onto the tissue sections and incubated for 10 minutes at 37^{0}C in a humidified chamber. The incubation with pepsin was followed by washing in PBS for 10 minutes at room temperature. In a second step tissue sections were incubated with pre-warmed proteinase K solution (40 µg/ml for cell cultures or 50-100 µg /ml for tissue sections in proteinase K buffer) for 10 minutes at 37^{0}C in a humidified chamber. Subsequently the sections were washed in 0.2 % glycine in PBS for 10 minutes at room temperature. Non-specific binding of the antibodies was inhibited by incubation with a blocking solution of 1 % casein in PBS for 30 minutes at room temperature. The samples were then incubated with a monoclonal antibody (R-C18) specific for Pt-GG adducts in DNA (0.1 µg/ml in 0.1 % BSA/PBS) over night at 4°C in the humidified chamber. Subsequently, the slides were washed in 0.05 % Tween 20 in PBS for 5 minutes at room temperature and then in PBS for 5 minutes. The incubation with secondary Cy3-labeled rabbit anti-(rat Ig) antibodies, was performed (0.2 µg/ml in 0.1 % BSA/PBS) for 60 minutes at 37°C in the humidified chamber, followed by washing in 0.05 % Tween 20 in PBS for 5 minutes at room temperature and then in PBS for 5

minutes. The nuclear DNA was counterstained with DAPI (1 µg/ml in PBS) for 30 minutes at room temperature. The slides were then washed in PBS. Finally, the samples were embedded with a densification compound “VECTASHIELD”. The quantification of immuno- and DNA-fluorescence was performed by means of a microscope-coupled digital image analysis system ACAS 6.0 Cytometry Analysis System. Adduct levels in the nuclear DNA of individual cells were calculated by normalizing antibody-derived fluorescence signals to the corresponding DNA content of the same nucleus, and were expressed as arbitrary fluorescence units (AFUs). Data were assigned to specific cell types as determined by histochemistry.

Solutions for ICA:

Alkali solution:

60 % 70 mM NaOH / 140 mM NaCl,

40 % methanol

Proteinase K-Buffer:

20 mM Tris

2 mM $CaCl_2$, pH 7.5

Glycin/PBS:

0.2 % Glycin in PBS

PBST:

0.05 % Tween 20 in PBS

2.2.5 Immunohistochemistry on frozen sections: visualization of OCT proteins

Slides with tissue sections were left at room temperature for 10 minutes and then fixed in pre-cooled ethanol at -20°C for 30 minutes. Subsequently, samples were washed three times in PBS for 5 minutes. Slides were then blocked in skim milk solution for 30 minutes. Immunohistochemical staining was accomplished with antibodies that recognize the target protein. First rabbit anti-(OCT) antibodies (OCT1-3 or OCTN 1-3; 0.5 µg/ml in 1m% BSA/PBS) were applied on slides and incubated in a humidified chamber at room temperature for 90 minutes. After that samples were washed three times in 0.1 % BSA/PBS. Secondary antibodies (0.2 µg/ml) were applied on the slides and incubated for 45 minutes at room temperature. Samples

were washed three times in 0.1 % BSA/PBS at room temperature. Counterstaining of DNA was performed with DAPI (1 µg/ml in PBS) for 30 minutes at room temperature. Slides were washed in PBS for 5 minutes and covered with “VECTASHIELD” mounting medium. Visualization of the protein localization was performed with a Zeiss Axioplan fluorescence microscope and documented with a charge-coupled device camera C4880.

2.2.6 Electrophysiological examination of the hearing capability of mice: auditory brainstem response evaluation

Auditory brainstem response or brainstem auditory evoked response (BAER) is an electrical signal evoked from the brainstem by the presentation of a sound such as a click. BAER is a clinical screening test to monitor for hearing loss or deafness assessing the functions of the ears, cranial nerves, and various brain functions of the lower part of the auditory system.

The cochlea acts as a mechanical demodulator in the hearing process and is responsible for converting sound vibrations into nerve impulses (Johnstone and Sellick, 1972). The stimulation of associated nerve endings and conduction signal through afferent nerves via the cochlear ganglia to the cochlear nucleus, then to the superior olivary complex, then to the inferior colliculus, then to the medial geniculate body and finally to the auditory cortex (Fig. 9).

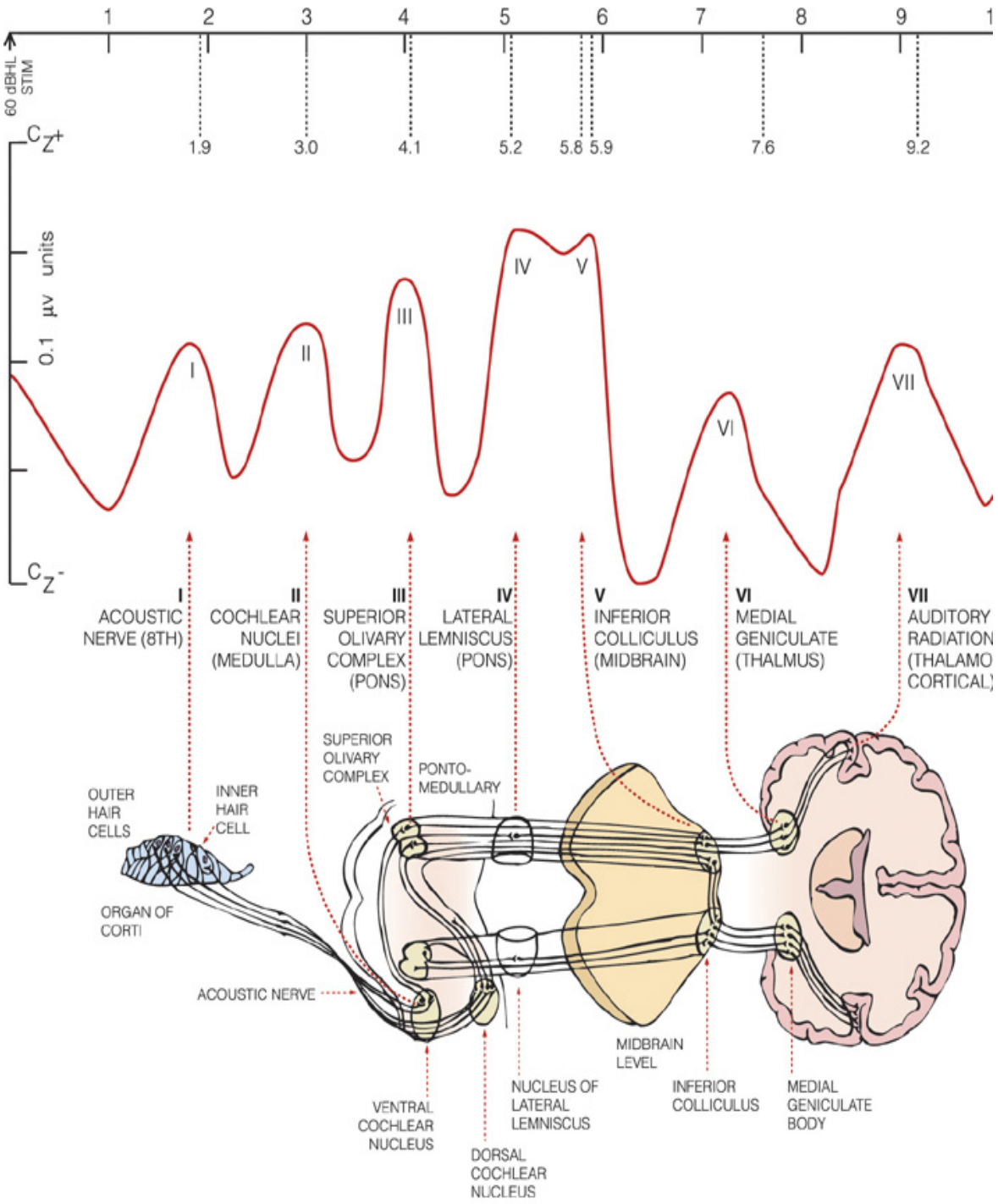

Fig. 9: The waveform of a normal brainstem auditory evoked response. Wave I represents the electrical potential from outer hair cell stimulation. Waves II, III, and IV derive from cochlear nucleus, superior olivary complex and lateral lemniscus potentials, respectively. Wave V is the response from the middle brain – inferor colliculus – which is measured by BAER to determine the level of hearing performance. (Figure adopted from Lippincott Williams & Wilkins Products).

All electrophysiological examinations were carried out under general anesthesia (xylazine, 20 mg/kg, plus ketamine, 100 mg/kg; i.p.). To minimize effects of body temperature on the evaluation process, animals were placed to a heated (37°C) thermal blanket.

Subdermal needle electrodes were inserted at vertex (active electrode), ventrolateral of left pinna (reference electrode) and ventrolateral of right pinna (ground electrode) (see Fig. 25). For acoustic stimulus presentation, auditory brainstem response recording and data management a modified clinical potential system (NeuroScreen Plus, Toennies, Germany) was used. Repetitive clicks (substantial energy: 1-3 kHz; duration: 10 ms, rate: 39 /s) were delivered through plastic tubes (diameter: 3 mm) to both ear canals (EAR-Auditory Systems, Indianapolis). BAER thresholds were determined by clicks beginning at 90 dB sound pressure level with decreasing intensity (10 dB-steps) until the waves have lost reproducible morphology. The BAER thresholds were determined separately for each ear and by repetitive measurements. Following BAER, mice were sacrificed by cervical dislocation and both cochleae were removed for ICA analysis.

2.2.7 Electron microscopy examination

C57BL/6J mice and BALB/c mice were used untreated or treated chronically with cisplatin (see 2.2.1). Dissected cochleae and pieces of kidney cortexes were fixed in 2.5% glutaraldehyde in cacodylat buffer (0.1M, pH = 7.4). The cochleae were decalcifyed in 10 % EDTA for 3 days. The samples were rinsed in several changes of phosphate buffer and fixed in 1 % osmium tetroxide for 3 hours with subsequent washing in PBS. Following dehydration through a graded series of ethanol, the tissues were washed with propylene oxide and immersed in a mixture of propylene oxide and Epon 812 (25:75 for 1 hour, 50:50 for 1 hour, 75:25 for 1 hour) and then Epon 812 pure over night. The next day samples were embedded in Epon 812 and left for 36 hours at 60°C for polymerization.

Ultrathin sections (90 nm) were taken from selected areas and mounted on grids. To increase structural contrast for electron microscopy, sections were counterstained with uranyl acetate and lead citrate (1:1). Tissue observation and photographic documentation were made with a transmission electron microscope Zeiss EM 902.

2.2.8 Annexin V apoptosis detection

Staining with FITC-labeled Annexin V was used to determine the percentage of cells within a population that are actively undergoing apoptosis. The method is based on the changes due to early stages of apoptosis: loosing membrane asymmetry due to the membrane phospholipid phosphatidyl serine (PS) that is translocated from the inner leaflet of the plasma membrane to the outer leaflet. After translocation, PS becomes exposed to the external environment. Annexin V is a calcium-dependent phospholipid-binding protein that has a high affinity for PS, and is used for identifying apoptotic cells with externally exposed PS (Fig. 10). Propidium iodide (PI) was used to distinguish viable from nonviable cells in flow cytometry as a standard test of cell viability. Living cells with intact membranes exclude PI whereas the membranes of dead or damaged cells are permeable to PI. Cells that stain positive for Annexin V and negative for PI are undergoing apoptosis. Cells that stain positive for both Annexin V and PI are either in the end stage of apoptosis, are undergoing necrosis, or are already dead. Cells that stain negative for both, Annexin V and PI, are alive and are not in the process of apoptosis.

Cells were cultivated in RPMI 1640 or DMEM medium with 10 % FCS in a humidified atmosphere containing 5% CO_2. After reaching 60 % confluence cells were treated with cisplatin alone (5 or 10 μg/ml), or in combination with DIPH (100 μg/ml), or with DIPH alone.

After 24 hours, cells were trypsinized, washed twice with PBS, and resuspended in 100 μl of Annexin–binding buffer (Annexin V-FITC Apoptosis Detection Kit I from BD). Cells were then stained with 5 μl of Annexin V-FITC and with 5 μl of PI for 15 minutes. Finally, 400 μl of Annexin-binding-buffer was added and cells were analysed by flow cytometry (FACScanto, BD) and evaluated with FACSdiva software.

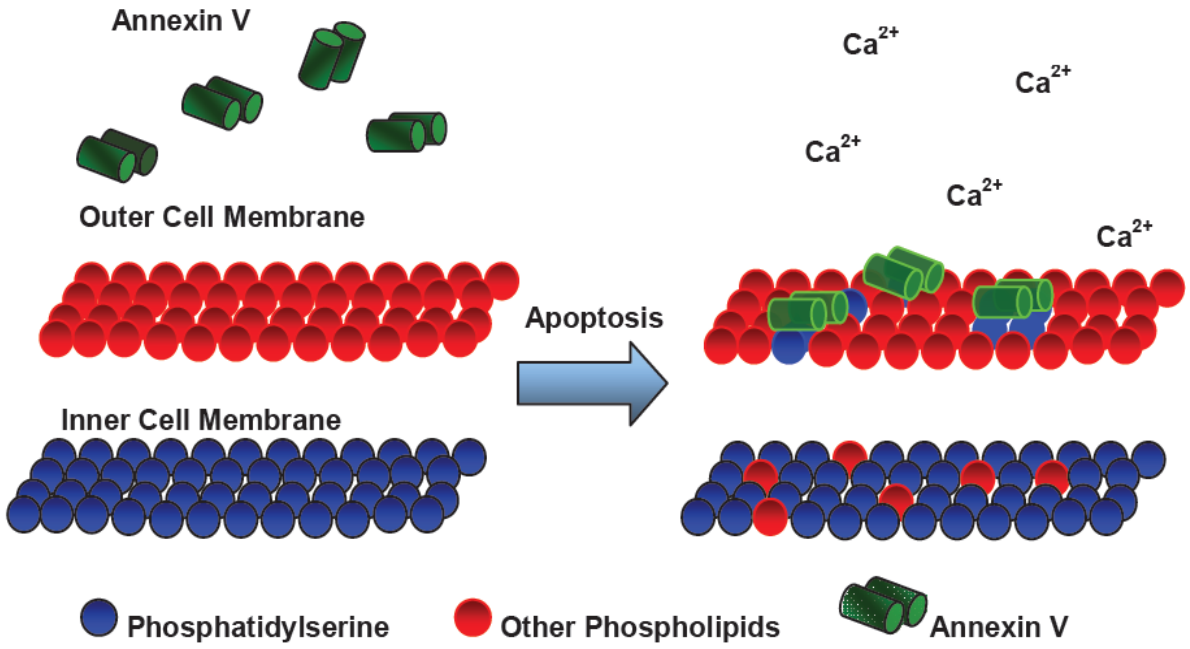

Fig. 10: Schematic scheme of apoptosis-induced membrane changes recognized by Annexin V. During early apoptosis, the plasma membrane loses asymmetry causing phosphatidylserine to be translocated from the cytoplasmic face of the plasma membrane to the external face which can be detected using Annexin V. (Figure adopted from R&D Systems).

3. Results

3.1 Establishing a mouse model for cisplatin–induced ototoxicity

The cellular and molecular mechanisms underlying the organ-specific toxicity of cisplatin in the inner ear and in the kidney have been studied predominantly in mammalian cell culture systems employing immortalized physiological cells such as proximal tubule cell lines. The majority of these studies were unable to explain the particular sensitivity of the target tissues to cisplatin because the cell systems resembled neither the complex pharmacokinetic situation within the affected organs nor the particular response of terminally differentiated, non dividing cells to the drug.
It is widely accepted that the cells of the kidney which are damaged predominantly during cisplatin treatment, and, are responsible for the nephrotoxicity and general renal dysfunction, are the epithelium cells of the proximal tubules (Arany and Safirstein, 2003). This had been evidenced by morphological studies in patients and animals treated with cispatin as well as by comparisons of various kidney cell lines developed from different cell types. The inner ear damage after cisplatin treatment was detected mainly by electron microscopic analysis but also by morphological studies of the cochlea (Klis *et al.*, 2002; Cardinaal *et al.*, 2004; Rybak and Ramkumar, 2007; Laurell *et al.*, 2007). The main conclusions from the aforementioned studies were that: (1) cisplatin-treated animals lost their cochlear hair cells, (2) the damage of the cochlea by cisplatin begins from the basal turn, (3) cisplatin causes degeneration of the stria vascularis and the spiral ganglion neurons. It has to be mentioned that almost all animal studies on the inner ear have been done so far with rats or guinea pigs, as cochleae of these animals are large enough to allow easy handling. The conclusions drawn from these studies neither provided clear evidence, how to design preventive treatment strategies, nor did they help to identify the primary molecular targets of cisplatin-ototoxicity and discriminate them from secondary effects. As no suitable transgenic rat or guinea pig strains for more detailed studies were available we first have established a mouse model to analyze the parameters targeting the toxicity of cisplatin to specific structures within the inner ear and the kidney.

3.1.1 Cochlea and kidney harbor specific target cells for cisplatin

According to our hypothesis that cisplatin mediates its toxic side effects in physiological cells also via the formation of cisplatin-DNA adducts the concentration and distribution of adducts was determined in different cell types of the inner ear and the kidney of drug-treated mice. For this purpose, male C57BL/6J mice (age 12 weeks) were injected i.p. with a single dose of cisplatin (10 mg/kg). Twenty four hours later, the inner ears and kidneys were dissected, kidneys were frozen immediately and cochleae were fixed and decalcified. Cryosections (10 µm) prepared from the tissues were placed onto specific adhesion slides. Slides were then immunostained for the visualization of platinum-guanine-guanine (Pt-GG) intrastrand adducts in the nuclei of individual cells by using the adduct-specific monoclonal antibody R-C18 in an immunocytological assay (ICA) developed in our lab (Liedert *et al.*, 2006). The tissue sections were then stained with a secondary Cy3-labeled goat-anti-rat antibody (red), counterstained with DAPI (blue) for nuclear DNA, and analyzed in the fluorescence microscope (Fig. 11). Serial sections from the same tissues were stained for morphological orientation with hematoxyline and eosin (H&E).

This analysis revealed a drastically unequal distribution of the nuclear DNA platination among cochlear cells. Two particular areas, parts of the organ of Corti and cells of the stria vascularis depicted extremely high levels of Pt-GG adducts whereas other structures were stained to a far lower degree (Fig. 11 A). A similar observation was made for kidney tissues, where the DNA of proximal tubular cells carried very high adduct burdens, whereas other types of cells depicted much lower levels of DNA platination (Fig. 11 B).

A

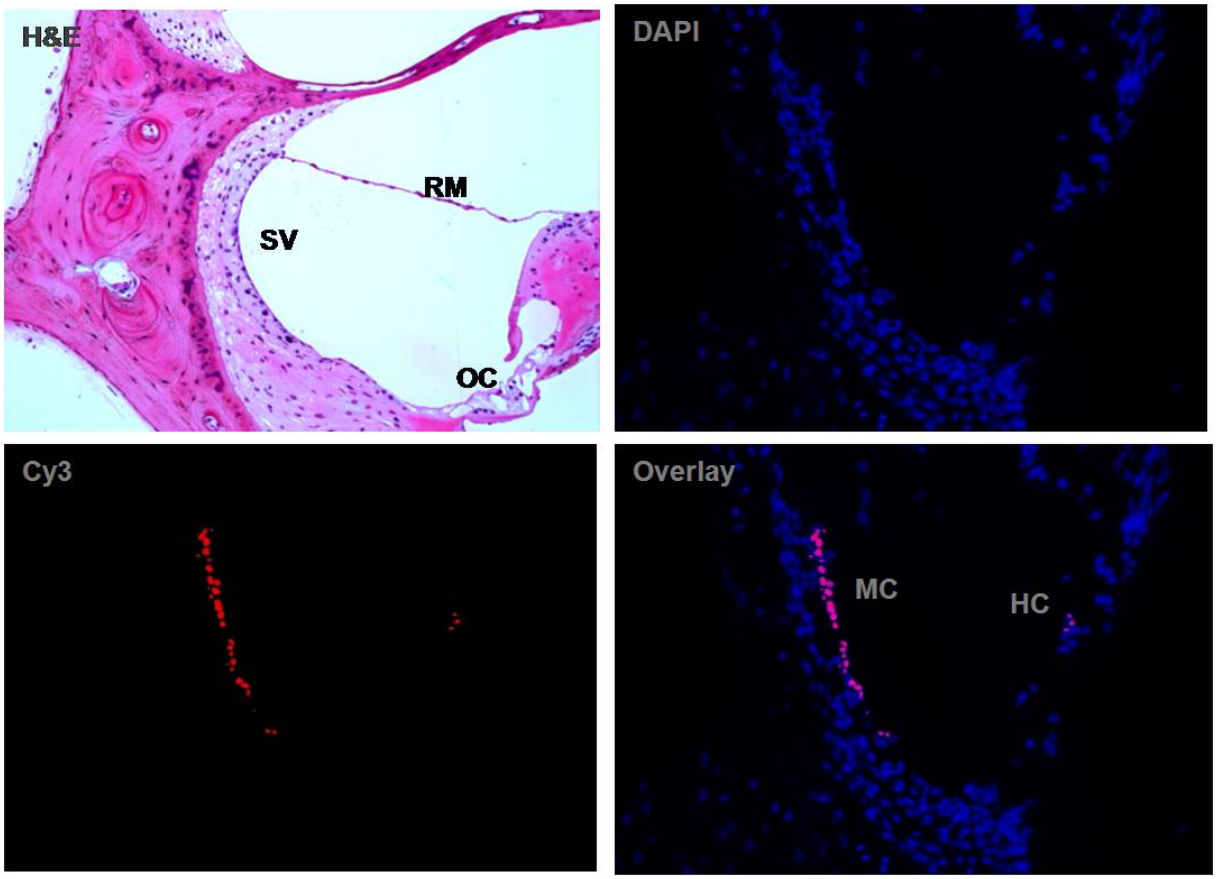

B

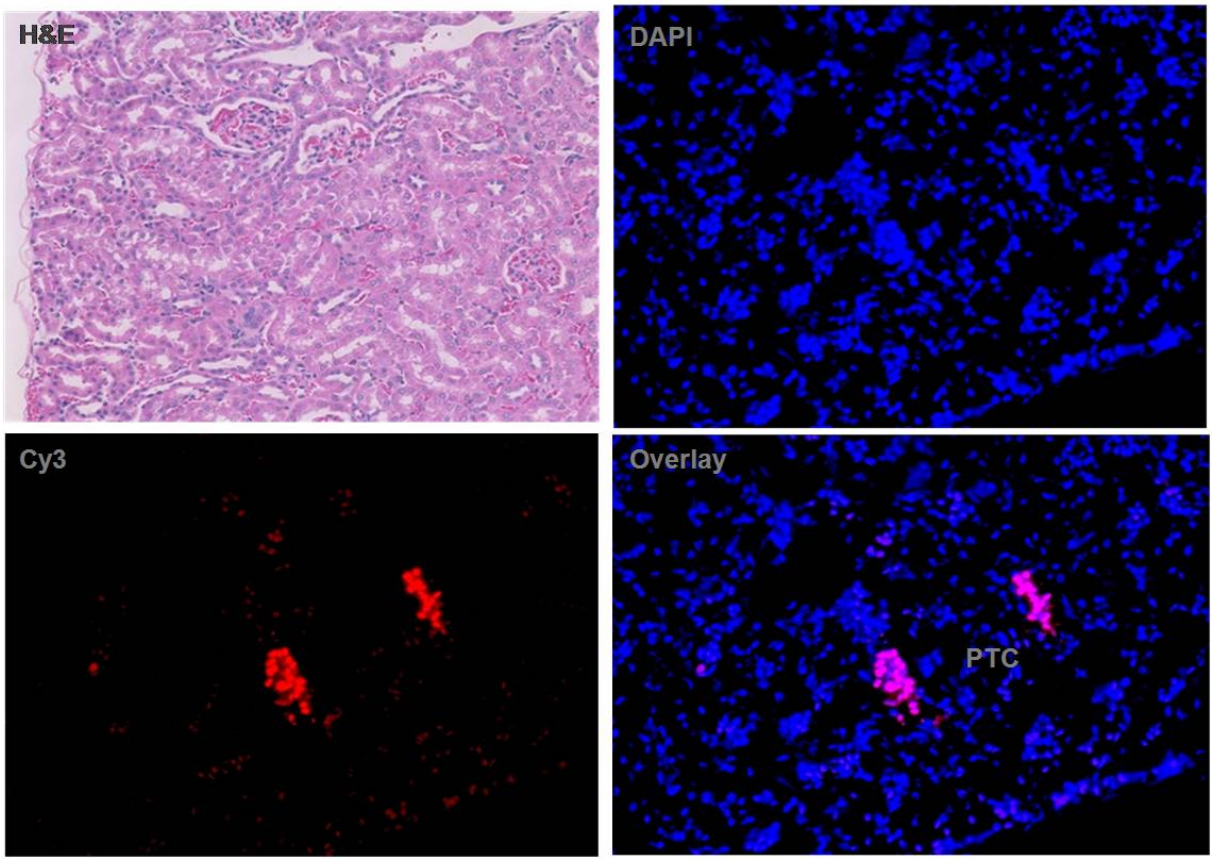

Fig. 11: High accumulation of platinum adducts in the DNA of particular cell types in the kidney and the cochlea of cisplatin-treated mice. 24 h after a single dose of cisplatin (10 mg/kg) Pt-GG intrastrand crosslinks in DNA were visualized by immunostaining of frozen sections with the adduct-specific antibody R-C18 (red) and counterstaining of the nuclear DNA with DAPI (blue). For morphological orientation serial sections of both organs were stained with hematoxyline and eosin (H&E; upper left micrographs). (A) Cochlea with high adduct levels in marginal cells (MC) in the stria vascularis (SV) and hair cells (HC) in the organ of Corti (OC). (B) Kidney with high adducts levels in proximal tubule cells (PTC). Magnification: 20x.

Micrographs of the organ of Corti at higher magnification (60x) clearly demonstrated high levels of DNA platination exclusively in the outer hair cells (OHC) but not in inner hair cells (IHC) or other cell types of organ of Corti (Fig.12 A). This observation is in line with structural damage in OHCs as seen in electron microscopy studies in cochleae from cisplatin treated rats (Hamers *et al.*, 2003).

More detailed analysis of the stria vascularis revealed a similar situation. High adduct levels were visible in this structure only in the outer cell layer representing the marginal cells, but not in the neighboring intermediate or basal cells (Fig. 12 B).

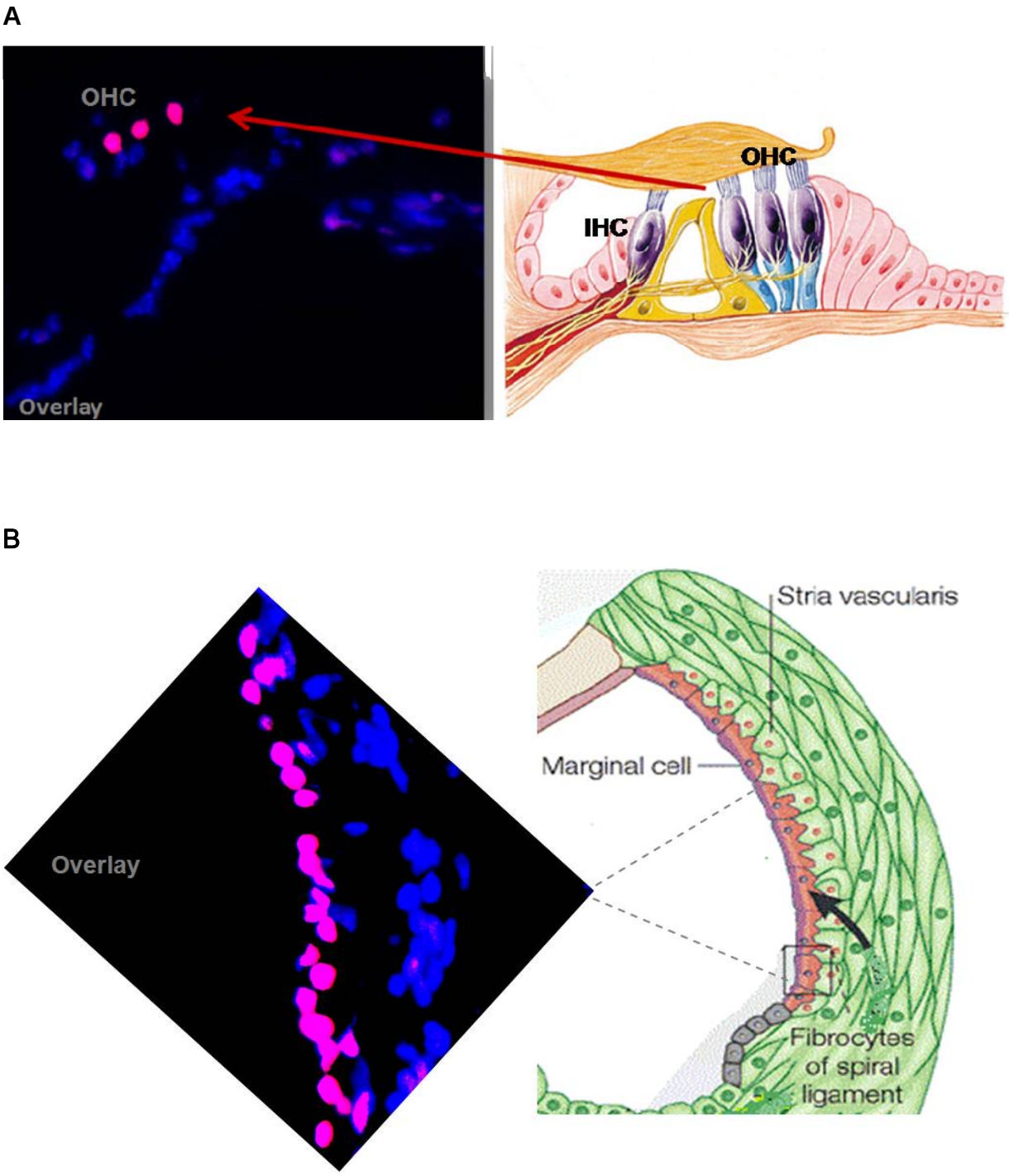

Fig. 12: Localization of Pt-GG adducts in cells of the inner ear. 24 h after a single dose of cisplatin (10 mg/kg) Pt-GG intrastrand crosslinks in DNA were visualized by immunostaining of frozen sections with the adduct-specific antibody (red) and counterstaining of the nuclear DNA with DAPI (blue). (A) Organ of Corti. Left: the nuclear DNA of the three outer hair cells is massively platinated (Magnification 60x). Right: schematic drawing of the organ of Corti with outer (OHC) and inner hair cells (IHC) (picture from Oxford Illustrated Science Encyclopedia, modified). (B) Detailed view of the stria vascularis. Left: stria vascularis with highly platinated marginal cells (magnification: 60x). Right: schematic drawing of the stria vascularis with localization of marginal, intermediate and basal cells and fibrocytes of the spiral ligament (Jentsch, 2000).

3.1.2 Quantification of Pt-GG adducts in the nuclei of cochlear cells

For the numerical determination of the DNA platination levels in the nuclei of individual cells, a Zeiss Axioplan fluorescence microscope coupled to a quantitative multichannel digital image analysis system (ACAS 2) was applied. This system automatically localizes single nucleus areas due to the DAPI-derived signals from DNA and integrates the intensities of the antibody-derived Cy3 signals for the same pixels (Liedert *et al.*, 2006). Relative adduct levels in the nuclear DNA of individual cells were calculated by normalizing antibody-derived fluorescence signals to the corresponding DNA content of the same cell (in order to correct for a possible DNA loss) and were expressed as arbitrary fluorescence units (AFUs). The AFU values were used as quantitative parameters and mean values (± SD) from 50 or 100 cells from the organ of Corti or the stria vascularis, respectively, were calculated to describe the relative adduct levels in particular cell types.

Mice were i.p. injected with 10 mg/kg of cisplatin and euthanized after 24 h or 48 h. Cryosections of cochlea and kidney tissues were stained with anti Pt-GG antibody and signals were measured from single nuclei of different types of cells. When analyzing the immunostained cochlea sections, four types of cells were measured separately: (1) outer hair cells, (2) surrounding cells (supporting cells of the organ of Corti), (3) marginal cells of the stria vascularis and (4) adjacent cells (intermediate and basal cells of the stria vascularis) (Fig. 13).

The levels of Pt-GG adducts in the highly platinated cells and directly neighboring cells of the cochlea were dramatically different being 11-fold higher in OHC vs. adjacent cells in the organ of Corti (13.26 AFUs vs. 1.19 AFUs), and 5-fold higher in the marginal cells as compared to the other cell types in the stria vascularis (9,85 AFUs vs. 2.08 AFUs).

In the kidney, proximal tubule cells, distal tubule cells and cells of the glomerulus were measured in the same way. The platination level in distal tubular cells was twice as high as that in glomerulus cells (2.61 AFUs vs. 0.97 AFUs) whereas the proximal tubular cells showed the highest level of platination (7-fold higher than distal tubular cells: (18.97 AFUs vs. 2.61 AFUs).

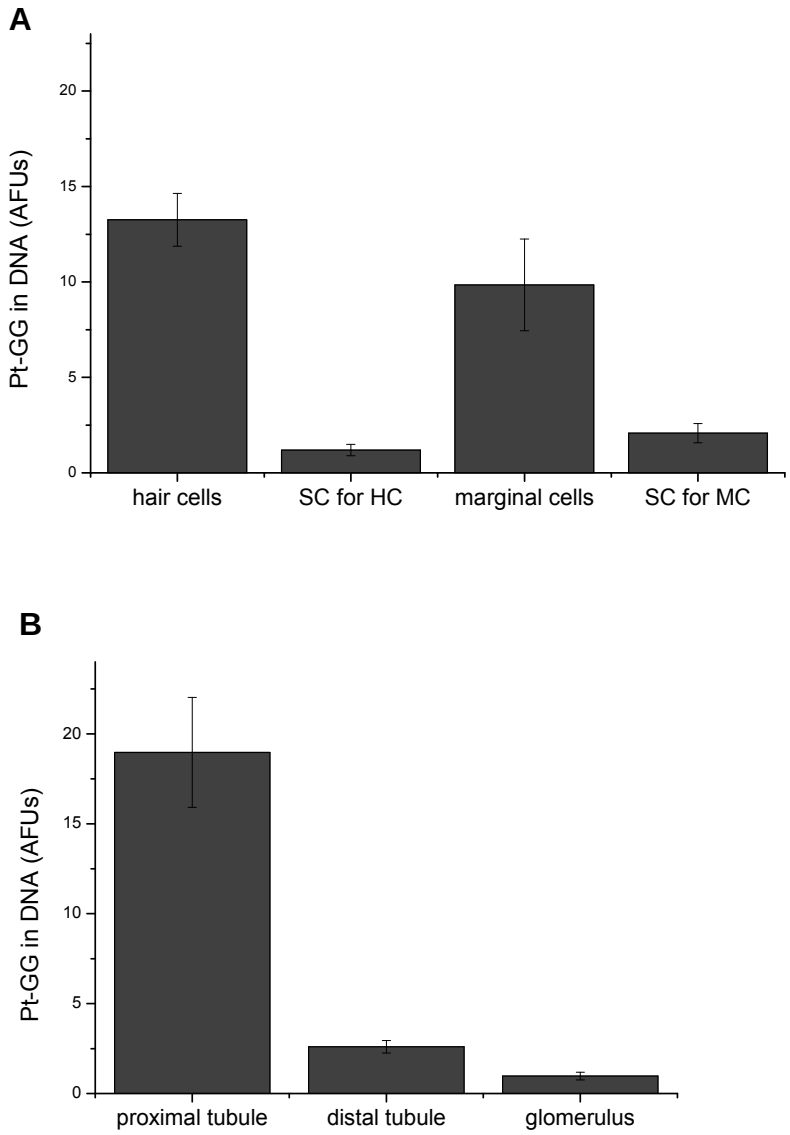

Fig. 13: Accumulation of platinum-DNA adducts in different cell types of the cochlea and the kidney cortex 24 h after cisplatin treatment. (A) Relative levels of Pt-GG adducts in outer hair cells (HC) and in marginal cells (MC) as compared to surrounding cells (SC). (B) Distribution of Pt-GG adducts in the kidney cortex: Comparison between cells of the proximal or distal tubules and cells of the glomeruli. The columns represent mean values (+/- SD) from 100 measured cells (for HC from 50 cells).

3.1.3 Different adduct levels in basal, middle and apical turns of the cochlea

A number of previous reports had described differences in the extent of morphological damage between basal and apical turns of the cochlea in the stria vascularis marginal cells of cisplatin-treated rats (Cardinaal *et al.*, 2004; van Ruijven *et al.*, 2005; Laurell *et al.*, 2007). To test whether such observations are correlated to differences in DNA platination, ICA analyses were performed with cryosections from all four turns of the cochlea from a mouse 24 h after cisplatin treatment. The quantitative measurement supported the structural observations by showing a decrease in marginal cell adduct levels from the basal to the apical turn (Fig. 14). A similar trend, although at nearly 10-fold lower levels, was also observed for the non-marginal cells of the stria vascularis. This finding corresponds to the clinical observations that cisplatin-induced hearing loss begins with high frequencies, which are recorded predominantly in the basal turn of the cochlea (Sluyter, 2003; Rybak and Ramkumar, 2007). The pharmacokinetic background for the unequal distribution of platinum-DNA adducts between upper and lower turns of the cochlea are not known.

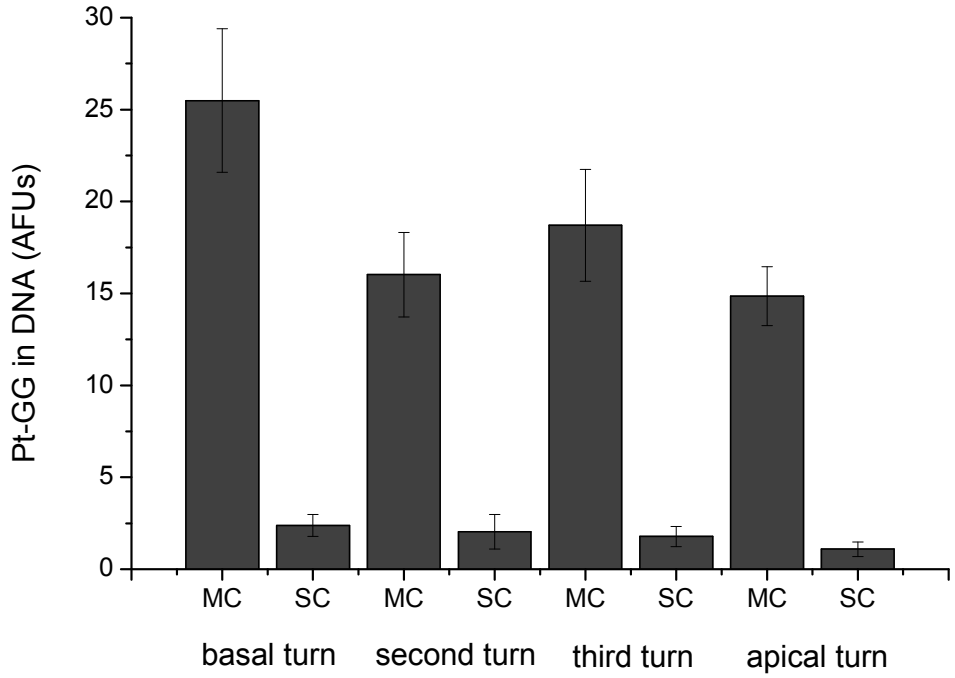

Fig. 14: Levels of Pt-GG adducts in cells of the stria vascularis from different turns of the cochlea. Cochleae were dissected from mice 24 h after a single dose of cisplatin (10 mg/kg) and serial cryosections were measured for DNA adduct levels in different cell types by ICA analysis. AFU values were significantly higher in marginal cells (MC) of the basal turn as compared to the apical turn.

A similar tendency was found for other cells of the stria vascularis (SC: intermediate and basal cells), however, on a 10-fold lower level of DNA platination.

3.2 The exploration of mechanisms underlying the excessive DNA platination in hair, marginal and proximal tubule cells

The dramatic accumulation of platinum adducts in particular cell types in the cochlea and the kidney of cisplatin-treated mice raised the question of the mechanisms underlying that observation. Basically, all the functions discussed for drug susceptibility of tumor cells (i.e. accelerated cellular uptake or decreased export of the drug, abrogation of the intracellular deactivation, or the incapability to repair adducts once formed in the DNA) might also be involved in physiological cells, and could all lead to the observed differential accumulation of platinum adducts.

3.2.1 Formation and repair of Pt-GG adducts in the DNA of different inner ear cells

It had been shown that Pt-GG intrastrand cross links can be removed efficiently from the nuclear DNA of cells in various mouse tissues by the nucleotide excision repair pathway (Dzagnidze *et al.*, 2007). Therefore, it was first analyzed whether a deficiency in DNA repair might be responsible for the high adduct accumulation in OHCs or marginal cells of the cochlea. C57BL/6 mice were treated with a single dose of cisplatin (12.5 mg/kg) and three animals were sacrificed at each of the different time points (2, 16, 48 and 72 h) after injection. Adduct levels were measured by ICA in three cell types of the cochlea, namely outer hair cells, marginal cells and cells of Reissner's membrane (Fig. 15). The latter only showed weak immunofluorescence signals at all time points after cisplatin treatment, and were chosen as an example for low adducted cochlear cells. The OHCs and the marginal cells depicted high levels of adduct formation after cisplatin treatment and were designated as target cells.

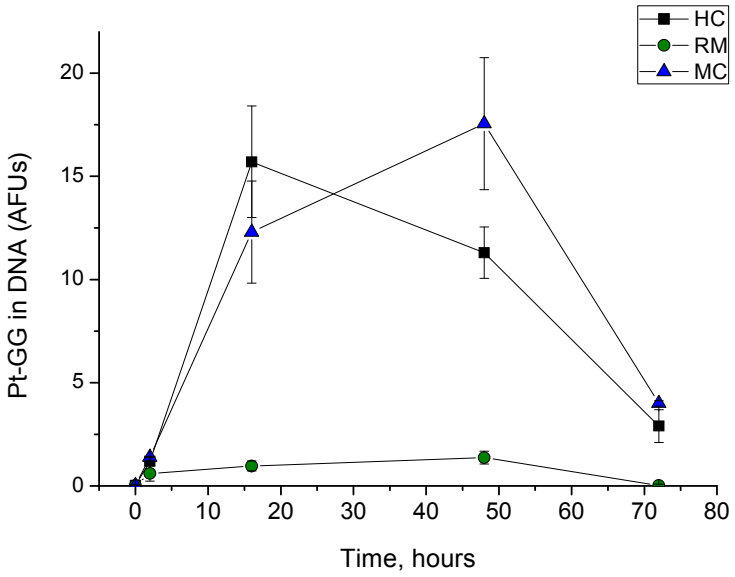

Fig. 15: Kinetics of Pt-GG adduct formation and repair in different cell types of the cochlea. Mice were treated with a single dose of cisplatin (12.5 mg/kg; i.p.) and were sacrificed at different time points. DNA adduct levels in outer hair cells (HC), in marginal cells (MC) and in cells of Reissner's membrane (RM) were measured by ICA analysis The data represent mean values (+/- SD) of >50 individual nuclei per cell type and from 2 independent experiments.

DNA platination was detectible in all three cell types already 2 hours after cisplatin administration (Fig. 15). The Pt-GG levels peaked after 16 hours in OHCs and after 48 hours in marginal and RM cells. They returned to comparatively low values in all three cell types 72 hours after treatment. As expected from the previous experiments, the adduct levels of the RM cells were only about 10 % of those of the two other cell types. The repair kinetics, however, clearly demonstrated that the excessive DNA platination in both OHC and marginal cells is not caused by their inability to repair such lesions.

This observation strongly implied that factors other than repair deficiency are responsible for the exorbitant DNA damage in the two target cell types. As mentioned above, proximal tubule cells of the kidney have physiological similarities with cochlear hair and marginal cells, namely their capacity of intensive unidirectional ion transport. Thus, in the next step we aimed to identify membrane transporters which are expressed in the highly adducted cells in the kidney and in the inner ear, but not in the surrounding cells, as a possible cause for an aberrant active uptake of cisplatin.

3.2.2 Localization of organic cation transporters in the cochlea

Based on experiments with cell culture systems, various types of membrane transporters have been suggested to be involved in the import and export of cisplatin, thereby modulating the cellular sensitivity to the drug (Ishida *et al.,* 2002; Samimi *et al.,* 2003; Yonesawa *et al.,* 2005; Burger *et al.,* 2010). One of these transporters is the organic cation transporter 2 (OCT2), which is highly expressed in the kidney cortex and is assumed to represent a specific marker for proximal tubule cells (Ciarimboli *et al.*, 2005). Therefore, it was tried to localize OCT2 and other members of the same transporter family in the murine inner ear. For this, cochleae were dissected from untreated 12-weeks old male C57BL/6 mice, fixed, and decalcified as described in Material and Methods (see 2.2.2). Eight micron thick tissue sections were prepared and immunostained for six different members of the OCT family, namely for OCT1, OCT2, OCT3, OCTN1, OCTN2 and OCTN3, using specific antibodies. No signals were detectable after staining for OCT1, OCTN1 or OCTN3 (data not shown). In contrast, OCT2 and OCT3 were positively stained in intermediate and basal cells of the stria vascularis, in supporting cells of the organ of Corti (cells surrounding the outer hair cells) and even in inner hair cells (Fig. 16). However, no signals were visible in the actual target cells of cisplatin, the marginal cells and the outer hair cells. From these findings it can be concluded that none of the six OCT family members tested here, is likely to be responsible for an aberrant import of cisplatin into the critical target cells.

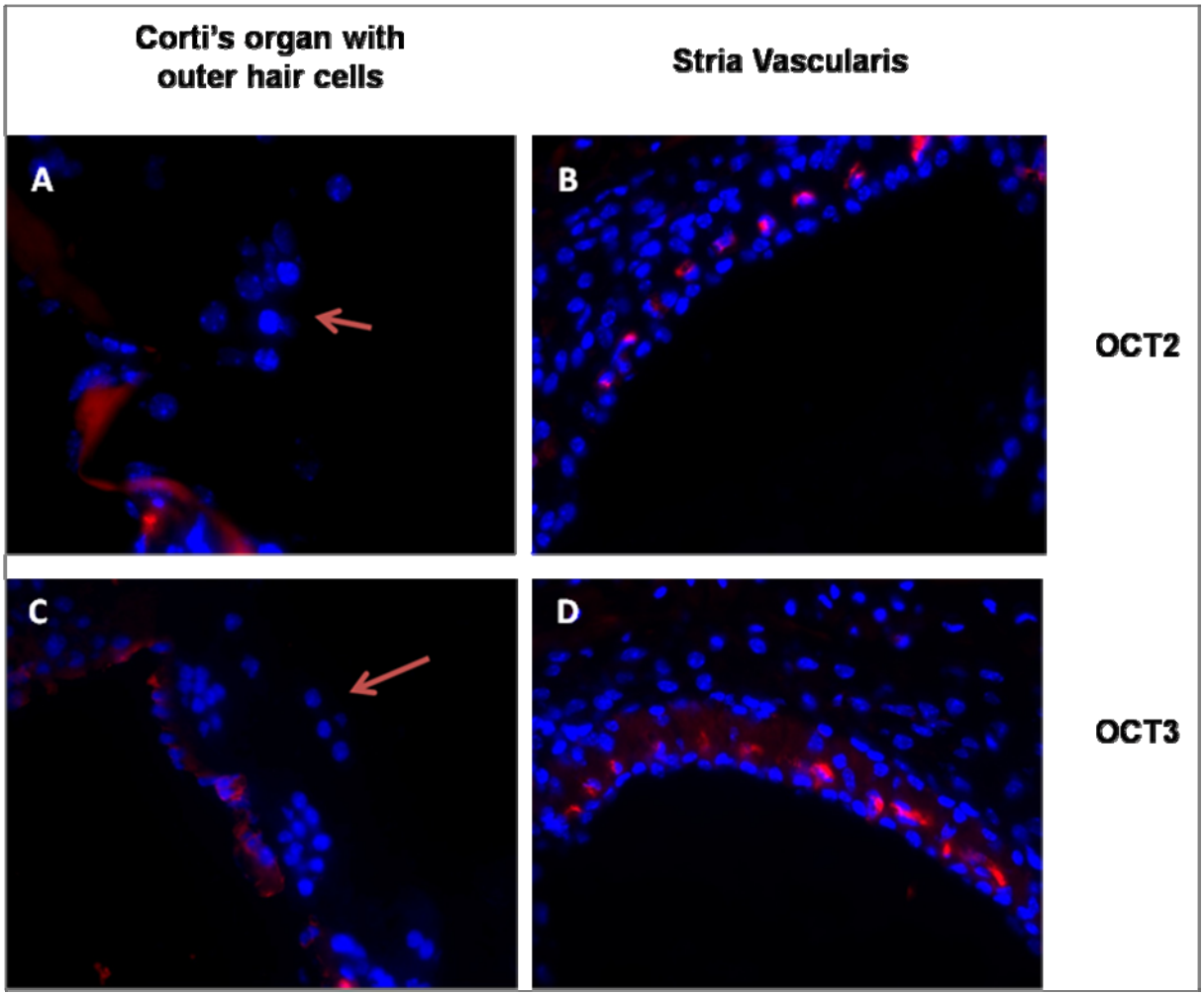

Fig. 16: Immunohistochemical localization of organic cation transporters in the organ of Corti and the stria vascularis of the cochlea. Cryosections of formalin-fixed cochleae were immunostained (red) with antibodies for the membrane transporters OCT2 (A, B) and OCT3 (C, D), and were counterstained for DNA with DAPI (blue). Arrows indicate the position of the outer hair cells in the organ of Corti. B and D :Cells of the stria vascularis with OCT2 and OCT3 located in the area of the intermediate cells. (Magnification: A: 60x; B, C, D: 40x).

3.3 Augmented levels of platinum-DNA adducts in cochlear cells of NER-deficient mice correlate with a higher degree of hearing loss

It is generally accepted that the antineoplastic effect of platinum anticancer drugs is mediated via the formation of adducts in the nuclear DNA of tumor cells and the subsequent induction of apoptotic pathways. For drug-induced damage and functional loss in physiological cells, however, this route of action is by far less well established and a matter of constant controversial discussion in the literature. The

neurotoxic effect of cisplatin was correlated to structural damage of the mitochondria in neurons and satellite cells of the dorsal root ganglia (Bottone *et al.,* 2008; Cavaletti, 2008). To investigate whether the accumulation of DNA platination products are really causing the ototoxicity in our *in vivo* model, two isogenic mouse strains (C57BL/6 NER wild type and XPA -/-) were compared which differ solely in their ability to repair cisplatin intrastrand adducts in their genomic DNA. While the wild type mice have a fully functional NER system, a homozygous deficiency for the xeroderma pigmentosum (XP) A protein, a major component of the NER pathway, has been shown to reduce (but not to completely abrogate) the repair capacity for Pt-GG intrastrand cross links in the DNA of various tissues (Liedert *et al.*, 2006; Dzagnidze *et al.*, 2007).

3.3.1 Increased cisplatin ototoxicity in XPA knockout mice

As a functional test for the hearing capability of mice we employed the method of brainstem auditory evoked response (BAER). This assay is based on the measurement of neurosensorial responses in the central auditory pathways of the brainstem after scaled acoustic stimulation by a sound generator. For this, mice were deeply anesthetized and electrodes were placed on the scalp and on each earlobe. A clicking sound was delivered via small earphones and the evoked waves of neuron activity were recorded.

XPA -/- mice and their wild type littermates were treated with cisplatin at a low cumulative dose of 3.5 mg/kg within two weeks (1^{st} week: 1 mg/kg; 2^{nd} week: 2.5 mg/kg). Control groups of both strains received PBS injections instead. The hearing capability of animals in all four experimental groups was determined by BAER measurement 48 hours after the last treatment. The treated and the control groups of the repair-proficient mice did not exhibit any sign of cisplatin ototoxicity (Fig. 17 A). The control group of the repair-deficient XPA-/- mice exhibited the same hearing threshold, indicating that the status of the NER system itself did not result in any hearing problems. In contrast, cisplatin treated NER-deficient XPA-/- mice exhibited a reduction of their hearing capability of nearly 50 %, indicating that unrepaired DNA adducts may indeed represent the initial molecular trigger for the functional hearing loss.

3.3.2 Higher accumulation of DNA adducts in cochlear cells of XPA-deficient mice

To further substantiate this indication, the mice of all four experimental groups were sacrificed immediately after the BAER test and cochleae were taken for adduct-specific immunostaining with anti-Pt-GG monoclonal antibodies. The ICA revealed about 2.7-fold higher levels of DNA damage in the marginal cells of cisplatin-treated XPA-/- mice compared to their wild type littermates (Fig. 17 B). Thus, the platinum adduct levels correlated well with the functional loss in the hearing system.

3.4 A strategy for the prevention of cisplatin-induced hearing loss

Having demonstrated the role of unrepaired cisplatin-DNA damage in hearing loss and its excessive formation rates in target cells of the affected tissues, the next logical step was to investigate preventive strategies for the severe side effects of cisplatin treatment, such as ototoxicity. Assuming that aberrant import of the drug by physiological membrane transporters gives rise to the high DNA platination in marginal and outer hair cells, the obvious strategy was to prevent the damage by trying to transiently block those transporters. As the molecular characterization of the responsible membrane pump by *in situ* immunostaining was not obvious, a functional *in vivo* screening was performed in the mouse model as an alternative strategy for the identification of possible pharmacological inhibitors.

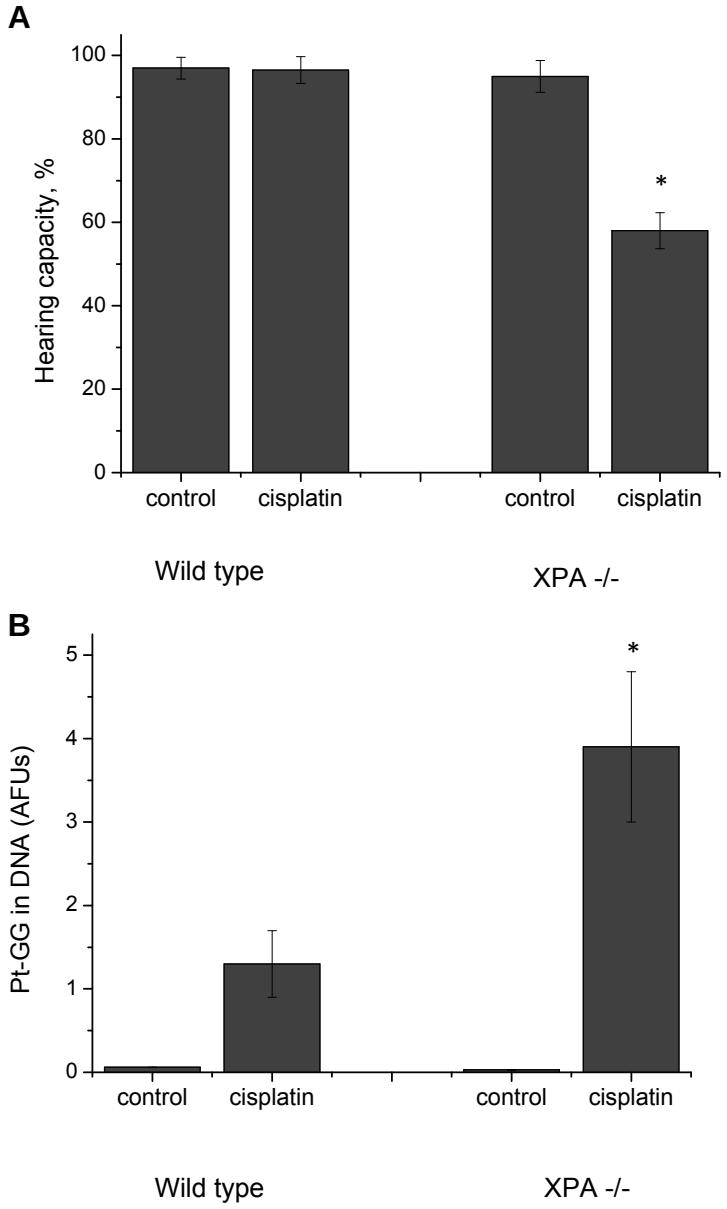

Fig. 17: Mice with reduced DNA repair capacity are more prone to cisplatin-induced ototoxicity and accumulate higher levels of Pt-GG adducts in the DNA of cochlear target cells. C57BL/6 (wild type) mice and syngenic DNA repair-deficient (XPA-/-) mice were repetitively treated with low doses of cisplatin (cumulated dose: 3.5 mg/kg) and the hearing capability was measured 24 h after the last dose by the BAER test in comparison to untreated controls. (A) The columns represent means (+/- SD) of three consecutive measurements per animal and of 5 mice per treatment group. The hearing capability was significantly reduced by 45 % in the group of cisplatin-treated XPA-/- mice whereas no effects were observed in untreated XPA-/- mice or in wild type mice after cisplatin exposure. (B) Levels of accumulated DNA adducts in the inner ear. All mice in the experiment were sacrificed immediately after the BAER test and cryosections of cochlea were analyzed for Pt-GG adduct levels by ICA analysis. After equal doses of cisplatin, inner ear cisplatin target cells of XPA -/- mice depicted more than 3 times higher adduct levels than those of the wild type littermates. * indicates $P \leq 0.001$ vs. wild-type.

3.4.1 Screening for cisplatin uptake inhibitors

According to reports on cisplatin transporters in various cell lines (Ciarimboli *et al.,* 2005; Müller *et al.,* 2005) a group of nine small molecules was chosen as candidate compounds for an *in vivo* screening for cisplatin uptake inhibitors (Fig. 18). Among them was cimetidine as a well known inhibitor of the OCT2 cation transporter. In a first set of experiments, four compounds were tested, namely quinine, butylscopolamine, diphenhydramine and ranitidine. The mice were separated into two groups for pretreatment with low or high doses of the test compounds. One hour before the treatment with cisplatin (10 mg/kg) the high dose group received i.p. injections of either quinine (100 mg/kg), ranitidine (100 mg/kg), diphenhydramine (60 mg/kg) or butylscopolamine (20 mg/kg). The low dose group received half the dose of the high dose group (50, 50, 30 or 10 mg/kg, respectively). As controls, two mice were treated with PBS instead of inhibitor prior to cisplatin (positive control) and two mice were treated with PBS only (negative control). All mice were sacrificed 24 hours after cisplatin treatment. Cochleae and kidneys were dissected for immunostaining and ICA analyses of Pt-GG adduct levels in specific cell types (Fig. 19).

In tissue sections from mice pretreated with quinine or butylscopolamine no inhibition of DNA platination was observed, independent of the dosing, in either of the three target cell types (renal tubulus epithelium cells, cochlear marginal and outer hair cells). In contrast, high dose treatment with ranitidine had a slightly protective effect (15 – 20 % reduction of adduct levels) in all three cell types, whereas the lower dose provided no protection. Pretreating the mice with diphenhydramine provided a dose-dependent and by far the strongest shielding from DNA damage, ranging from 75 % in proximal tubule cells over 70 % in cochlear marginal cells to about 50 % in outer hair cells at the high dose of 60 mg/kg (Fig. 19). No significant inhibition by any of the four inhibitors was observed in the low-adduct “non-target” cells of Reissner’s membrane of the cochlea (Fig. 19).

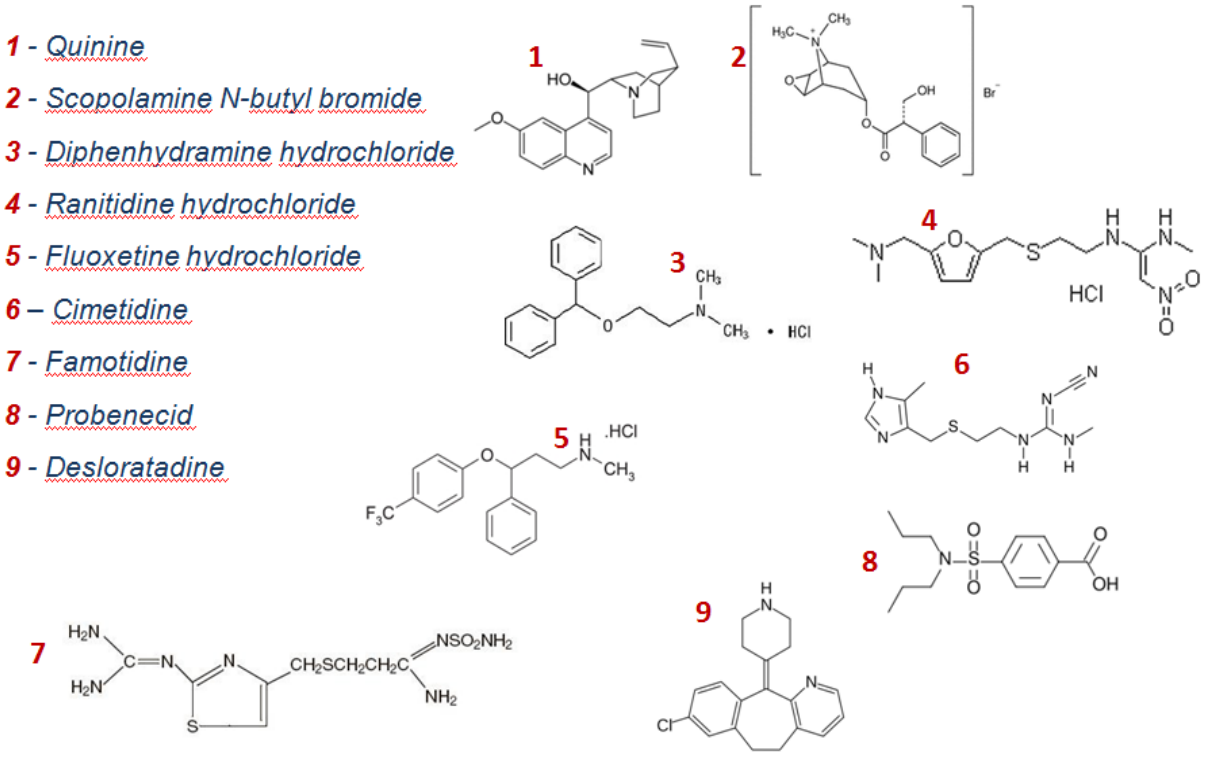

Fig. 18: Small molecules investigated for their applicability as import inhibitors for cisplatin *in vivo*.

Having identified diphenhydramine (DIPH) as a potent pharmacological inhibitor of the excessive DNA platination in critical renal and cochlear cells, it was of interest to pinpoint the specific functions that might be affected by the compound. DIPH has been shown to have a rather broad spectrum of physiological effects (Garnett, 1986; Harris, 2008). Therefore, we intended to use a panel of other small molecules which might mimic specific effects of DIPH in our mouse model. In the first instance, DIPH was characterized for its antihistaminic activity by blocking the pertinent H2 receptors. Therefore, we tested two other H2 receptor antagonists, cimetidine and famotidine, in addition to ranitidine (Fig. 18 and 20), as well as desloratadine as a highly specific H1 antagonist. Furthermore, we included cimetidine and famoditine because of their known activity as OCT2 inhibitors, fluoxetine as a serotonin re-uptake inhibitor, and butylscopolamine, which was described to be an anticholinergic agent and a muscarinic receptor antagonist. All these functions have also been associated with the pharmacologic activity of DIPH. Finally, probenecid was included in these experiments as a presumed inhibitor of members of the organic anion

transporter (OAT) family. All these compounds were applied separately to two mice at concentrations representing half of the LD50 dose one hour before cisplatin treatment. Mice were sacrificed 24 hours after cisplatin treatment and adduct levels in cochleae and kidneys were determined as above**.** No significant inhibitory effects on the DNA platination in the target cells were detected for any of the compounds (Fig. 20).

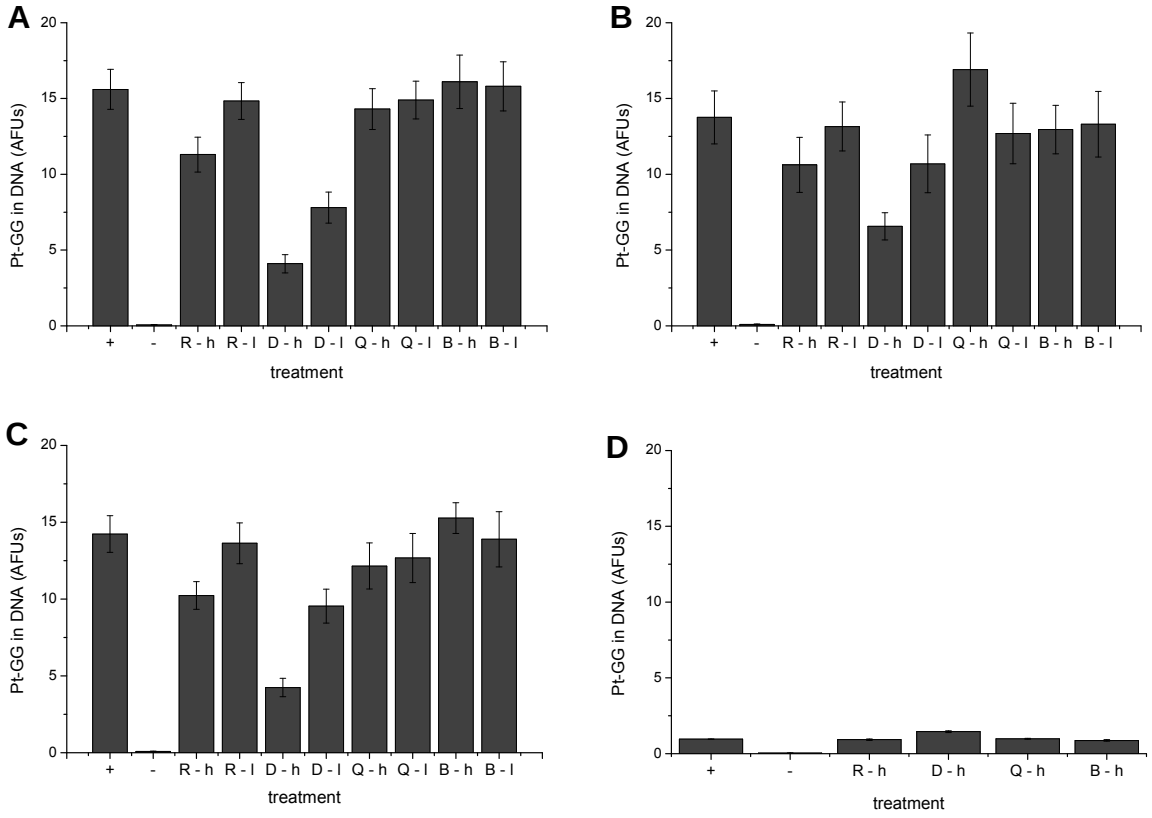

Fig. 19: Accumulation of the Pt-GG adducts in cells of the kidney and the inner ear of cisplatin-treated mice with co-administration of transport inhibitors. Potential inhibitors were i.p.-injected at two different doses 1 h before cisplatin treatment (10 mg/kg). Mice were sacrificed 24 h after cisplatin treatment and Pt-GG adducts were measured in the DNA of target and non-target cells by ICA analysis. (A) Proximal tubule cells of the kidney. (B) Outer hair cells of the cochlea. (C) Stria vascularis marginal cells of the cochlea. (D) Cells of Reissner's membrane. (+): cisplatin; (-): PBS treated control; R: Ranitidine, D: Diphenhydramine; Q: Quinine; B: Butylscopolamine; h: high dose; l: low dose.

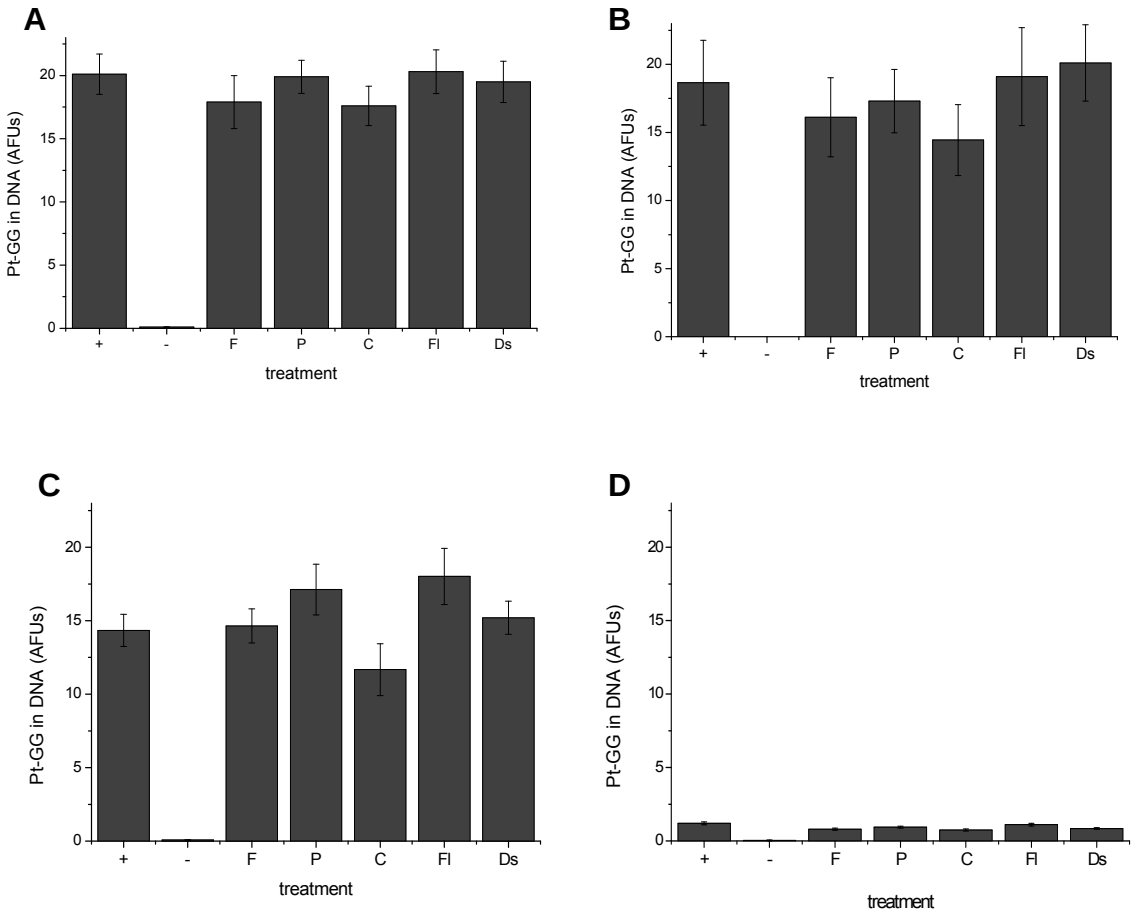

Fig. 20: A**ccumulation of the Pt-GG adducts in cells of kidney and inner ear of cisplatin-treated mice with co-administration of transport inhibitors.** Potential inhibitors were i.p.-injected at the maximum tolerated dose 1 h before cisplatin treatment (10 mg/kg). Mice were sacrificed 24 h after cisplatin treatment and Pt-GG adducts were measured in the DNA of target and non-target cells by ICA analysis. (A) Proximal tubule cells of the kidney. (B) Outer hair cells of the cochlea. (C) Stria vascularis marginal cells of the cochlea. (D) Cells of Reissner's membrane. (+): cisplatin; (-): PBS-treated control; F: Famotidine (20 mg/kg); P: Probenecis (150 mg/kg); C: Cimetidine (15 mg/kg); Fl: Fluoxetine (30 mg/kg); Ds: Desloratadine (240 mg/kg, oral). For none of the compounds a significant reduction in DNA adduct levels was observed in comparison to the cisplatin alone treatment.

3.4.2 DIPH reduces the DNA platination in cochlear marginal cells and in kidney cortex cells in a dose-dependent manner

In the first set of experiments the applied doses of DIPH to reduce the adduct formation in the target cells were corresponding to 50 % and 25 % of the LD50 dose for mice. Therefore, it was tested next whether the inhibitory effect of DIPH is dose-dependent and whether it is possible to reduce the dose while maintaining the preventive activity on adduct formation. For this, mice were pre-treated by i.p.

injections with DIPH at different doses between 0 and 57 mg/kg (two mice per group) 30 minutes prior to a single dose of cisplatin (10 mg/kg). The ICA for Pt-GG adducts in kidney and cochlear cells revealed a dose-dependent inhibition of the adduct accumulation in proximal tubule cells and in marginal cells (Fig. 21). No significant alterations were observed in the low-platinated distal tubule cells of the kidney and in the basal and intermediate cells of the stria vascularis. This shows that the inhibitor has a specific effect on proximal tubule cells and marginal cells but has no effect on the surrounding cells (such as distal tubule cells; Fig. 21 B).

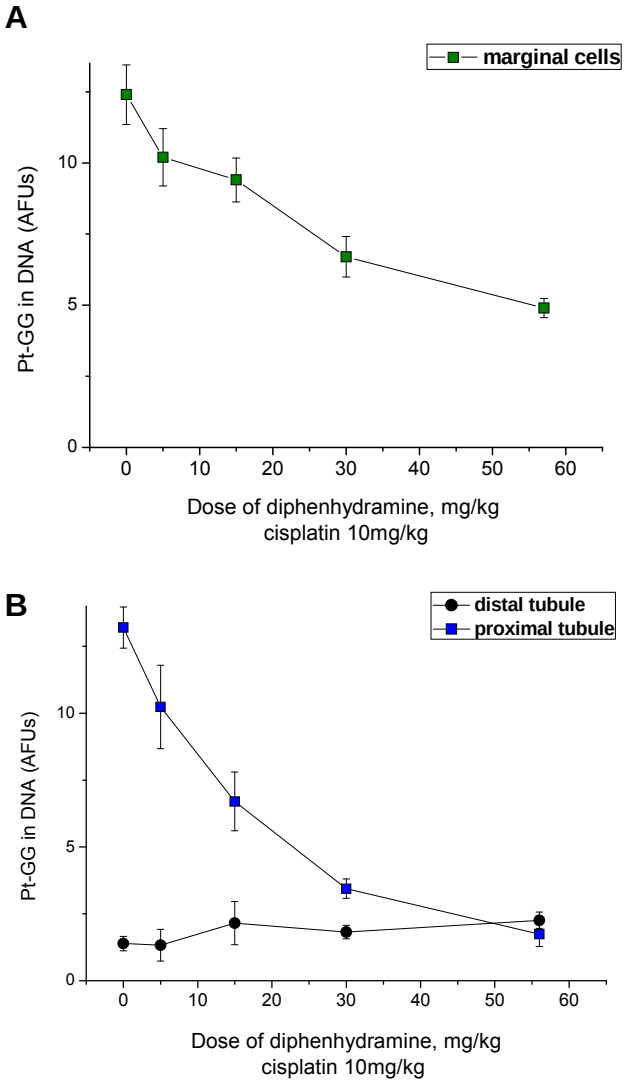

Fig. 21: Dose-dependent effect of DIPH on adducts accumulation in different cell types. Mice were treated with cisplatin alone (0) or in combination with different doses of DIPH (5, 15, 30, 57 mg/kg), sacrificed 24 h later and the DNA adduct levels were measured in kidney and cochlear cells by ICA analysis. (A) Marginal cells of the inner ear (green squares). (B) Proximal (blue squares) and distal tubules (black circles) of the kidney.

3.4.3 No interference of DIPH with the repair capacity for cisplatin-DNA adducts in cochlear target cells

As shown above the pre-treatment with DIPH prior to cisplatin injections leads to lower levels of DNA adduct accumulation in the target cells. This could be caused by reduced intracellular drug concentrations, or alternatively, by augmented removal of those lesions from the genomic DNA of the target cells. To elucidate a possible interaction of DIPH with the DNA repair machinery, we functionally analyzed its efficiency by measuring adduct kinetics. Mice were pretreated with DIPH (57 mg/kg) and 30 minutes later with a single dose of cisplatin (12.5 mg/kg). Three mice per time point were sacrificed at 2, 16, 48 and 72 hours after cisplatin treatment and cochleae were measured for Pt-GG adduct levels by ICA (Fig. 22). The kinetics revealed drastically decreased DNA platination in marginal and outer ear cells in DIPH pre-treated animals as compared to the corresponding cisplatin alone group at all time points, but no obvious differences in their capability to repair the damage.

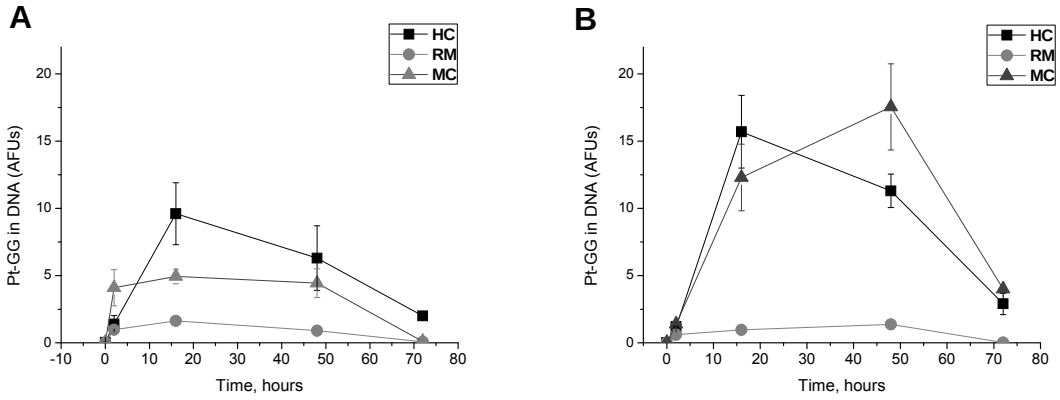

Fig. 22: Influence of DIPH co-application on the formation and repair kinetics of Pt-GG adducts in the DNA of different cochlear cell types of cisplatin-treated mice Animals were pre-treated or not with DIPH (57 mg/kg) and were i.p. injected 30 minutes later with cisplatin (12.5 mg/kg). Each two mice were sacrificed at 2, 16, 48, or 72 hours after cisplatin and Pt-GG adduct levels in the DNA of inner ear cells were determined by ICA analysis. (A) With DIPH. (B) Without DIPH. HC: outer hair cells; MC: marginal cells; RM: cells of Reissner's membrane.

3.4.4 DIPH does not lead to reduced DNA damage *in vitro*

When it was evident that renal proximal tubule cells as well as cochlear marginal and outer hair cells, share a unique mechanism to accumulate cisplatin and that DIPH can block this mechanism *in vivo*, the next step was to find an easier access to further characterize the transporter(s) involved in this process in more detail. For combining functional with molecular analyses, permanent cell lines established from the primary target cells would be very valuable tools. As no established lines from stria vascularis marginal cells were available, a functional analysis was done with an epithelium cell line (TKPTS) deduced from proximal tubules of normal mouse kidney tissue.

To investigate whether the protective effect of DIPH could be reproduced under *in vitro* conditions, TKPTS mouse kidney cells and, as a control, GM637 human skin fibroblasts were pre-incubated or not with DIPH (0.3 mM) and then treated with cisplatin in a dose-dependent manner. The accumulation of Pt-GG adducts in the nuclear DNA was analyzed at different time points by ICA analysis.

No inhibitory effects of DIPH on the formation of cisplatin-DNA adducts were observed in both cell lines at four hours after drug exposure (Fig. 23). A similar result was obtained when the mouse kidney cells were incubated with cisplatin for 12 or 24 hours (data not shown). Signs of apoptosis were visible in TKPTS cells when analyzed at 24 hours after cisplatin, independently whether they were pre-treated or not with DIPH (data not shown).

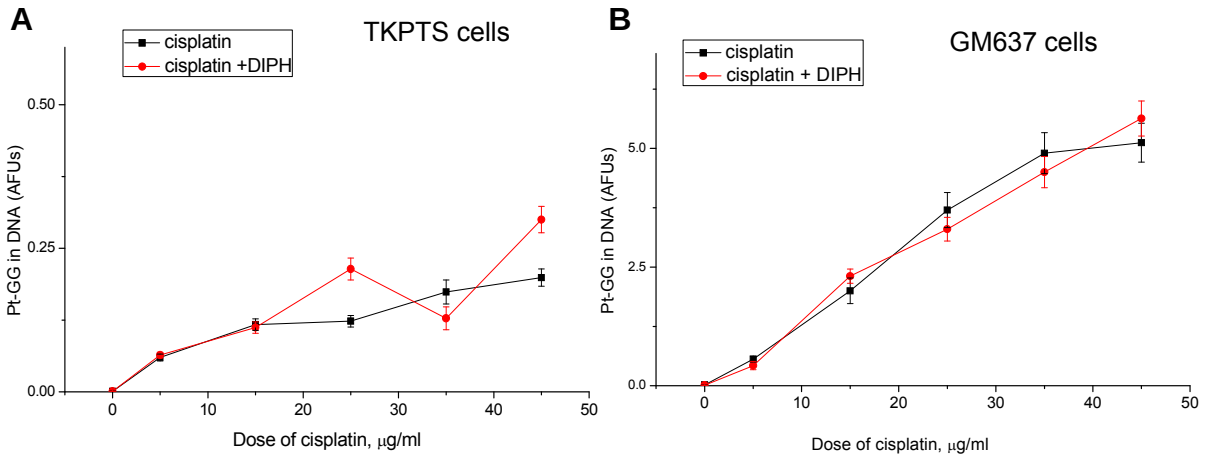

Fig. 23: Null effect of DIPH on the formation of Pt-GG adducts in the DNA of cisplatin-exposed murine proximal tubule cells and of human fibroblast cells *in vitro.* Cells of the lines TKPTS (established from renal proximal tubule of the mouse; A) and GM637 (human skin fibroblasts; B) were treated with different concentrations of cisplatin (black squares) or cisplatin plus DIPH (0.3 mM; 30 minutes before cisplatin). After 4 hours cells were trypsinized, placed on slides, stained for Pt-GG adducts and measured by ICA analysis.

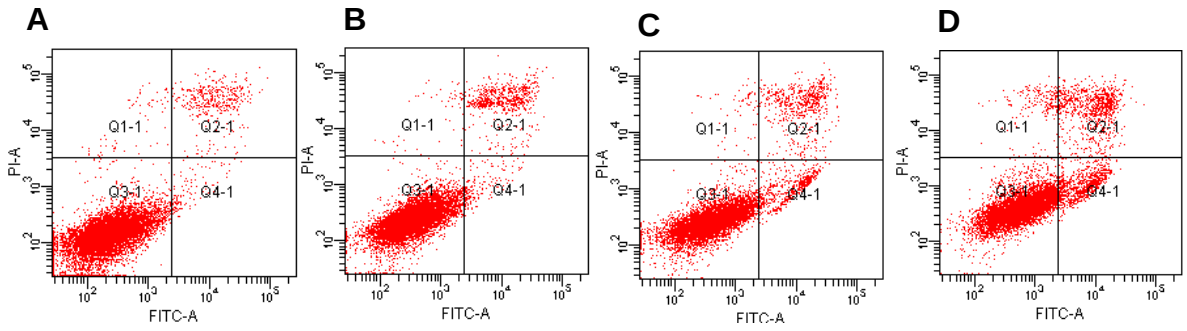

Fig 24: DIPH does not reduce the cytotoxic effect of cisplatin in human lung cancer cells *in vitro*. Human lung carcinoma cells were left untreated (A), treated with 0.3mM DIPH (B), 5 µg/ml cisplatin (C) or cisplatin plus DIPH (D) for 24 hours. The percentages of apoptotic and necrotic cells were measured 24 h later by Annexin V-FITC and propidium iodide (PI) staining and FACS analysis. Early apoptotic cells are plotted in Q4 (Annexin V-FITC positive) and late apoptotic or necrotic cells in Q2 (Annexin V-FITC and propidium iodide positive) and and viable cells (unstained, Q3). The fraction of apoptotic cells was significantly increased in cisplatin- (8 %; plot C) and cisplatin plus DIPH (11.2 %; plot D) treated cells as compared to the untreated control (2.3 %; plot A) and to cells exposed to DIPH alone (3 %; plot B) with no significant difference between the two cisplatin-treated cultures.

The results suggest that the mechanism leading to the excessive DNA platination in proximal tubule cells *in vivo* is not active in the TKPTS cell line. This may be due to the fact that these cells have lost the expression of putative transporter for cisplatin

uptake during the establishment of the permanent line from primary tubulus epithelium cells, or somehow have an altered their sensitivity to the inhibition by DIPH.

In an additional set of experiments, several human cancer cell lines established from tumors, which are usually treated with cisplatin (lung, bladder, testis) were treated with cisplatin alone or in combination with DIPH. Also here, inhibitory effects of DIPH were detected neither on the formation of DNA adducts (as measured by ICA) or on the induction of apoptosis (as measured by Annexin V staining and FACS analysis) (Fig.24 and data not shown).

3.5 Co-administration of DIPH with repetitive cisplatin treatments diminishes the functional hearing loss in mice

The next question asked was whether the DIPH-mediated protection of the cochlear target cells from excessive DNA platination also leads a reduction of the cisplatin-induced hearing loss. In the clinical setting the ototoxic effect of cisplatin chemotherapy is observed only after several treatment cycles. To mimic this situation in our mouse model, animals were treated every second day with comparably moderate doses of cisplatin (5 mg/kg). A subgroup of the animals was additionally injected with DIPH (57 mg/kg) 30 minutes before each dose of cisplatin. Both groups received additional i.p. injections with saline solution (500 µl) in order to protect the mice from kidney injury. As controls, two further groups of animals received either only the inhibitor (DIPH group) or saline solution (negative control). At different cumulative doses of cisplatin all mice were measured for their functional hearing capability using the BAER test. For this test, the mice were relaxed by complete anaesthesia, positioned on a reclining table and clicks with a substantial frequency in the 1-3 kHz range were administrated at increasing levels of sound pressure between 30 and 100 dB via adapted earphones. The neurosensoric waves along the central auditory pathway of the brainstem were measured by electrodes placed on the scalp and on each earlobe and were record as shown in Fig. 25. Like in the clinical BAER tests for humans, the hearing threshold was determined as the disappearance of wave V (Fig. 25 and Fig. 9). This value was converted into percentage of hearing capability as compared to the untreated controls (dB to %). The test was done for all

animals in this experiment also prior to treatment showing that they had a normal hearing capability. The mean value of the untreated mice was set as 100 %.

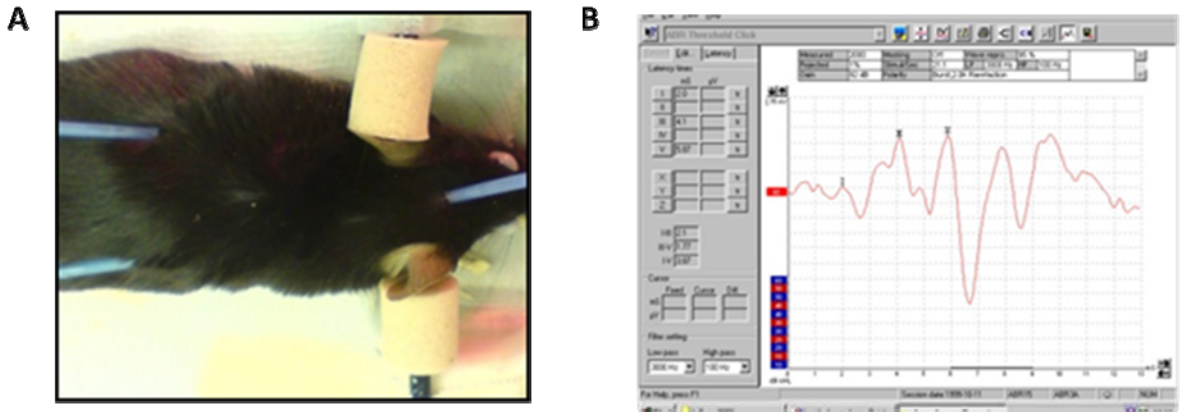

Fig. 25: The measurement of hearing capacity in mice. (A) BAER test adapted to mice. Three needle electrodes were applied to pick up neuroelectrical signals from the hearing transmittal pathway. (B) Typical neurographic curve as recorded from sound stimulated, untreated control mice by the BAER test system for one sound pressure range.

After reaching a cumulated cisplatin dose of 20 mg/kg, the BAER test was performed 24 h after the last treatment. Mice that received only cisplatin showed a reduction of their hearing capability to about 50 % of the controls (Fig. 26). In contrast, the same dose of cisplatin, but in combination with DIPH, induced a hearing loss of only 20 % (Fig.26). Mice of the control and the DIPH alone groups did not show any difference in their hearing ability throughout the experiment.

Another group of mice that received cisplatin in cumulated doses of 40 mg/kg plus DIPH still maintained a mean hearing capability of about 70 % of the untreated controls (Fig. 26). Importantly, all animals from the corresponding cisplatin-alone group displayed severe signs of acute toxicity before reaching that dose and had to be euthanized.

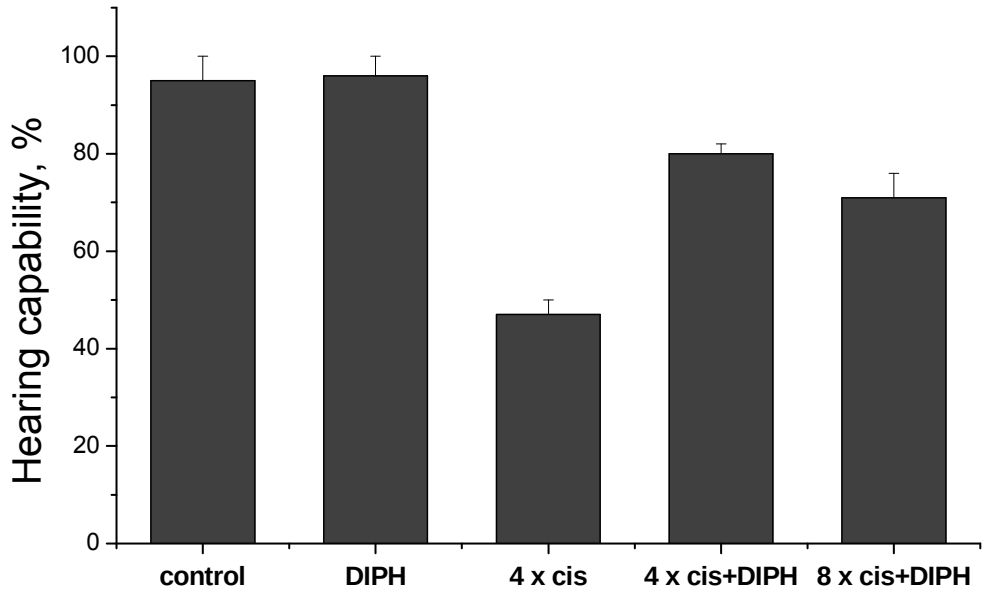

Fig. 26: Protective effect of DIPH on the hearing capability of cisplatin-treated mice. To induce functional loss in the hearing system mice were treated repetitively 4 times with cisplatin alone (5mg/kg every second day, cumulated dose: 20 mg/kg) or with concomitant injections of DIPH (57 mg/kg) 30 minutes before each dose of cisplatin. Additional groups were injected accordingly only with PBS or only with DIPH or were treated with cisplatin + DIPH eight times (cumulated dose of cisplatin: 40 mg/kg). All animals were measured for their hearing capability with the BAER test 24 h after the last dose of cisplatin was applied. The columns represent mean values (+/- SD) from five animals per treatment group and were calculated as percentage of the control group.

In all treatment groups of this experiment the mice were sacrificed immediately after the final BAER test and cochleae and kidneys were resected for the measurement of DNA platination by ICA analysis.

A comparison of adduct levels in the different treatment groups was performed to find out whether repetitive low dose application of cisplatin induced the same pattern of DNA platination in both tissues as the acute high dose application, and whether the reduced hearing loss in the cisplatin plus inhibitor group was associated with a lower adduct accumulation in the critical target cells under these conditions. Massive adduct accumulation was found in the target cells of the two investigated organs, kidney and inner ear, from mice of the cisplatin alone group. In contrast, by far less adducts were found in the pertinent cells of the cisplatin plus DIPH treatment group. In the kidney all cells of the cortex depicted similarly low adduct levels with no

protruding proximal tubules visible (Fig. 27). Similarly, in the marginal and hair cells of the cochlea much lower adduct accumulation was observed in animals co-treated with DIPH as compared to the cisplatin alone group (Fig. 28). This protective effect was observed in all turns of the cochlea and was more pronounced in the marginal than in the outer hair cells. The adduct levels in other cell types of the inner ear remained unchanged by DIPH.

Taken together, the results of this experiment strongly supported the notion that the excessive DNA damage in cochlear cells is the key trigger for the cisplatin-induced hearing loss and that an inhibitor-mediated reduction of that damage is a successful strategy to significantly prevent the functional loss. Noteworthy, the general health status of the mice in the cisplatin plus inhibitor group was better and weight loss was less severe than in the cisplatin alone group. A prolonged treatment of mice with DIPH alone up to eight applications had no obvious side effects.

As it was assumed that the protective effect of DIPH for the cochlea was mediated by blocking an ion transporter being relevant for the physiological function of the target cells, an additional experiment was done to verify whether a treatment with DIPH alone alters the hearing capability of the mice. For this, five animals measured for their basal auditory sensitivity with the BAER test were treated 24 h later with a single dose of DIPH (57 mg/kg), and were re-examined one hour later again by the BAER test. All mice depicted a slight reduction in their hearing capability from 100% down to 70%. When the BAER test was repeated 24 hours later all mice had regained their normal hearing sensitivity (graphs not shown). This observation further confirmed the idea that DIPH temporally blocks ion transporters in the inner ear and by that prevents cisplatin accumulation in the cochlear cells.

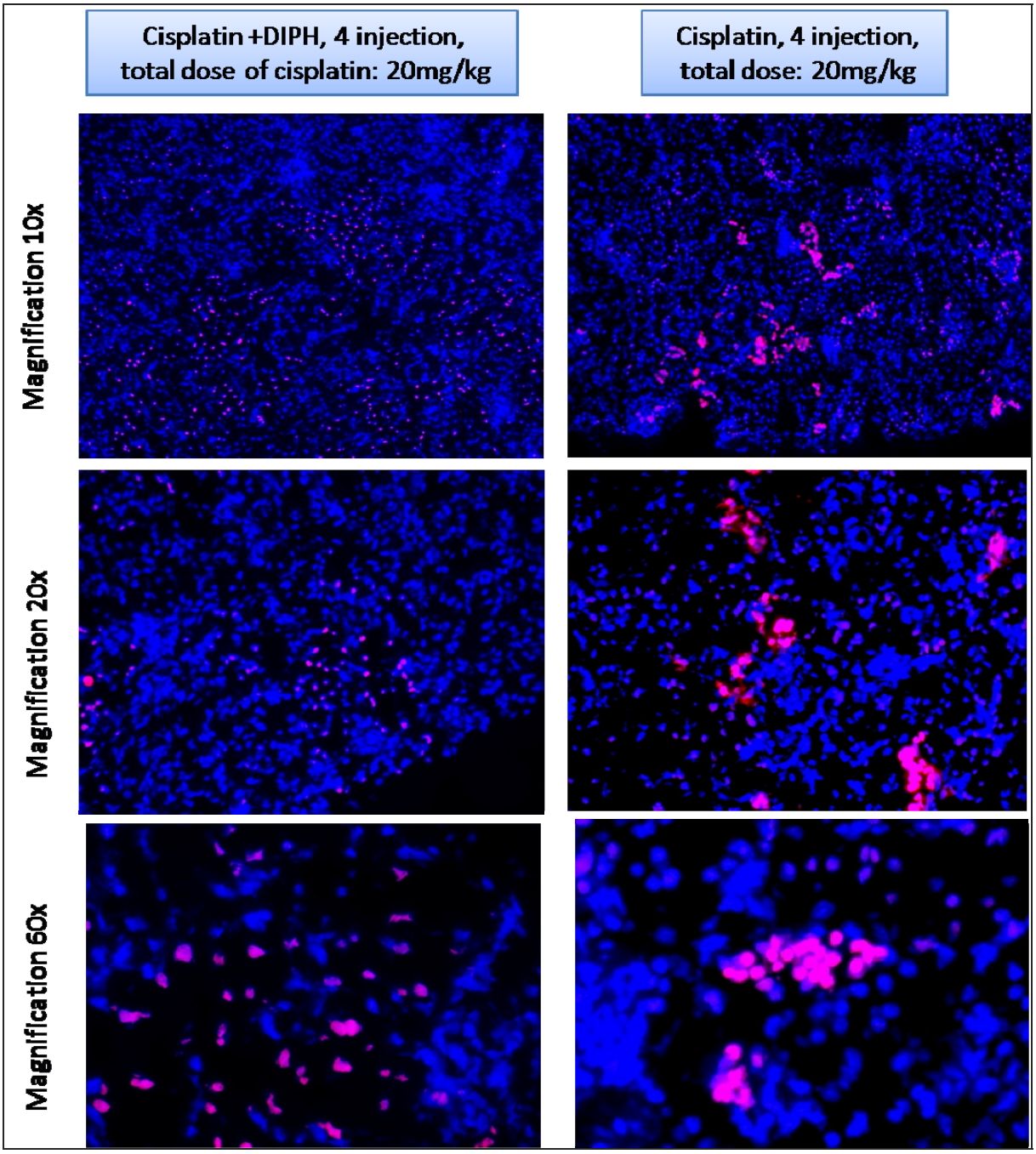

Fig. 27: Distribution of platinum adducts between different cells of the kidney cortex after repetitive cisplatin and cisplatin plus DIPH treatment. Mice were treated repetitively 4 times with cisplatin alone (5 mg/kg every second day, cumulated dose: 20 mg/kg) or with concomitant injections of DIPH (57 mg/kg) 30 minutes before each dose of cisplatin. Animals were sacrificed after the last BEAR test and Pt-GG levels in the DNA of kidney cells were visualized by immunostaining (red); DAPI - DNA (blue). Shown are representative micrographs of the adduct distribution in kidney cortex sections from both treatment groups. Left side: cisplatin plus DIPH; right side: cisplatin only.

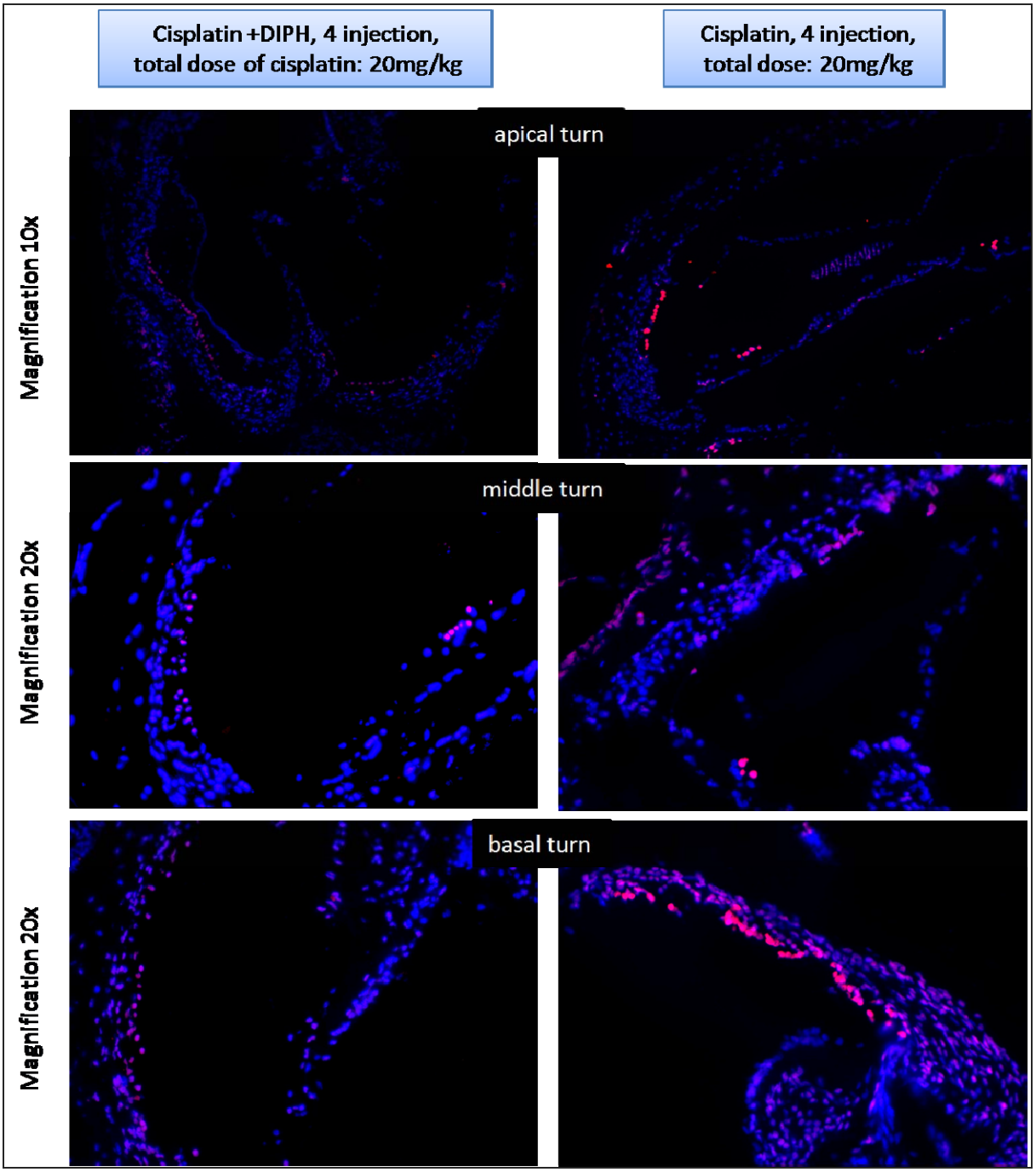

Fig. 28: Distribution of platinum adducts between different cells of the cochlea after cisplatin and cisplatin plus DIPH treatment. Mice were treated repetitively 4 times with cisplatin alone (5 mg/kg every second day, cumulated dose: 20 mg/kg) or with concomitant injections of DIPH (57 mg/kg) 30 minutes before each dose of cisplatin. Animals were sacrificed after the last BEAR test and Pt-GG levels in the DNA of kidney cells were visualized by immunostaining (red); DAPI - DNA (blue). Shown are representative micrographs of the adduct distribution in kidney cortex sections from both treatment groups. Left side: cisplatin plus DIPH; right side: cisplatin only.

3.6 DIPH does not affect the therapeutic efficacy of cisplatin

The pronounced protective effect of DIPH on both, DNA platination and functional loss in physiological target cells, made it an interesting candidate for co-application during cisplatin-based cancer therapy to reduce the side effects. An important factor that had to be controlled in this respect is whether DIPH not only reduces the severity of the side effects but also diminishes the efficacy of cisplatin-based cancer chemotherapy. Although experiments with various human cancer cell lines had indicated no inhibitory effect of DIPH on adduct formation and cytotoxicity induced by cisplatin (Fig. 24 and data not shown), the relevant mechanisms in primary tumor cells *in situ* might be completely different. Therefore, a suitable rodent tumor model was employed to further investigate this question.

3.6.1 A mouse model for human lung cancer

Oncogenic mutations in the gene encoding the small GTPase *K-ras* are among the most frequently detected alterations in human lung cancer and approximately 30 % of all cases of human non-small cell lung cancer (NSCLC) carry such an activated *K-ras* allele with mutations predominantly located in codons 12, 13 or 61. Based on this observation a mouse model for NSCLC was recently established (Sweet-Cordero *et al.*, 2006; Oliver *et al.*, 2010). The local activation of a silent transgenic *K-ras*^{G12D} allele in these mice is achieved by intratracheal adenoviral transfection with the Cre recombinase (AdCre). The Cre recombinase cuts out a “stop” cassette and allows for expression of the oncogenic *K-ras* protein in transfected lung cells. When the initiation is performed at the age of 8 weeks, mice are diagnosed 16 weeks later with lung tumors at 100 % penetrance. The morphology and molecular characteristics of the tumors are very similar to human NSCLC and they respond with regression to chemotherapy with cisplatin (Oliver *et al.*, 2010). Because cisplatin is a first line drug in treating human NSCLC, we employed this mouse model to investigate possible effects of DIPH on the treatment outcome of chemotherapy with cisplatin. The experiments were performed in the laboratory of Dr. Tyler Jacks at the MIT in Cambridge, Massachusetts.

3.6.2 No effect of DIPH on the DNA platination in primary lung tumor cells of cisplatin–treated mice

*M*ice bearing *K-ras*^{G12D} -induced lung tumors were divided into two groups for acute high dose and for chronic low dose treatment. Animals received mock-treatment with PBS or cisplatin alone or cisplatin plus pretreatment with DIPH. For acute treatment, the mice were i.p.-injected once with cisplatin (10 mg/kg) and for chronic treatment every second day with 5 mg/kg (4 consecutive injections, cumulative dose: 20 mg/kg). DIPH was given at a dose of 57 mg/kg 30 minutes prior to each dose of cisplatin. All mice were sacrificed 24 hours after the last treatment and cochleae, kidneys and lungs were resected for analysis of DNA adduct accumulation. Whereas the protective effect of DIPH on the DNA platination in renal and cochlear target cells was present as expected from the previous experiments (data not shown), no reduction of the Pt-GG levels by DIPH co-treatment was measurable in lung tumor cells, independent from the treatment schedule (Fig. 29). Adduct levels were about two-fold higher after repetitive treatment as compared to single high dose treatment. These observations suggest that the pharmacodynamics of cisplatin in primary lung tumor cells of mice is different from the situation in the kidney and the cochlea, allowing for the severe side effects of the drug. Active uptake of the drug by a DIPH-sensitive transporter does not seem to play a major role in the malignant lung cells, but could be confirmed for kidney and cochlear cells.

3.6.3 Tumor growth controlled by cisplatin is not affected when combined with DIPH

In addition to the analysis of adduct levels in the *K-ras* mouse model, we analyzed whether the co-administration of DIPH negatively affected the therapeutic efficacy of cisplatin in the NSCLC tumors. A cohort of tumor-bearing mice was randomly divided into three subgroups receiving different treatment regimens. Group one (mock treatment control) received i.p. injections once per week with PBS for 4 weeks. The second group received cisplatin treatment (7 mg/kg) once per week for 4 weeks, and mice of the third group were additionally pre-treated with DIPH (57 mg/kg) 30 minutes

before each dose of cisplatin. Mice were sacrificed 5 days after the last dose; lungs were resected and prepared for paraffin sections. Following H&E staining for morphological structures, the percentage tumor burden, the number of tumors per lung and the average tumor size was determined microscopically (Fig. 30, 31). In addition, kidneys were resected from all mice as internal control for correct cisplatin treatment and cryosections were analyzed by ICA for DNA platination (data not shown). By microscopic inspection of the stained lung section, it became obvious that the number of tumors per lung were higher in PBS-treated mice as compared to animals of the two cisplatin-treated groups (Fig. 30). For quantitative analysis we used the Bioquant image analysis software to blindly and randomly quantify the area of all lung tumors and the total lung surface area in 4 lung sections per mouse. The measurement revealed significantly lower average tumor sizes in both groups with cisplatin treatment as compared to the PBS control group and no difference between the cisplatin alone and the cisplatin plus inhibitor group (Fig. 31). The mean tumor burden in the lung, (as calculated from total area of tumor divided by total lung area), too, was significantly lower in both groups of cisplatin-treated mice with no significant difference if given alone or in combination with DIPH (Fig. 31). Tumor number was reduced in cisplatin and cisplatin plus DIPH treated mice, but these values were not statistically significant. This suggests that the drugs mainly reduce tumor growth and have less of an effect on tumor initiation. This hypothesis is further supported by the average tumor size data, and an observation that tumor growth is inhibited by cisplatin treatment as monitored by micro-CT (Oliver *et al.,* 2010). In summary, the co-application of DIPH neither influenced the DNA damage level induced by cisplatin in primary lung tumors nor did it significantly hamper the therapeutic efficacy of the drug as determined by tumor burden and average lung tumor size.

Based on all results obtained so far in our mouse models, it is concluded that during cancer chemotherapy with cisplatin the concomitant application of DIPH is a suitable and safe pharmacological strategy to prevent structural and functional damage in the inner ear and in the kidney without affecting the therapeutic response.

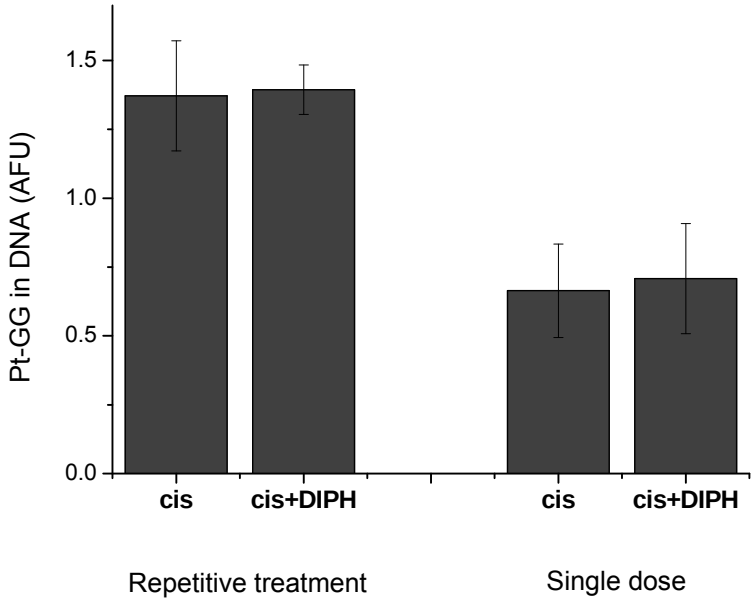

Fig. 29: Accumulation of platinum-DNA adducts in primary mouse lung tumors during acute and chronic treatment by cisplatin or cisplatin plus inhibitor is not affected by the co-application of DIPH. Animals were sacrificed 24 h after the last drug injection and lung cryosections were measured by ICA analysis The two left columns represent mean adduct levels (+/- SD) in lung tumors cells of mice treated with cisplatin four times (5 mg/kg, every second day) with (cis+DIPH) or without (cis) co-application of DIPH (57 mg/kg). The two right columns refer to the respective adduct levels after a single high dose of cisplatin (10 mg/kg).

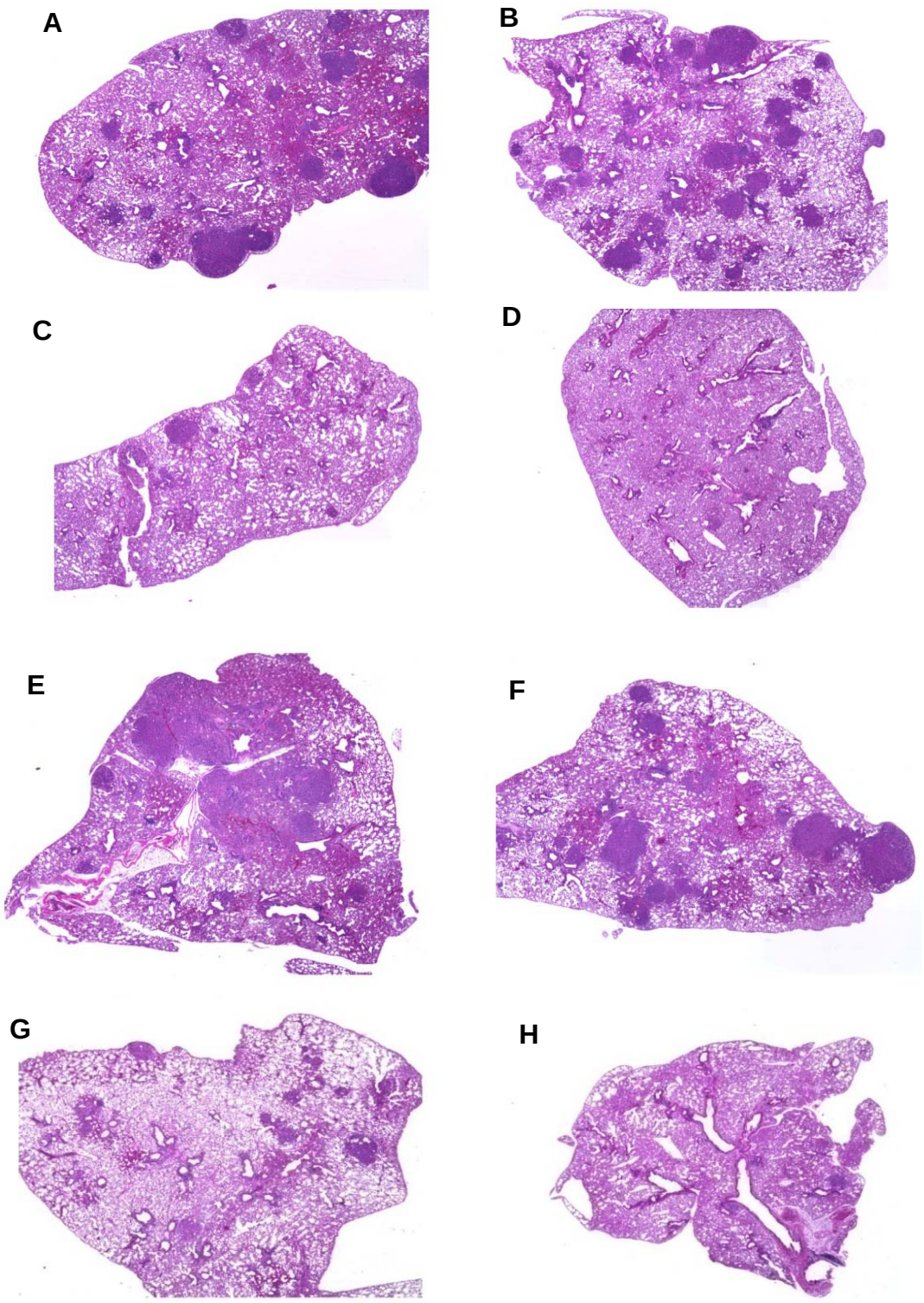

Fig. 30: Representative photographs of the H&E stained lung sections from tumor-bearing mice of from three treatment groups. Twelve weeks after tumor initiation mice were treated with cisplatin alone (7 mg/kg once a week for 4 weeks; C, D) or in combination with DIPH (57 mg/kg; G, H)) or were mock-treated with PBS (A, B, E, F). Five days after the last treatment lungs were resected, fixed in formalin and embedded in paraffin. Morphological structures were visualized in tissue sections (6 µm) by H&E staining (magnification: 2x). Tumor areas are stained dark purple.

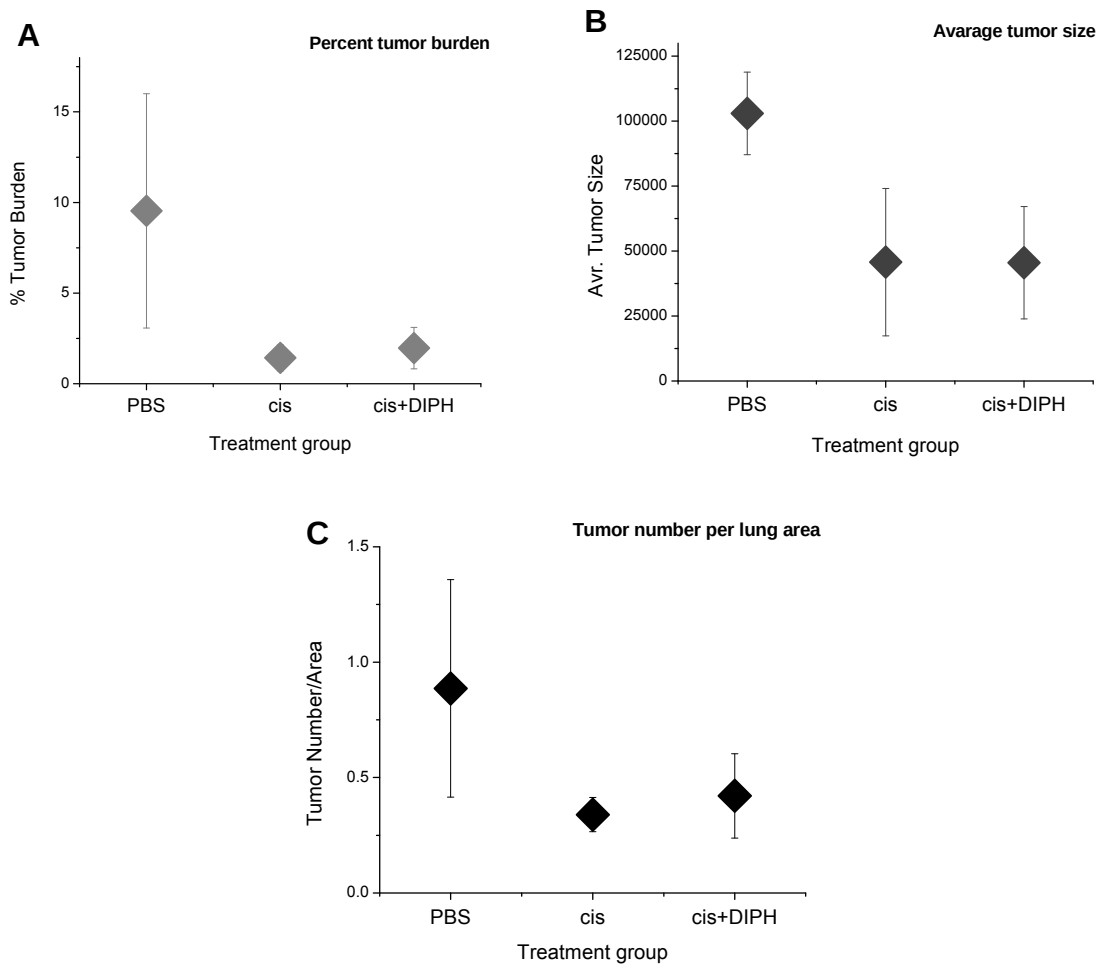

Fig. 31: The co-application of DIPH had no inhibitory effect on the therapeutic efficacy of cisplatin on primary lung tumors in mice. Four tumor-bearing animals were treated with cisplatin alone or in combination with DIPH or were mock-treated with PBS. H&E-stained lung sections were analyzed quantitatively for the percentage of tumor burden (A), the average tumor size (B), and the number of tumors per section (C) by using Bioquant image analysis software. For none of these parameters a significant alteration was observed when comparing cisplatin and cisplatin plus DIPH treatment schedules.

3.7 Cisplatin resistance in the NSCLC mouse model

Once the mouse model of human lung cancer was introduced, it was intensively studied for mechanisms of drug resistance as, similar to the clinical situation, a subset of tumors lost their responsiveness to cisplatin after several treatment cycles (Sweet-Cordero *et al.*, 2006; Oliver *et al.*, 2010). In the context of this study such tumors were investigated for the formation and persistence of platinum-DNA adducts in comparison to tumors still responding to the drug.

3.7.1 Long-term cisplatin-treated lung tumors in mice exhibit reduced levels of DNA damage in response to a final dose of cisplatin

30 mice bearing *K-ras*^{G12D} -induced lung tumors were randomly divided into two groups and were long-term treated with cisplatin (7 mg/kg, i.p. once per week for four weeks) to select for drug resistance or were mock treated with PBS accordingly. After two weeks without treatment all mice got a final dose of cisplatin (7 mg/kg) and three animals were sacrificed at 4, 8, 16, 24 and 48 hours after the injection. Lungs were resected and cryosections were immuno-stained for Pt-GG adducts. In mice long-term treated with PBS lung tumor cells regularly depicted Pt-GG adduct levels which were comparable to those in the surrounding normal lung cells, suggesting that formation and repair rates were similar in malignant and non-malignant cells (Fig. 32) The picture was different in the group of long-term cisplatin-treated mice where about 20 % of the individual lung tumors analyzed by fluorescence microscopy showed strongly reduced or nearly undetectable levels of platinum-DNA adducts as early as 4 h after a final dose of cisplatin (Fig. 32, lower panel). Interestingly, big differences were observed between single tumors from one animal (Fig. 33). However, tumors that had undetectable levels of platinum-DNA adducts at all time point were found only in lungs from long-term cisplatin-treated animals.

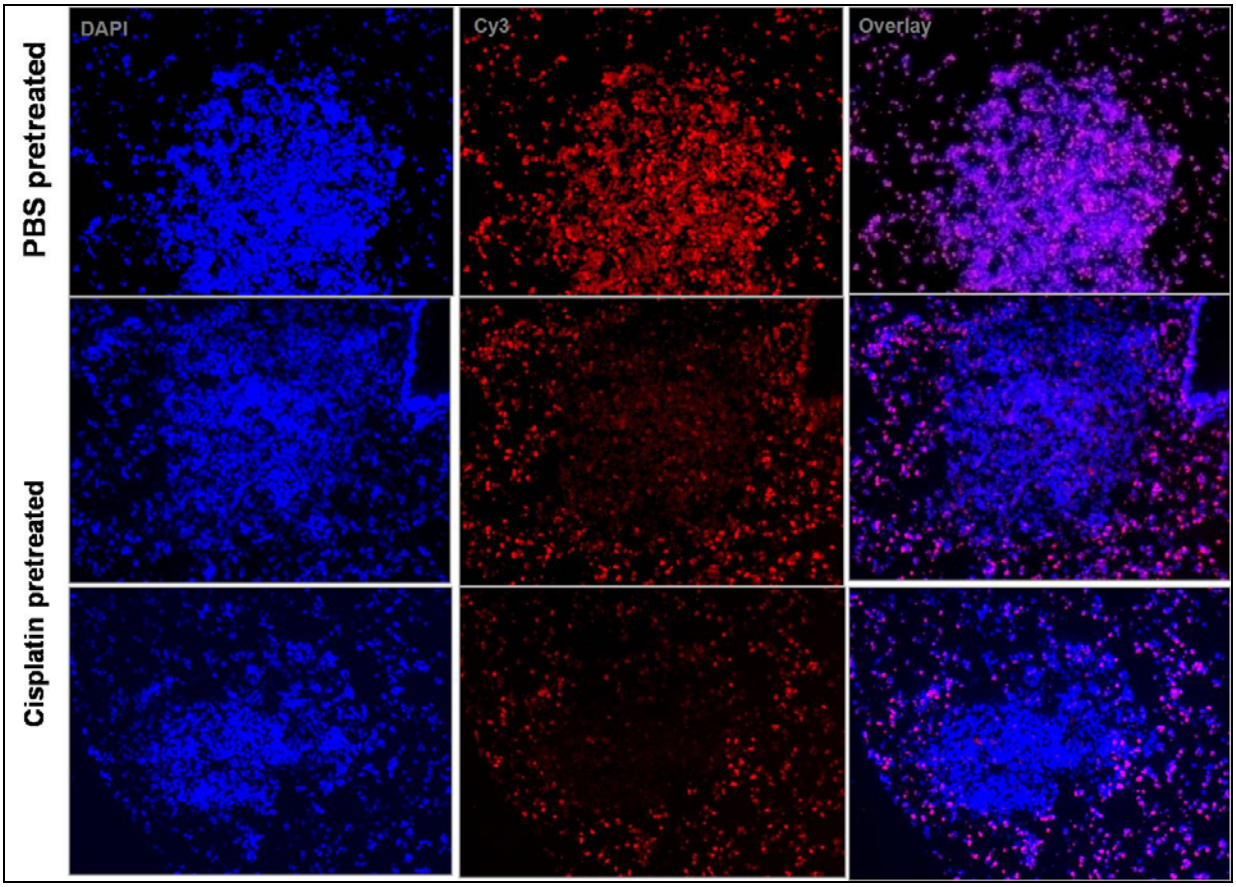

Fig. 32: Representative images of individual lung tumors stained for cisplatin-induced Pt-GG adducts in the nuclear DNA. Tumor-bearing mice were either long-term pre-treated with PBS (upper panel) or with cisplatin (lower panels) and were sacrificed 24 hours after a final dose of cisplatin. Left column: DAPI staining for DNA, medium column: immunostaining for DNA adducts, left column: overlay. Magnification: 10x.

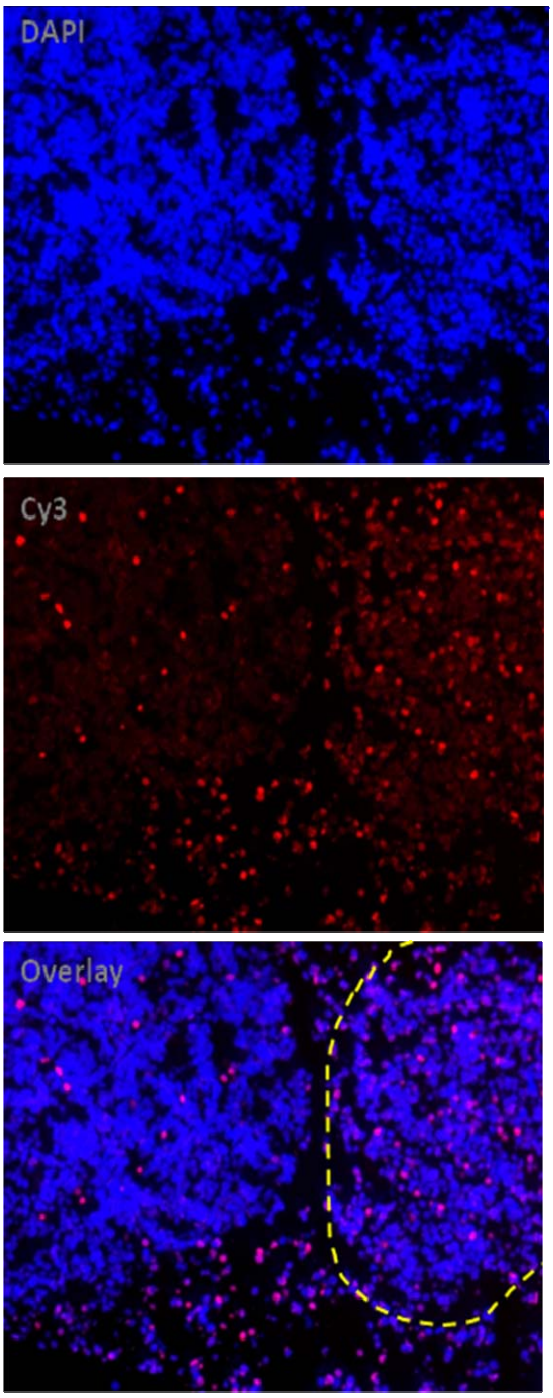

Fig. 33: Individual tumors in the same lung area of a cisplatin-treated mouse exhibit different level of adduct accumulation. A mouse with lung tumors was long-term pretreated with cisplatin and was sacrificed 4 h after last administration. The immunostaining of lung sections for Pt-GG adducts revealed two adjacent tumors with different levels of DNA platination. The cells of the tumor on the left depicted none or very low adduct staining (red) whereas the nuclei of the tumor on the right (separated by the dotted line) show immuno-fluorescece signals similar to those of the surrounding normal lung tissue. Magnification: 20x.

3.7.2 Heterogeneity between individual lung tumors in mice

To verify heterogeneity between all tumors, we scored all tumors blindly for absence, or presence of Pt-GG adducts. The numbers of tumors varied between the cisplatin and the PBS treatment groups, so we grouped the tumors into three categories: tumors with very low or absent adducts, tumors with low adducts and tumors with the same adduct level as the surrounding tissue (Fig. 32). This analysis was done at four time points: 4, 8, 16 and 24 hours. At the latter time point, the tumor cells may already have replicated their DNA and underwent cell division, which would reduce the adduct levels independently from repair processes.

It was noted that the percentage of tumors with low or absent adducts in the long-term cisplatin-treated group increased with time (Fig. 34). These data allow to conclude that Pt-GG adducts are present in sensitive and most resistant tumors at early time points, but are cleared more rapidly in non-responsive tumors pretreated with cisplatin.

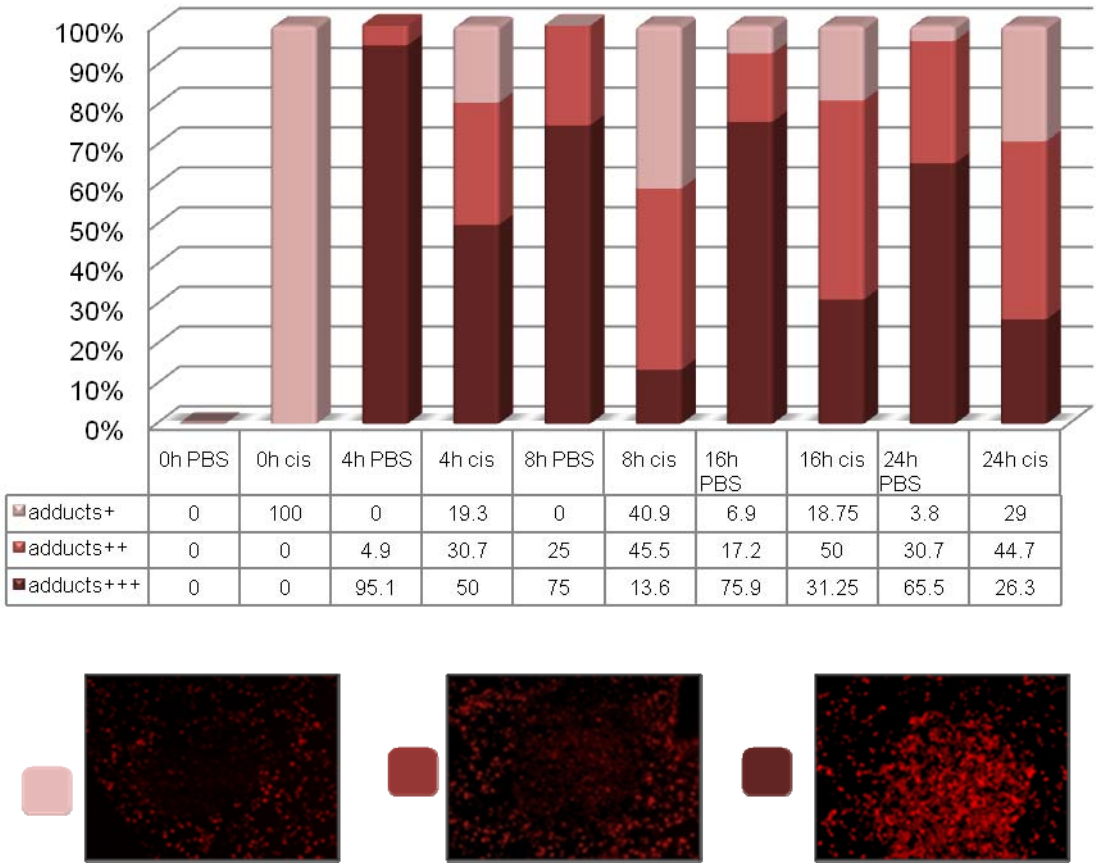

	0h PBS	0h cis	4h PBS	4h cis	8h PBS	8h cis	16h PBS	16h cis	24h PBS	24h cis
adducts+	0	100	0	19.3	0	40.9	6.9	18.75	3.8	29
adducts++	0	0	4.9	30.7	25	45.5	17.2	50	30.7	44.7
adducts+++	0	0	95.1	50	75	13.6	75.9	31.25	65.5	26.3

Fig. 34: Number of lung tumors with different levels of DNA platination in two treatment group. Tumor-bearing mice were either long-term (4 weeks) pretreated with cisplatin (cis) or were mock-treated (PBS), All animals received a final dose of cisplatin (7 mg/kg) in week 6 and 3 mice were sacrificed at 4, 8, 16 or 24 h after the last dose of cisplatin (0h PBS and 0h cis: without last dose). Deep red – sensitive to cisplatin tumors (high adduct level), red – low adduct level tumors, light pink – tumors with very few adducts. In cisplatin treated group number of tumors analyzed: 4 hours - were analyzed 26 tumors; 8 hours - were analyzed 22 tumors; 16 hours - were analyzed 32 tumors; 24 hours - were analyzed 38 tumors. In long-term PBS treated group: 4 hours - were analyzed 41 tumors; 8 hours – were analyzed 20 tumors; 16 hours - were analyzed 29 tumors; 24 hours – were analyzed 26 tumors. The table below indicates exact percentage number with different adducts.

4. Discussion

The antineoplastic chemotherapy with cisplatin, although, effective in many cases, is hampered by serious limiting factors such as severe side effects and primary or acquired resistance often occurring during repetitive courses of treatment. Such side effects make the reduction of dosage, frequency or duration of cisplatin therapy necessary. One of the major side effects of cisplatin, its nephrotoxicity, can be reduced by forced diuresis before and after drug administration. The ototoxicity of cisplatin is still a serious clinical problem. Future efforts should be aimed at the development of methods to efficiently protect the inner ear tissue during chemotherapy. In the recent years, numerous suggestions have been made for pharmacological strategies to prevent cisplatin-induced hearing loss (van den Berg *et al.,* 2006). From the clinical perspective, it is absolutely necessary that such a preventive strategy does not interfere with the antineoplastic efficacy of the drug. To develop rational strategies for preventive interventions, it is crucial to investigate the molecular mechanisms underlying the hypersensitivity of cochlear cells to cisplatin. The primary aim of this thesis was to study the molecular events resulting in cell damage in the inner ear and in hearing dysfunction after cisplatin administration, as well as to identify putative inhibitors of cisplatin cytotoxicity in normal tissues.

4.1 Cell type-specific accumulation of Pt-DNA adducts coincides with the cytotoxicity of cisplatin in normal tissues

The main mechanism by which cisplatin exerts its cytotoxicity in tumor cells is believed to involve the formation of intra- and interstrand adducts in the nuclear DNA. Persisting platinum adducts may lead to the inhibition of replication and transcription processes as well as to cell cycle arrest, and can result in apoptotic cell death (Jordan *et al*., 1998; Ang *et al.,* 2010).

Regarding cisplatin ototoxicity, numerous mechanisms that may lead to functional disturbance or death of non- or slow-dividing cells of normal tissues were suggested during the recent years. Most frequently discussed are (i) the generation of reactive oxygen species (ROS), (ii) damage of mitochondrial membranes and (iii) drug-

induced mitochondrial apoptosis (Devarajan *et al.,* 2002; Peters *et al.,* 2003; Santos *et al.,* 2007; Kim *et al.,* 2010). However, previous *in vivo* studies in our own group in cisplatin-treated guinea pigs observed that the level of 8-oxoguanine (a lead type of ROS-induced DNA damage) was not increased in the DNA of inner ear cells after cisplatin administration (Thomas *et al.,* 2006). Most other investigations detected ROS production only in cisplatin-exposed cochlear explants and in short-term cultures *ex vivo* (Dehne *et al.,* 2001).

The formation rate of cisplatin-induced DNA damage is cell-type specific, and occurs in the inner ear predominantly in two types of cells, the marginal cells of the stria vascularis and the outer hair cells of the organ of Corti. Early observations on cell type specificity of cisplatin-induced damage in the inner ear were made using electron microscopy (Nakai *et al.,* 1982; Kohn *et al.,* 1988), and were supported by DNA damage analysis in guinea pigs later on (Thomas *et al.,* 2006). In the present study, it was aimed to further clarify the molecular mechanisms of cisplatin ototoxicity. Thus, a mouse model was established, which allowed the analysis of electrophysiological parameters of hearing capability and, simultaneously, of the formation and processing of Pt-DNA adducts at the level of individual cells. The degree of cisplatin-induced DNA damage and its repair was measured in different types of inner ear and kidney cells. This study shows for the first time that the DNA in outer hair cells and marginal cells of the cochlea is extensively damaged in cisplatin-treated mice. Up to eight-fold differences between the various cells layers in the stria vascularis as well as between the outer hair cells and other cell types of the organ of Corti were observed. A similar erratic distribution of the DNA platination was detected throughout kidney cortex cells, with high levels in proximal tubular cells as compared to other kidney cortex cells. These observations strictly contradict the assumption of passive diffusion as the exclusive or main route of cisplatin to enter such cells. More likely, the active import of cisplatin by membrane transporters may play a role for the distinct distribution of DNA platination products within a given tissue. The finding of similarly high platinated cells within two structurally and functionally unrelated tissues might indicate a causative role of channels or transporters expressed in the kidney as well as in the cochlea. Such a common mechanism was recently discussed by Lang *et al.* who suggested that simultaneous dysfunction of seemingly unrelated organs might be based on a common defect of channels or transporters (Lang *et al.,* 2007).

A number of clinical observations documented that almost all ototoxic agents also have nephrotoxic effects (Rybak and Ramkumar, 2007; Lang *et al.,* 2007). Due to its comparatively small size (MW: 300), it is likely that cisplatin is aberrantly recognized as a substrate by specific membrane transporters in the target cells of the inner ear and the kidney (Lang *et al.,* 2007).

4.2 Quantification of Pt-DNA adducts in different turns of the cochlea

Cisplatin-induced dysfunction of the hearing system has been shown to begin in the basal turn of the cochlea, leading to a functional loss for high frequencies (Böheim and Bichler, 1985; Sluyter, 2003; Laurell *et al.,* 2007). In this study, remarkable differences were found in DNA adduct accumulation between the basal and the apical turn, not only for the marginal cells, but also for other cells of stria vascularis. The mechanism underlying the differential distribution of cisplatin between the cochlea turns is not known, but might be determined by the morphological structure of the cochlea and the blood stream through the stria vascularis. Indirect measurements have shown that radioactively labeled cisplatin is first accumulated in the stria vascularis and then distributed among other cells of the inner ear (Schweitzer *et al.,* 1986). The higher content of DNA adducts in the basal turn marginal cells found in this study corresponds to the higher degree of destruction of the tissue in the basal turn of the cochlea, and is in line with the early onset of hearing loss for high frequencies recorded in rodents and humans (Sluyter, 2003; Rybak and Ramkumar, 2007).

4.3 The activity of nucleotide excision repair in processing of Pt-DNA lesions in inner ear cells

The adduct formation in DNA by cisplatin is influenced by different pharmacokinetic and pharmacodynamic factors of the drug, such as chemical absorption, distribution, metabolism or renal excretion (O'Dwyer *et al*., 2000). Once adducts are formed, their removal depends on the activity of DNA repair processes. In the case of cisplatin, the elimination of adducts is mediated predominately by the nucleotide excision repair (NER) system. The functional capacity of NER is assumed to be rather

inhomogeneous among different cell types (Kelland, 1994) and the deficiency for distinct repair proteins leads to an increased vulnerability of the cell. For example, deficient repair of Pt-DNA adducts was identified in human testicular cancer cells, which are highly sensitive to cisplatin (Bedfort *et al.,* 1988; Hill *et al.,* 1994; Köberle *et al.,* 1997; Köberle et al., 2010). The *in vivo* measurement of repair kinetics in this study showed high NER activities in the target cells of the inner ear and were comparable to those in the non-target cells of Reissner's membrane. The data exclude insufficient DNA repair as the cause of the excessive DNA platination in outer hair cells and marginal cells. Furthermore, these findings in mice were in line with previous observations in guinea pigs (Thomas *et al.,* 2006). Interestingly, long term kinetics in other tissues (e.g. liver, kidney and neurons) of cisplatin-treated, NER-proficient mice, revealed that a certain proportion of adducts persisted unrepaired even five days after drug administration (Liedert *et al.,* 2006; Dragnidze *et al.,* 2007).

4.4 The role of the NER protein XPA in the cells of the hearing system

Functional DNA repair is critical for the viability of cells, particularly during acute genotoxic stress. The XPA protein plays a central role in the NER pathway by recruiting several other NER proteins, which build the repair incision complex at the damaged site.

In the present work, XPA-knockout mice defective in both sub-pathways of the NER, were used to study the influence of this repair system on the cytotoxicity of cisplatin and the processing of Pt-GG adducts. The experiments revealed that XPA-deficient mice were highly sensitive to the general toxicity of cisplatin, accompanied by a high accumulation of adducts in cochlear cells and a decrease in hearing performance. The data presented here strongly supports the hypothesis that the cisplatin-induced DNA adducts initially trigger cellular processes finally leading to functional sensorineural hearing loss. In contrast, several other reports have accused the generation of ROS to be causative for the ototoxicity of the drug by promoting apoptotic and necrotic cell death in cochlear tissue (Albinger-Hegyi *et al.,* 2006; Santos *et al*., 2007; Rybak *et al.,* 2007; Rybak and Ramkumar, 2007). However, none of the preventive approaches for ototoxicity (as well as nephrotoxicity) based on

the reduction of ROS during cisplatin treatment were ever validated in clinical trials (van den Berg *et al.,* 2006; Yao *at al.,* 2007). In addition, no convincing biochemical mechanism has been suggested until now to explain the direct or indirect modulation of ROS levels by cisplatin.

4.5 A putative transport system for cisplatin in normal tissues

Several previous studies on the cellular uptake of cisplatin assumed an inert transport through the membrane as the predominant route of entrance of the drug (Gale *et al.,* 1973; Ogawa *et al.,* 1975; Andrews *at al.,* 1988; Mann *et al.,* 1990). Experiments with cancer cell lines revealed passive transport to be responsible for 50% of the influx (% of drug molecules per cell). The other half of influx of cisplatin molecules was attributed to unknown transporters (Dornish *et al.,* 1986; Gately and Howell, 1993). More recent studies further support the concept of active transport mechanisms in distinct cell types (Andrews and Albright, 1991; Komatsu *et al.,* 2000; Katano *et al.,* 2003; Sinani *et al.,* 2007; Blair *et al.,* 2010).

Two main families of importers that recognize cisplatin as a substrate have been described so far (Pabla and Dong, 2008). One of them is the high-affinity copper transporter CTR1. However, organs with a high copper metabolism, such as liver and brain, accumulate comparatively low levels of Pt-DNA adducts (Liedert et al, 2006; Dzagnidze *et al.*, 2007) and do not show signs of cisplatin toxicity. In contradiction, an increase of cellular uptake of either copper or cisplatin by CTR1 was shown to reduce the uptake of the other, and the exposure to both substances trigger the delocalization of CTR1 from the membrane. Cells lacking functional CTR1 lost their sensitivity to cisplatin (Ishida *et al.,* 2002) and overexpression of CTR has been shown to increase the cellular sensitivity to cisplatin (Song *et al.,* 2004). Inversely, the overexpression of the copper efflux transporter ATP7B (ATPase, Cu++ transporting, beta polypeptide), was associated with resistance of cancer cells to cisplatin (Nakayama *et al.,* 2002, Kuo *et al.,* 2007). The role of these transporters in ototoxicity or nephrotoxicity has not yet been investigated in animal models despite of some evidence for CTR1 being highly expressed in mouse kidney cells (Kuo *et al.,* 2006). In addition to increasing the cellular sensitivity for cisplatin, CTR1 overexpression has also been shown to increase the cellular sensitivity to carboplatin (Song *et al.,* 2004).

This finding may mean that CTR1 is unlikely to represent the major mechanism for the ototoxic effect of cisplatin, since carboplatin is not particularly ototoxic in patients, and does not depict high adduct accumulation in marginal cochlear cells or renal proximal tubular cells of drug-exposed guinea pigs (Thomas *et al.,* 2006).

The second transporter family which may be involved in the import of platinum complexes are the organic cation transporters (OCTs). OCTs mediate the transport of cationic compounds through the basolateral membrane of epithelial cells (Fig. 35). Three members of this family, OCT1, OCT2 and OCT3, are currently under discussion to account for the side effects of cisplatin (Motohashi *et al.,* 2002; Yonezawa *et al.,* 2005). In a study with MDCK canine kidney tubular cells it was demonstrated that the drug-induced nephrotoxicity was related to basolateral transport of cisplatin into proximal tubular cells (Ludwig *et al.,* 2004). The toxic effect was higher when the drug was administrated to the basolateral side of the cells as compared to the apical side. OCT2 has been reported to be highly expressed in the kidney, while other members of the OCT family are expressed predominantly in other tissues: OCT1 in the liver and OCT3 in the heart, intestine and brain (Alnouti *et al*., 2006; Nies *et al.,* 2009). Only very few published data are available about the expression and distribution of OCT transporters in the cochlea.

The functional inhibition of membrane transporters by small molecules is a possible strategy to pharmacologically modulate the uptake of substrate molecules. For the family of OCT transporters, several potential inhibitors have been tested so far. Cimetidine has been reported to specifically interfere with OCT2, and to reduce the influx of cisplatin into proximal tubular cells (Ludwig *et al.,* 2004). Conversely, the overexpression of OCT2 highly sensitized human embryonic kidney cells to the cytotoxic effects of cisplatin (Müller *et al.,* 2005; Yonezawa *et al.,* 2005; Ciarimboli *et al.,* 2005). A further proof for OCT2 to represent a main factor for the nephrotoxicity of cisplatin came from the observation that proximal tubule cells established from a human diabetic kidney exhibited reduced uptake of in the drug. This observation might be connected to the lower expression of OCTs in diabetes (Thomas *et al*., 2004; Yao *et al*., 2007). Finally, the two other platinum complexes, carboplatin and oxaliplatin, which were shown to have no noteworthy ototoxic or nephrotoxic potentials, were demonstrated not to interact with OCT2 (Ciarimboli *et al.,* 2005).

Due to the above mentioned reasons, the local expression in the inner ear of six different proteins of the OCT family was determined in this study by immunostaining of mouse cochlea tissue using a panel of specific antibodies. Only the transporters OCT2 and OCT3 were found to be present at high levels, whereas the other four (OCT1, OCTN1, OCTN2, OCTN2) were not detected. This finding correlates with a recently published study showing OCT2 expression in the organ of Corti and the stria vascularis of mice (Ciarimboli *et al.,* 2010). It is interesting to note that the expression of OCT2 and OCT3 transporters in intermediate and basal cells of the stria vascularis and in the supporting cells of the organ of Corti does not fit to the distribution of DNA adducts in the cochlear which is comparatively low in just those cells. In conclusion, the identity of the hypothetical membrane transporter importing cisplatin into the critical target cells remains obscure yet. Another model for the particular cytotoxicity of cisplatin in the marginal cells was published by Laurell *et al*. (2006), The authors suggested that the drug is actively imported into the intermediate cells of the stria vascularis, which contain high levels of melanin. This pigment is known to form complexes and, thereby, detoxifies cisplatin. As soon as this protective mechanism is exhausted and the cells have lost their structural integrity the neighboring marginal cells are targeted by the cytotoxic effect of the cisplatin (Schweitzer, 1993; Takeuchi *et al*., 2000). However, this model is not supported by our data since the high accumulation of DNA adducts in the marginal cells is observed already a few hours after application of the drug and long time before structural alterations can be detected .

4.6 Screening for a pharmacological inhibitor of cisplatin-induced ototoxicity

Although there had been numerous attempts to identify molecules which modulate the transport of cisplatin into physiological cells or diminish its toxicity, in most cases the protective activity of such compounds was proven only in cell culture systems and not under *in vivo* conditions (Pfaller and Gstraunthaler, 1998; Chan *et al.,* 2007; Rybak *et al.,* 2007). In this study, several of those compounds were examined in an established mouse model for cisplatin-induced ototoxicity. Here, it was clearly demonstrated that famotidine, probenecid, fluoxetine, desloratadine, quinine and butylscopolamine do not reduce the accumulation of cisplatin-DNA damage in the

target cells of renal and inner ear tissues. There had been reports on *in vivo* experiments for ranitidine and cimetidine without conclusive results (Dorr and Soble, 1988; Ott *et al.,* 1991; Fisher and le Couteur, 2001; Erhsson and Wallin, 2010). In the present study, it was demonstrated for the first time that the co-application of diphenhydramine (DIPH) significantly reduces both, the excessive DNA platination in the critical inner ear cells and the functional loss in the hearing system.

DIPH was discovered initially as an antihistaminic agent, which ameliorates motion sickness (Garnett, 1986; Harris, 2008). Since then, a number of structurally or functionally related substances have been evaluated, some of which were also included in this study (fluoxetine, ranitidine, cimetidine, desloratadine). They differ only slightly in their antihistaminic activity, mostly with respect to duration. The precise mechanism, however, is not completely understood. They have little effect on either apomorphine- or copper sulfate-induced emesis and there is little correlation between their antihistaminic or anticholinergic potency and their antiemetic effects. All compounds were shown to have a narrower spectrum of antiemetic activity than compounds of the phenothiazine group, being used predominantly for the treatment of motion sickness and vestibular disturbances (Harris, 1978). Among the drugs tested in this study, DIPH was the only antihistaminic agent that displayed a significant activity in preventing the formation of platinum adducts in critical target cells. Therefore, the pharmacological effects such as histamine antagonism, serotonin re-uptake inhibition, anti-cholinergic activity or muscarinic receptor antagonism, which DIPH has in common with other antihistamines, could most likely be excluded from being responsible for the reduced accumulation of DNA adducts in cochlear and kidney cells. Thus, the nephro- and oto-protective activity of DIPH is more likely to be due to the interference with a so far unidentified transporter expressed in the target cells.

Theoretically, there are different mechanisms that could be triggered by DIPH leading to reduced levels of DNA platination in the target cells: (i) a decrease of the uptake or an increase of the export of cisplatin in such cells, (ii) its accelerated metabolic deactivation, or (iii) an augmented repair of the DNA adducts. The findings in this study clearly exclude an effect of DIPH on the DNA repair capacity of cochlear and kidney cells.

The cells in focus are all characterized by their distinct profiles of multiple membrane transporters ensuring their functionality in the respective tissues (Kendall *et al.,* 1983; Inui, Masuda and Saito, 2000; Lang *et al.,* 2007). The strictly dose-dependent pharmacological inhibition of DNA platination by DIPH in the target cells, but no influence on other surrounding cells supports the hypothesis of DIPH binding to, and thereby blocking, specific transporters on the target cells. In an attempt to further characterize this transport mechanism, the influence of DIPH on the accumulation of Pt-GG adducts was analyzed in a cell line established from kidney proximal tubule cells of the mouse. The null-effect of DIPH in that cell system points to a functional loss of the putative drug importer, and again underlines the basic necessity of analyzing such mechanisms under *in vivo* conditions. One reason for seeing no protective activity of DIPH may be the due to the fact that epithelial cells of the proximal tubules are highly orientated in the kidney. There are a number of transporters in the basolateral membrane of the kidney, and different patterns of transporters in the brush border membrane orientated to the inner lumen of the tubule (Fig. 35). These transporters are regulated by the concentrations of different ions and molecules around both membranes. When cultivating such cells *ex vivo*, they do not have natural barriers as they would in the intact kidney tissue, and might have lost the expression of cell-type specific membrane components during the process of immortalization.

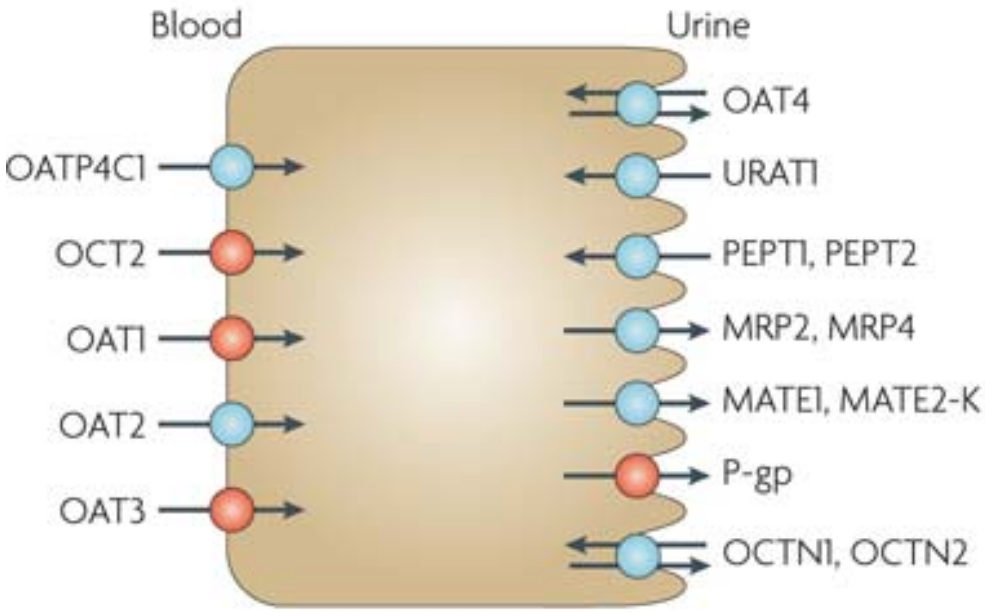

Fig. 35: Uptake and efflux transporters in proximal tubule epithelium cells of the kidney. The figure depict the localization of some transporters in the basolateral (left) and the brushborder (right) membranes. OCT: organic cation transporter; OAT: organic anion transporter; OATP: organic anion transporting polypeptides; URAT1: urate transporter 1: PEPT1-2: solute carrier for oligopeptides; MRP: multidrug resistance-related protein transporter; MATE: multidrug and toxin extraction protein; PgP; P-glycoprotein; OCTN1: organic cation/ergothioneine transporter; OCTN2: organic cation/carnitine transporter. (Figure adopted from Giacomoni *et al.,* 2010)

4.7 DIPH prevents cisplatin-induced ototoxicity in mice

Cisplatin chemotherapy is usually applied in the clinic in repetitive treatment cycles, and thus, leads to progressive and permanent hearing loss. In cases of successful therapy, most of the patients, and in particular treated children, suffer from the toxic side effects for the rest of their lives. In this study, clinically relevant degrees of hearing loss were measurable in mice treated repetitively with low doses of cisplatin and a strong reduction of this side effect was observed when DIPH was given prior to each treatment cycle. Furthermore, it was demonstrated for the first time that unrepaired platinum-DNA adducts in the target cells represent the critical triggers for cisplatin toxicity and that the severity of the side effects is strictly correlated to the amount of drug-induced DNA damage. The precise mechanism by which persisting Pt-(GG) intrastrand cross links lead to structural alterations and functional impairment in terminally differentiated G0 cells is still unknown. One current hypothesis highlights

the role of autophagy in this process. Autophagy is a genetically programmed mechanism for cell survival during different stress conditions, such as energy starvation or exposure to cytotoxic agents (Rosenfeld and Ryan, 2009). The underlying processes are complicated and usually mediate the balance between pro-apoptotic and pro-survival signals (Tang *et al.,* 2010). Autophagy has been observed in a variety of tumors as a response to DNA damaging agents (Degenhardt *et al.,* 2006; Jin and White, 2007). This study suggests that a similar process might also be triggered in the highly damaged cochlear cells of mice after repetitive treatments with cisplatin. Micromorphological analyses by electron microscopy revealed numerous large autophagosomes containing a bulk of cytoplasmic organelles in these cells (Fig. 36 and 37). Such alterations are generally indicative for autophagic or necrotic processes rather than for survival or apoptosis (Yu *et al.,* 2006; Gozuacik and Kimchi, 2007; Galuzzi *et al.,* 2008). No signs of autophagy or necrosis were recorded in the respective cells from animals treated with DIPH alone or from untreated controls, and autophagosomes were much less frequent and properly shaped in cochlear cells of mice treated with cisplatin plus DIPH.

A possible model to explain how cisplatin-induced DNA adducts may trigger physiological, non-dividing cells to undergo such dramatic alterations and finally lose their functionality might be based on the following observations: The activation of autophagic rescue programs after cytotoxic stress strictly depends on the availability of the “high mobility group” protein HMGB1 in the cytoplasm of cells (Tang *et al*., 2010). Earlier studies have shown a very strong binding of HMGB1 to cisplatin-modified DNA structures (Chow *et al.,* 1995; He *et al*., 2000), so that high levels of Pt-GG adducts may trap all of the protein in the nucleus, and thereby, prevent its role in balancing the autophagic process in favor of cell survival. According to this model a reduced adduct accumulation in the target cells by co-application of DIPH would result in diminished functional impairment of those cells. Whether this hypothesis reflects the mechanism of cisplatin ototoxicity in mice as well as in patients remains to be proven.

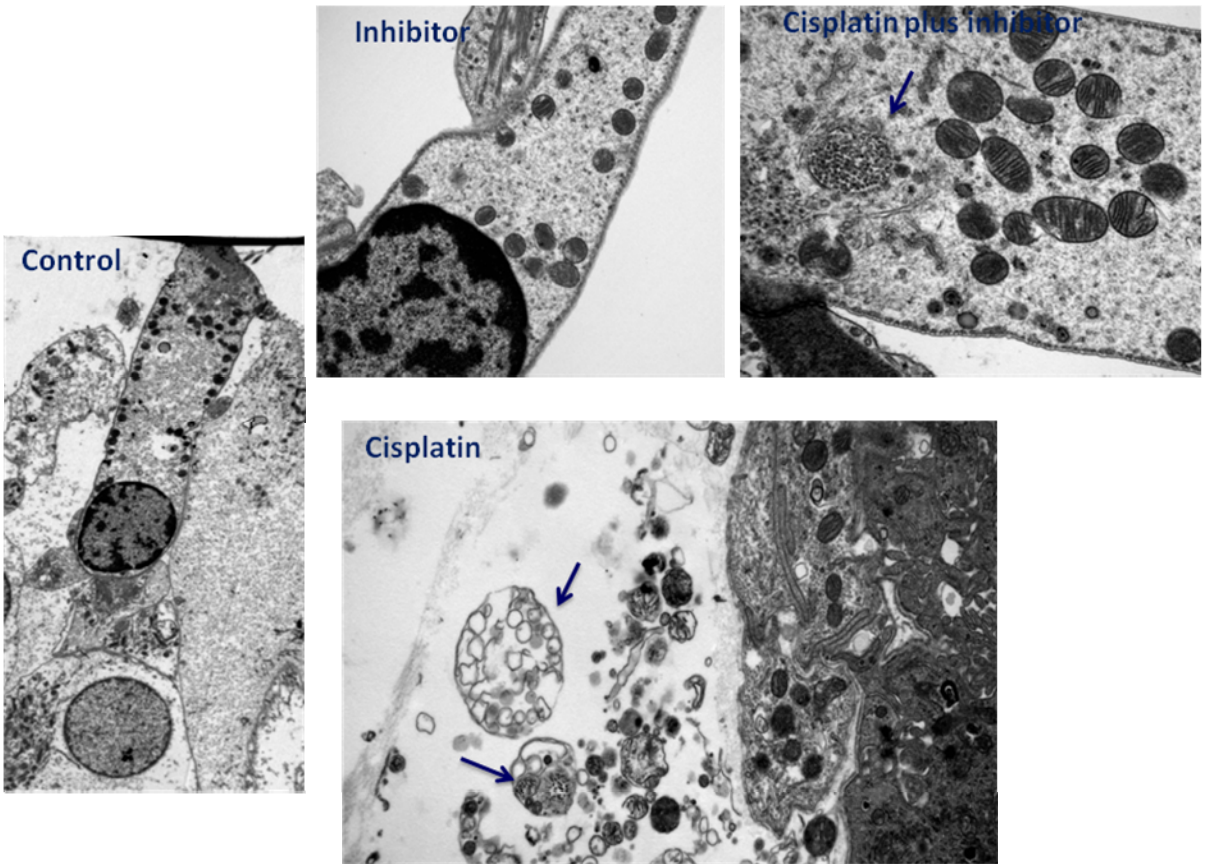

Fig. 36: Micromorphology of outer hair cells in the cochlea of mice: Comparison of different treatment conditions. Mice were repetitively treated every second day for four times with PBS ("Control"), or with DIPH (57 mg/kg; "Inhibitor"), or with cisplatin (5 mg/kg; "Cisplatin") or with both drugs ("Cisplatin plus Inhibitor") and outer hair cells in the middle turns of the cochleae were visualized in ultrathin sections by electron microscopy. The morphology of the cytoplasm was normal without any sings of autophagy in PBS- as well as in only DIPH-treated mice. Cochleae from mice treated with cisplatin plus DIPH depicted rare autophagosome-like structures (arrow). in the cytoplasm. Treatment with cisplatin alone caused necrotic cell death as indicated by incomplete and lumpy autophagosomes (arrow) as well as cellular swelling, and scattered chromatin condensation.

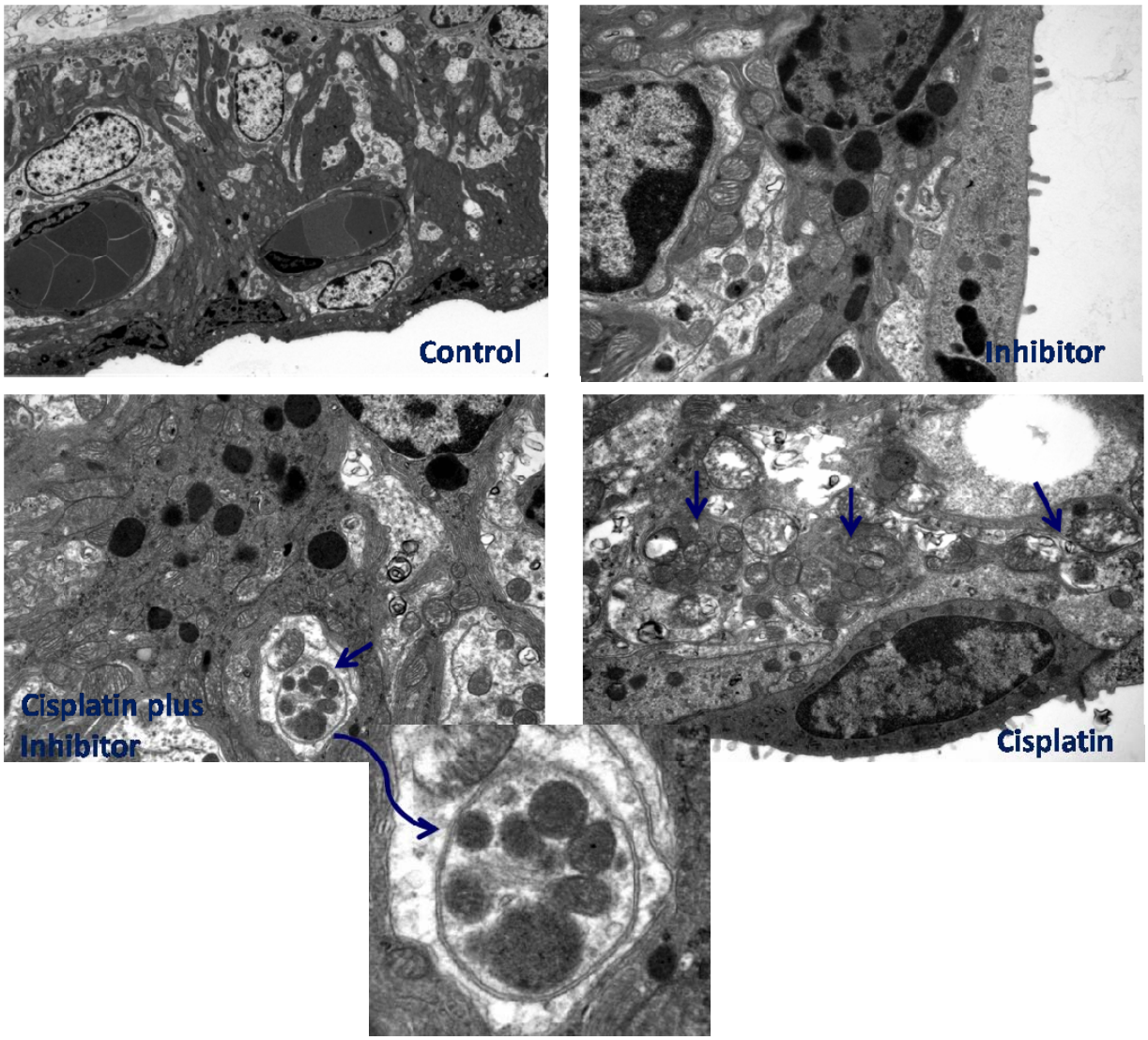

Fig. 37: Micromorphology of stria vascularis marginal cells in the cochlea of mice: Comparison of different treatment conditions. Drug exposure and analyses were done as given in Fig. 36. No signs of autophagic processeses were observed in control as well as in DIPH allone-treated animals ("Inhibitor"), whereas rare, well-shaped autophagosomes were detectable after a combined application of DIPH and cisplatin ("Cisplatin plus Inhibitor"). At a higher magnification (bottom image) embedded mitochondrial bodies became visible in such double membrane-coated phagosomes. After cisplatin alone-treatment (lower right) most of the marginal cells contained multiple, densely packed autophagic vesicles (see arrows).

4.8 DIPH diminishes side effects of cisplatin without affecting the anti-cancer efficacy

Since the severe side effects of cisplatin were already recognized in early clinical trials, numerous pharmacological, molecular, and genetic approaches have been suggested to circumvent the neuro-, nephro- and ototoxicity of the drug (Hanigan *et al.,* 1994; Hanigan *et al.,* 2001; Tsuruya *et al.,* 2003; Yu *et al.,* 2005; Jiang *et al.,* 2007; Santos *et al.,* 2008). None of these preventive strategies reached the clinical level, although the majority of them had demonstrated their effectiveness in animal models. The major obstacles derived from warrantable concerns regarding putative negative effects of such strategies on the tumor-therapeutic efficacy of cisplatin, Therefore, there was an urgent need to address this problem carefully when developing novel approaches.

Lung cancer is the leading cause of cancer death world wide, and non-small cell lung cancer (NSCLC) accounts for approximately 80 % of the cases (Greenlee *et al.,* 2001). This malignancy is frequently associated with mutations in the gene coding for the small GTPase *K-ras* and is usually treated with cisplatin-based combination therapies. The use of genetically engineered mice carrying a silent oncogenic *K-ras* transgene, which can be activated in a controlled manner, provides a model that closely recapitulates many aspects of human lung oncogenesis (Johnson *et al.,* 1997; Jackson *et al.,* 2001; Guerra *et al.,* 2003; Sweet-Cordero *et al.,* 2004). The molecular similarity between *K-ras*-initiated murine lung tumors and the human NSCLC suggests that this is a relevant model to investigate the molecular mechanisms of chemotherapy response. In order to explore whether DIPH might have an effect on the anticancer activity of cisplatin in this model, renal, cochlear and lung tumor tissues were examined for DNA adduct accumulation after short-term and long-term treatments. Furthermore, the average tumor volume and the percentage of tumor burden were measured in animals treated with cisplatin alone or in combination with the inhibitor The results clearly support the hypothesis that DIPH, while efficiently protecting the target cells in the kidney and the inner ear, did not have any significant effect on the levels of DNA adduct accumulation in the tumor cells. Moreover, DIPH did not influence the tumor response during several cycles of chemotherapy with cisplatin. In conclusion, this study uncovered the highly protective

role of DIPH for the target cells of cisplatin toxicity, while retaining the pro-apoptotic role of cisplatin in primary lung tumor cells *in vivo*.

4.9 Enhanced DNA repair in a mouse model of cisplatin-resistant lung cancer

Despite the widespread clinical use of conventional chemotherapeutic agents such as cisplatin, the precise mechanisms underlying the non-responsiveness of tumors to these drugs are still poorly understood. This lack of knowledge is, at least partly, due to the fact, that most of the previous studies on cisplatin sensitivity / resistance have utilized tumor cell lines *in vitro* to generate resistant sub-clones. While this experimental approach has revealed a broad spectrum, of particular mechanisms which can alter the cellular drug sensitivity *in vitro,* they may differ significantly from those used in primary tumor cells *in vivo* (Fink *et al.,* 1997; Siddik, 2003; Wang and Lippard, 2005). A major reason for the diverse behavior could be, that *In vivo* resistance develops in response to repeated low doses of cisplatin whereas *in vitro* resistance is a rapid adaptation to high doses of the drug given over a short period of time.

Genetically engineered animal models for particular malignant diseases are powerful tools, which have not yet been fully exploited to address the problem of drug resistance. Here, the effects of cisplatin treatment in an oncogenic *K-ras*-driven mouse model of human lung cancer were characterized.

The loss of sensitivity to cisplatin-based chemotherapies in human cancer is assumed to be a complex, multifactorial process, as no single factor has been able to explain resistance in full. The mechanisms most frequently discussed during the last years were decreased uptake, intracellular detoxification, increased efflux, tolerance to high adduct levels by translesion DNA synthesis via specialized polymerases or accelerated repair of drug-induced DNA damage. In the murine lung cancer model employed in this study, significantly decreased levels of platinum adducts were observed 24 hours after a final dose of cisplatin in resistant tumors of long-term treated mice as compared to still responding tumors in the control group (Fig. 32 and 34, Oliver *et al.,* 2010). Adduct levels in normal lung cells adjacent to the resistant tumors were generally unaltered (Oliver *et al.,* 2010). Furthermore, atomic absorption

spectroscopy studies did not reveal a significantly decreased overall concentration of platinum within the tumor areas, demonstrating that cisplatin was able to enter tumors similarly in long-term cisplatin and in PBS-treated tumors (Oliver *et al.,* 2010). The repair kinetics in the analyzed tumors support the idea of increased repair capacity, rather than reduced adduct formation rates, as the reason for the low levels of DNA damage in malignant cells no longer responding to the therapy. These findings are in line with clinical observations of NSCLC tumors having a comparatively poor prognosis for treatment outcome. These tumors often depict high expression levels of the DNA repair protein ERCC1, a rate-limiting component of the NER pathway (Olaussen *et al.,* 2006).

The data presented here demonstrated for the first time that enhanced DNA repair causes chemotherapy resistance in an *in vivo* NSCLC mouse model. In combination with the data from a recently published paper (Oliver *et al.,* 2010), this supports the idea that the predominant mechanism leading to the therapeutic failure of cisplatin treatments *in vivo* may be based on accelerated DNA repair (Read, 1998; Martin *et al*., 2008).

4.10 Conclusions and outlook

The results obtained in this study strongly highlight the analytical power of the antibody-based measurement of cisplatin-induced DNA adducts at the level of individual cells. In combination with informative mouse models this technique enabled new insights into the cellular mechanisms which underlie the two major clinical problems associated with cisplatin-based chemotherapies, the occurrence of tissue-specific toxicity and the development of drug resistance in tumors. The precise knowledge of these mechanisms is an indispensable prerequisite for the development of successful interventions aiming to reduce or eliminate the side effects ant to improve the therapeutic benefit. Thus, the identification of DIPH as a potent inhibitor of the cisplatin-mediated oto- and nephrotoxicity was enabled after aberrant import of the drug into the target cells was pinpointed as the critical mechanism. After having shown that primary lung tumor cells in mice and also human lung cancer cell lines lack such transporter activities the clinical application of DIPH during cisplatin treatment can be promoted. The design of future clinical studies

with DIPH is facilitated to a great deal because it is an approved drug and has already been used in cancer chemotherapies as an anti-vomiting agent.

With respect to the problem of drug resistance this study demonstrated for the first time that the non-responsiveness observed in individual lung tumors after several cycles of cisplatin treatment is correlated to strongly reduced levels of drug-induced DNA damage. The data obtained so far in this study argue for the enrichment of highly repair competent cells in such tumors under the selective pressure of repetitive cisplatin chemotherapy. Future clinical studies with NSC lung cancer patients have to show whether this mechanism is also relevant for human malignancies.

5. Summary

Cisplatin is one of the most commonly used tumor-chemotherapeutic agents. It is highly effective in testicular cancer and is a central component of treatment regimens for several other malignancies including esophageal and lung cancer. While much is known about the molecular mechanism by which cisplatin induces apoptosis in proliferating tumor cells, it is still poorly understood, why this drug also leads to fatal dysfunction and cell loss in particular normal tissues such as the inner ear, the kidney, and the peripheral nervous system. These side effects strictly limit desirable dose escalations and severely reduce the quality of life of treated patients. This work aimed to answer some of the open questions and, based on the results, tried to develop a novel strategy for reducing the systemic toxicity of cisplatin in normal tissues.

Employing a mouse model for cisplatin-induced ototoxicity and a sensitive, antibody-based technique to measure cisplatin-DNA adducts in the nuclei of individual cells it was possible to identify two particular cell types in the inner ear which accumulated excessive amounts of DNA damage after drug treatment. These cells are the marginal cells in the stria vascularis and the outer hair cells in the organ of Corti, both indispensable components for the process of hearing. A corresponding observation was made in the second target tissue of cisplatin toxicity, the kidney, where the epithelium cells of the proximal tubules carried a similarly high adduct burden. By analyzing mice with a genetically reduced DNA repair capacity it was possible to pinpoint the platinum adducts as the relevant initial trigger for the drug-induced cell damage and the functional loss in both tissues.

As all three affected cell types are characterized by the presence of multiple, highly active membrane transporters, it was hypothesized that aberrant import of cisplatin by one of these transporters may cause the vast levels of DNA damage. The *in vivo* screening for potential small molecule inhibitors identified diphenhydramine hydrochloride (DIPH) to efficiently reduce the excessive DNA platination in the target cells of cisplatin-treated mice, and thereby, significantly protect their hearing capability.

To test whether the co-application of DIPH is specifically preventive for the cochlear and kidney target cells and does not reduce the therapeutic efficacy of cisplatin for

primary tumors a mouse model for human lung cancer was studied in detail. Neither the formation of DNA adducts in the tumor cells nor the reducing effect of cisplatin with respect to number and volume of the tumors were negatively influenced by the concomitant DIPH treatment. The data strongly suggest a clinical applicability of this strategy, in particular as DIPH is an approved drug.

Finally, the mouse lung cancer model was investigated for mechanisms underlying the development of non-responsiveness during repetitive treatment cycles with cisplatin. The cells in drug-resistant tumors accumulated much lower amounts of DNA platination as compared to tumors still responding to cisplatin chemotherapy, and time-resolved analyses hint to augmented DNA repair as the responsible mechanism.

The results of this study contribute to a better understanding of the *in vivo* effects of cisplatin-based chemotherapies and may pave the way to circumvent some of the major clinical obstacles.

Zusammenfassung

Cisplatin gehört zu den in der onkologischen Klinik am häufigsten verwendeten Zytostatika und wird beispielsweise sehr effektiv bei der Behandlung von Hodentumoren eingesetzt. Cisplatin ist zudem zentraler Bestandteil in Therapie-Konzepten für eine Zahl anderer solider Tumore, wie Ösophagus- oder Lungenkarzinome. Neben der anti-neoplastischen Wirkung induziert Cisplatin aber auch eine Reihe schwerwiegender, oft Dosis-begrenzender Nebenwirkungen. Dazu zählt neben der Schädigung der Niere und des peripheren Nervensystems vor allem die ausgeprägte Toxizität im Innenohr mit nachfolgendem irreversiblem Hörverlust. Die molekularen Mechanismen dieser spezifischen Wirkung auf terminal-differenzierte Normalzellen waren bisher unbekannt und wurden hier an verschieden Mausmodellen *in vivo* untersucht. Eingesetzt wurden dazu vor allem immunanalytischen Nachweisverfahren zur quantitativen Messung von Cisplatin-induzierten Schäden in der Kern-DNA einzelner Zellen.

Dabei zeigte sich, dass es nach einer Cisplatin-Behandlung sowohl im Innenohr als auch in der Niere in bestimmten Zellarealen (Marginalzellen und äußere Haarzellen der Cochlea, Epithelzellen der proximalen Tubuli der Niere) zu einer extrem hohen Anreicherung von DNA-Läsionen kommt und dass diese Schäden ursächlich für die Funktionsverluste bei beiden Organe sind.

Da dieses Schädigungsprofil sehr wahrscheinlich auf einem hochwirksamen, aberranten Import des Medikamentes durch physiologische Membrantransporter in den betroffenen Zellen beruht, wurde im nächsten Schritt nach einem spezifischen Inhibitor für diesen Mechanismus gesucht. Mit Diphenylhydramin (DIPH) konnte ein solcher *in vivo*-wirksamer Inhibitor identifiziert werden, der Dosis-abhängig sowohl die Akkumulation von DNA-Schäden in den Zielzellen als auch den Cisplatin-induzierten Funktionsverlust blockierte.

An einem Mausmodell für das nicht-kleinzellige Lungenkarzinom (NSCLC) konnte anschließend gezeigt werden, dass eine effiziente pharmakologische Oto- und Nephroprotektion durch DIPH weder die DNA-Platinierung in primären Tumorzellen noch die therapeutische Wirksamkeit einer Cisplatin-Behandlung negativ beeinflusst. Damit sind die wichtigsten Grundlagen für eine klinische Erprobung dieser neuen

Protektionsstrategie gelegt, da es sich bei DIPH um ein zugelassenes Medikament handelt.

In einem weiteren Teilabschnitt dieser Arbeit wurden an dem NSCLC-Mausmodell auch die Mechanismen einer Cisplatin-Resistenz genauer untersucht, da die molekularen Ursachen für das häufig auftretende klinische Therapieversagen beim behandelten Lungenkarzinom nicht genau verstanden sind. Es konnte hier erstmals nachgewiesen werden, dass nach mehrmaligen Behandlungszyklen die Zellen Therapie-refraktärer Tumore eine deutlich reduzierte Akkumulation von Cisplatin-DNA-Schäden aufwiesen. Ursächlich dafür ist sehr wahrscheinlich eine selektiv gesteigerte DNA-Reparatur-Kapazität dieser Zellen.

Die hier erhobenen Befunde tragen wesentlich zum besseren Verständnis der Wirkungsmechanismen einer Therapie mit Platin-Zytostatika bei und bieten damit wichtige Ansatzpunkte für einen effizienteren klinischen Einsatz dieser Medikamente.

6. References

Albertella, M.R., Green, C.M., Lehmann, A.R. & O'Connor, M.J. A role for polymerase eta in the cellular tolerance to cisplatin-induced damage. *Cancer Res* **65**, 9799–9806 (2005).

Albinger-Hegyi, A., *et al*. Alteration of activator protein 1 DNA binding activity in gentamicin-induced hair cell degeneration. *Neuroscience* **137**, 971–980 (2006).

Alnouti, Y., Petrick, J.S. & Klaassen, C.D. Tissue distribution and ontogeny of organic cation transporters in mice. *Drug Metab Dispos* **34**, 477-482 (2006).

Andrews, P.A. & Albright, K.D. Role of membrane ion transport in cisplatin accumulation. *Plenum Press, New York*, 151–159 (1991).

Andrews, P.A., Velury, S., Mann, S.C. & Howell, S.B. cis-Diamminedichloroplatinum(II) accumulation in sensitive and resistant human ovarian carcinoma cells. *Cancer Res* **48**, 68-73 (1988).

Ang, W.H., Myint, M. & Lippard, S.J. Transcription inhibition by platinum−DNA cross-links in live mammalian cells. *J Am Chem Soc* **132**, 7429–7435 (2010).

Arany, I. & Safirstein, R.L. Cisplatin nephrotoxicity. *Semin Nephrol* **23**, 460-464 (2003).

Armstrong, D.K., *et al.* Intraperitoneal cisplatin and paclitaxel in ovarian cancer. *N Engl J Med* **354**, 34-43 (2006).

Arslan, E., Orzan, E. & Santarelli, R. Global problem of drug-induced hearing loss. *Ann N Y Acad Sci* **884**, 1–14 (1999).

Badary, O.A., Abdel-Maksoud, S., Ahmed, W.A. & Owieda, G.H. Naringenin attenuates cisplatin nephrotoxicity in rats. *Life Sci* **76**, 2125-2135 (2005).

Bajorin, D.F., *et al*. Pharmacokinetics of cis-diamminedichloroplatinum(II) after administration in hypertonic saline. *Cancer Res* **46**, 5969–5972 (1986).

Bedford, P., Fichtinger-Schepman, A.M., Shellard, S.A., Walker, M.C., Masters, J.R. & Hill, B.T. Differential repair of platinum-DNA adducts in human bladder and testicular tumor continuous cell lines. *Cancer Res* **48**, 3019-3024 (1988).

Bellon, S.F., Coleman, J.H. & Lippard, S.J. DNA unwinding produced by site-specific intrastrand cross-links of the antitumor drug cis-diamminedichloroplatinum(II). *Biochemistry* **30**, 8026–8035 (1991).

Bellon, S.F., Rodgers, K.K., Schatz, D.G., Coleman, J.E. & Steitz, T.A. Crystal structure of the RAG1 dimerization domain reveals multiple zinc-binding motifs including a novel zinc binuclear cluster. *Nature Struct Biol* **4**, 586-591 (1997).

Berclaz, G., Gerber, E., Beer, K., Aebi, S., Greiner, R., Dreher, E. & Buser, K. Long-term follow-up of concurrent radiotherapy and chemotherapy for locally advanced cervical cancer: 12-year survival after radiochemotherapy. *Int J Oncol* **20**, 1313-1318 (2002).

Bertolini, P., Lassalle, M., Mercier, G., Raquin, M.A., Izzi, G., Corradini, N. & Hartmann, O. Platinum compound-related ototoxicity in children: long-term follow-up reveals continuous worsening of hearing loss. *J Pediatr Hematol Oncol* **26**, 649-655 (2004).

Blair, B.G., Larson, C.A., Adams, P.L., Abada, P.B., Safaei, R. & Howell, S.B. Regulation of copper transporter 2 expression by copper and cisplatin in human ovarian carcinoma cells. *Mol Pharmacol* **77**, 912-921 (2010).

Blanc, C., *et al.* Caspase-3 is essential for procaspase-9 processing and cisplatin-induced apoptosis of MCF-7 breast cancer cells. *Cancer Res* **60**, 4386-4390 (2000).

Böheim, K. & Bichler, E. Cisplatin-induced ototoxicity: audiometric findings and experimental cochlear pathology. *Arch Otorhinolaryngol* **242**, 1-6 (1985).

Bottone, M.G., Soldani, C., Veneroni, P., Avella, D., Pisu, M. & Bernocchi, G. Cell proliferation, apoptosis and mitochondrial damage in rat B50 neuronal cells after cisplatin treatment. *Cell Prolif* **41**, 506-520 (2008).

Burger, H., *et al*. Differential transport of platinum compounds by the human organic cation transporter hOCT2 (hSLC22A2). *Br J Pharmacol* **159**, 898-908 (2010).

Cardinaal, R.M., de Groot, J.C., Huizing, E.H., Smoorenburg, G.F. & Veldman, J.E. Ultrastructural changes in the albino guinea pig cochlea at different survival times following cessation of 8-day cisplatin administration. *Acta Otolaryngol* **124**, 144-154 (2004).

Cavaletti, G. Peripheral neurotoxicity of platinum-based chemotherapy. *Nat Rev Cancer* **8**, p1 (2008).

Chan, D.K., *et al*. Protection against cisplatin induced ototoxicity by adeno-associated virus-mediated delivery of the X-linked inhibitor of apoptosis protein is not dependent on caspase inhibition. *Otol Neurotol* **28**, 417–425 (2007).

Chow, C.S., Barnes, C.M. & Lippard, S.J. A single HMG domain in High-Mobility Group 1 protein binds to DNAs as small as 20 base pairs containing the major cisplatin adduct. *Biochemistry* **34**, 2956–2964 (1995).

Ciarimboli, G., *et al*. Cisplatin nephrotoxicity is critically mediated via the human organic cation transporter 2. *Am J Pathol* **167**, 1477-1484 (2005).

Ciarimboli, G., *et al*. Organic cation transporter 2 mediates cisplatin-induced oto- and nephrotoxicity and is a target for protective interventions. *Am J Pathol* **176**, 1169-1180 (2010).

Ciarimboli, G. & Schlatter, E. Regulation of organic cation transport. *Pflugers Arch* **449**, 423-441 (2005).

Cornelison, T.L. & Reed, E. Nephrotoxicity and hydration management for cisplatin, carboplatin, and ormaplatin. *Gynecol Oncol* **50**, 147–158 (1993).

Cross, R.H.M. A reliable epoxy resin mixture and its application in routine biological transmission electron microscopy. *Micron Microsc Acta* **20**, 1-7 (1989).

Cullen, K.J., Yang, Z., Schumaker, L. & Guo, Z. Mitochondria as a critical target of the chemotheraputic agent cisplatin in head and neck cancer. *J Bioenerg Biomembr* **39**, 43–50 (2007).

Cummings, B.S. & Schnellmann, R.G. Cisplatin-induced renal cell apoptosis: caspase 3-dependent and independent pathways. *J Pharmacol Exp Ther* **302**, 8–17 (2002).

Dallos, P., Popper, A. & Fay, R. The Cochlea. *Springer handbook of auditory research* **8**, (1996).

Degenhardt, K., *et al.* Autophagy promotes tumor cell survival and restricts necrosis, inflammation and tumorigenesis. *Cancer Cell* **10**, 51-64 (2006).

Dehne, N., Lautermann, J., Petrat, F., Rauen, U. & de Groot, H. Cisplatin ototoxicity: involvement of iron and enhanced formation of superoxide anion radicals. *Toxicol Appl Pharmacol* **174**, 27–34 (2001).

de La Motte Rouge, T., *et al*. Survival and reproductive function of 52 women treated with surgery and bleomycin, etoposide, cisplatin (BEP) chemotherapy for ovarian yolk sac tumor. *Ann Oncol* **19**, 1435-1441 (2008).

Dentino, M., Luft, F.C., Yum, M.N., Williams, S.D. & Einhorn, L.H. Long term effect of cis-diamminedichloride platinum (CDDP) on renal function and structure in man. *Cancer* **4**, 11274-11281 (1978).

Devarajan, P., *et al*. Cisplatin-induced apoptosis in auditory cells: role of death receptor and mitochondria. *Hear Res* **174**, 45-54 (2002).

Dive, C. & Hickman, J.A. Drug target interactions: only the first step in the commitment of a cell to a programmed cell death. *Br J Cancer* **64**, 192-196 (1991).

Dornish, J.M., Melvik, J.E. & Pettersen, E.O. Reduced cellular uptake of cis-dichlorodiammineplatinum(II) by benzaldehyde. *Anticancer Res* **6**, 583-588 (1986).

Dorr, R.T. & Soble, M.J. Cimetidine enhances cisplatin toxicity in mice. *J Cancer Res Clin Oncol* **114**, 1-2 (1988).

Dzagnidze, A., *et al*. Repair capacity for platinum-DNA adducts determines the severity of cisplatin-induced peripheral neuropathy. *J Neurosci* **27**, 9451-9457 (2007).

Durak, I., Ozbek, H., Karaayvaz, M. & Oztürk, H.S. Cisplatin induces acute renal failure by impairing antioxidant system in guinea pigs: effects of antioxidant supplementation on the cisplatin nephrotoxicity. *Drug Chem Toxicol* **25**, 1-8 (2002).

Ehrsson, H. & Wallin, I. Cimetidine as an organic cation transporter antagonist. *Am J Pathol* **177**, 1573-1574 (2010).

Einhorn, E.H. Testicular cancer: an oncological success story. *Clin Cancer Res* **3**, 2630-2632 (1997).

Ekborn, A., Laurell, G., Andersson, A., Wallin, I., Eksborg, S. & Ehrsson, H. Cisplatin-induced hearing loss: influence of the mode of drug administration in the guinea pig. *Hear Res* **140**, 38-44 (2000).

Fan, J. & Bertino, J.R. Modulation of cisplatinum cytotoxicity by p53: effect of p53-mediated apoptosis and DNA repair. *Mol Pharmacol* **56**, 966-972 (1999).

Fauser, A.A., *et al*. Guidelines for anti-emetic therapy: acute emesis. *Eur J Cancer* **35**, 361-370 (1999).

Fink, D., *et al*. The role of DNA mismatch repair in platinum drug resistance. *Cancer Res* **56**, 4881-4886 (1996).

Fink, D., *et al. In vitro* and *in vivo* resistance to cisplatin in cells that have lost DNA mismatch repair. *Cancer Res* **57**, 1841-1845 (1997).

Finley, R.S., Fortner, C.L. & Grove, W.R. Cisplatin nephrotoxocity: a summury of preventative interventions. *Drug Intell Clin Pharm* **19**, 362-367 (1985).

Fisher, A.A. & Le Couteur, D.G. Nephrotoxicity and hepatotoxicity of histamine H2 receptor antagonists. *Drug Saf* **24**, 39-57 (2001).

Fraser, M., *et al.* p53 is a determinant of X-linked inhibitor of apoptosis protein/Akt-mediated chemoresistance in human ovarian cancer cells. *Cancer Res* **63**, 7081-7088 (2003).

Fulda, S., Los, M., Friesen, C. & Debatin, K.M. Chemosensitivity of solid tumor cells *in vitro* is related to activation of the CD95 system. *Int J Cancer* **76**, 105-114 (1998).

Furukawa, T., Komatsu, M., Ikeda, R., Tsujikawa, K. & Akiyama, S. Copper transport systems are involved in multidrug resistance and drug transport. *Curr Med Chem* **15**, 3268-3278 (2008).

Gale, G.R., Morris, C.R., Atkins, L.M. & Smith, A.B. Binding of an antitumor platinum compound to cells as influenced by physical factors and pharmacologically active agents. *Cancer Res* **33**, 813-818 (1973).

Galluzzi, L., Vicencio, J.M., Kepp, O., Tasdemir, E., Maiuri, M.C. & Kroemer, G. To die or not to die: that is the autophagic question. *Curr Mol Med* **8**, 78-91 (2008).

Garnett, W.R. Diphenhydramine. *Am Pharm* **26**, 35-40 (1986).

Gately, D.P. & Howell, S.B. Cellular accumulation of the anticancer agent cisplatin: a review. *Br J Cancer* **67**, 1171-1176 (1993).

Giacomini, K.M., *et al*. Membrane transporters in drug development. *Nat Rev Drug Discov* **9**, 215-236 (2010).

Gifford, G., Paul, J., Vasey, P.A., Kaye, S.B. & Brown, R. The acquisition of hMLH1 methylation in plasma DNA after chemotherapy predicts poor survival for ovarian cancer patients. *Clin Cancer Res* **10**, 4420-4426 (2004).

Gniazdowski, M. & Czyz, M. Transcription factors as targets of anticancer drugs. *Acta Biochim Pol* **46**, 255-262 (1999).

Gonzalez, V.M., Fuertes, M.A., Alonso, C. & Perez, J.M. Is cisplatin-induced cell death always produced by apoptosis? *Mol Pharmacol* **59**, 657-663 (2001).

Gonzales-Vitale, J.C., Hayes, D.M., Cvitkovic, E. & Sternberg, S.S. The renal pathology in clinical trials of cis-platinum(II)diamminedichloride. *Cancer* **39**, 1362-1371 (1977).

Gozuacik, D. & Kimchi, A. Autophagy and cell death. *Curr Top Dev Biol* **78**, 217-245 (2007).

Graham, M. & Mead, M.D. Changing role of chemotherapy in treatment of head and neck cancer. *Am J Med* **73**, 582-595 (1982).

Greenlee, R.T., Hill-Harmon, M.B., Murray, T. & Thun, M. Cancer statistics, 2001. *CA Cancer J Clin* **51**, 15-36 (2001).

Guerra, C., *et al.* Tumor induction by an endogenous *K-ras* oncogene is highly dependent on cellular context. *Cancer Cell* **4**, 111-120 (2003).

Hamers, F.P., Wijbenga, J., Wolters, F.L., Klis, S.F., Sluyter, S. & Smoorenburg, G.F. Cisplatin ototoxicity involves organ of Corti, stria vascularis and spiral ganglion: modulation by alphaMSH and ORG 2766. *Audiol Neurootol* **8**, 305-315 (2003).

Hanigan, M.H., *et al*. Inhibition of gammaglutamyl transpeptidase activity by acivicin *in vivo* protects the kidney from cisplatin-induced toxicity. *Cancer Res* **54**, 5925-5929 (1994).

Hanigan, M.H., *et al*. Gamma-glutamyl transpeptidase-deficient mice are resistant to the nephrotoxic effects of cisplatin. *Am J Pathol* **159**, 1889-1894 (2001).

Harris, J.G. Nausea, vomiting and cancer treatment. *CA Cancer J Clin* **28**, 194-201 (1978).

He, Q., Liang, C.H. & Lippard, S.J. Steroid hormones induce HMG1 overexpression and sensitize breast cancer cells to cisplatin and carboplatin. *Proc Natl Acad Sci USA* **97**, 5768-5772 (2000).

Helleman, J., *et al.* Mismatch repair and treatment resistance in ovarian cancer. *BMC Cancer* **6**, 201 (2006).

Helm, C.W. & States, J.C. Enhancing the efficacy of cisplatin in ovarian cancer treatment - could arsenic have a role. *J Ovarian Res* **2**, 2 (2009).

Herceg, Z. & Wang, Z.Q. Functions of poly(ADP-ribose) polymerase (PARP) in DNA repair, genomic integrity and cell death. *Mutat Res* **477**, 97-110 (2001).

Hibino, H. & Kurachi, Y. Molecular and physiological bases of the K^+ circulation in the mammalian inner ear. *Physiology (Bethesda)* **21**, 336-345 (2006).

Hill, B.T., *et al*. Deficient repair of cisplatin-DNA adducts identified in human testicular teratoma cell lines established from tumours from untreated patients. *Eur J Cancer* **30**, 832-837 (1994).

Hill, J.M. & Speer, R.J. Organo-platinum complexes as antitumor agents (review). *Anticancer Res* **2**, 173-186 (1982).

Huang, J.-C., Zamble, D B., Reardon, J.T., Lippard, S.J. & Sancar, A. HMG-domain proteins specifically inhibit the repair of the major DNA adduct of the anticancer drug cisplatin by human excision nuclease. *Proc Natl Acad Sci USA* **91**, 10394-10398 (1994).

Inoue, K., *et al*. Cisplatin-induced macroautophagy occurs prior to apoptosis in proximal tubules *in vivo. Clin Exp Nephrol* **14**, 112-122 (2009).

Inui, K.I., Masuda, S. & Saito, H. Cellular and molecular aspects of drug transport in the kidney. *Kidney Int* **58**, 944-958 (2000).

Ishida, S., Lee, J., Thiele, D.J. & Herskowitz, I. Uptake of the anticancer drug cisplatin mediated by the copper transporter Ctr1 in yeast and mammals. *Proc Natl Acad Sci USA* **99**, 14298-14302 (2002).

Ishida, S., McCormick, F., Smith-McCune, K. & Hanahan, D. Enhancing tumor-specific uptake of the anticancer drug cisplatin with a copper chelator. *Cancer Cell* **17**, 574-583 (2010).

Ishikawa, T. The ATP-dependent glutathione S-conjugate export pump. *Trends Biochem Sci* **17**, 463-468 (1992).

Jackson, E.L., Willis, N., Mercer, K., Bronson, R.T., Crowley, D., Montoya, R., Jacks, T. & Tuveson, D.A. Analysis of lung tumor initiation and progression using conditional expression of oncogenic *K-ras*. *Genes Dev* **15**, 3243-3248 (2001).

Jamieson, E.R. & Lippard, S.J. Structure, recognition, and processing of cisplatin-DNA adducts. *Chem Rev* **99**, 2467-2498 (1999).

Jiang, M., *et al*. Nutlin-3 protects kidney cells during cisplatin therapy by suppressing Bax/Bak activation. *J Biol Chem* **282**, 2636-2645 (2007).

Jin, S. & White, E. Role of autophagy in cancer: management of metabolic stress. *Autophagy* **3**, 28-31 (2007).

Jo, S.K., *et al*. MEK inhibitor, U0126, attenuates cisplatin-induced renal injury by decreasing inflammation and apoptosis. *Kidney Int* **67**, 458-466 (2005).

Johnson, S., *et al.* Relationship between platinum–DNA adduct formation and removal and cisplatin cytotoxicity in cisplatin-sensitive and -resistant human ovarian cancer cells. *Cancer Res* **54**, 5911-5916 (1994).

Johnson, L., *et al. K-ras* is an essential gene in the mouse with partial functional overlap with *N-ras*. *Genes Dev* **11**, 2468-2481 (1997).

Johnstone, B.M. & Sellick, P.M. The peripheral auditory apparatus. *Q Rev Biophys* **5**, 1-57 (1972).

Jones, M.M., Basinger, M.A. & Holscher, M.A. Control of the nephrotoxicity of cisplatin by clinically used sulfur-containing compounds. *Fundam Appl Toxicol* **18**, 181-188 (1992).

Jordan, P. & Carmo-Fonseca, M. Cisplatin inhibits synthesis of ribosomal RNA *in vivo*. *Nucleic Acids Res* **26***,* 2831-2836 (1998).

Kang, H., Kim, T.J., Kim, W.Y., Choi, C.H., Lee, J.W., Kim, B.G. & Bae, D.S. Outcome and reproductive function after cumulative high-dose combination chemotherapy with bleomycin, etoposide and cisplatin (BEP) for patients with ovarian endodermal sinus tumor. *Gynecol Oncol* **111**, 106-110 (2008).

Karimi, G., Ramezani, M. & Tahoonian, Z. Cisplatin nephrotoxicity and protection by milk thistle extract in rats. *Evid Based Complement Alternat Med* **2**, 383-386 (2005).

Kartalou, M. & Essigmann, J.M. Recognition of cisplatin adducts by cellular proteins. *Mutat Res* **478**, 1-21 (2001).

Katano, K., Safaei, R., Samimi, G., Holzer, A., Rochdi, M. & Howell, S.B. The copper export pump ATP7B modulates the cellular pharmacology of carboplatin in ovarian carcinoma cells. *Mol Pharmacol* **64**, 466-473 (2003).

Kelland, L. The resurgence of platinum-based cancer chemotherapy. *Nat Rev Cancer* **7**, 573-584 (2007).

Kelland, L.R. The molecular basis of cisplatin sensitivity/resistance. *Eur J Cancer* **30**, 725-727 (1994).

Kendall, M.D., Warley, A., Nicholson, J.K. & Appleton, T.C. X-ray microanalysis of proximal and distal tubule cells in the mouse kidney, and the influence of cadmium on the concentration of natural intracellular elements. *J Cell Sci* **62**, 319-338 (1983).

Kigawa, J., *et al.* Effect of p53 gene transfer and cisplatin in a peritonitis carcinomatosa model with p53-deficient ovarian cancer cells. *Gynecol Oncol* **84**, 210-215 (2002).

Kim, H.J., *et al*. Roles of NADPH oxidases in cisplatin-induced reactive oxygen species generation and ototoxicity. *J Neurosci* **30**, 3933-3946 (2010).

Klionsky, D.J. & Emr S.D. Autophagy as a regulated pathway of cellular degradation. *Science* **290**, 1717-1721 (2000).

Klis, S.F., O'Leary, S.J., Wijbenga, J., de Groot, J.C., Hamers, F.P. & Smoorenburg, G.F. Partial recovery of cisplatin-induced hearing loss in the albino guinea pig in relation to cisplatin dose. *Hear Res* **164**, 138-146 (2002).

Köberle, B., Grimaldi, K.A., Sunters, A., Hartley, J.A., Kelland, L.R. & Masters, J.R. DNA repair capacity and cisplatin sensitivity of human testis tumour cells. *Int J Cancer* **70**, 551-555 (1997).

Köberle, B., Tomicic, M.T., Usanova, S. & Kaina, B. Cisplatin resistance: preclinical findings and clinical implications. *Biochim Biophys Acta* (2010).

Kohn, S., Fradis, M., Pratt, H., Zidan, J., Podoshin, L., Robinson, E. & Nir, I. Cisplatin ototoxicity in guinea pigs with special reference to toxic effects in the stria vascularis. *Laryngoscope* **98**, 865-871 (1988).

Komatsu, M., *et al.* Copper-transporting P-type adenosine triphosphatase (ATP7B) is associated with cisplatin resistance. *Cancer Res* **60**, 1312-1316 (2000).

Konishi, T., Hamrick, P.E. & Walsh, P.J. Ion transport in guinea pig cochlea. *Acta Otolaryngol* **86**, 22-34 (1978).

Konstantakou, E.G., *et al.* Human bladder cancer cells undergo cisplatin-induced apoptosis that is associated with p53-dependent and p53-independent responses. *Int J Oncol* **35**, 401-416 (2009).

Kortmann, R.D., *et al.* Current and future strategies in radiotherapy of childhood low-grade glioma of the brain. Part I: Treatment modalities of radiation therapy. *Strahlenther Onkol* **179**, 509-520 (2003).

Kroemer, G., *et al*. Clasification of cell death: recommendations of the Nomenclature Committee on Cell Death. *Cell Death Differ* **12**, 1463-1467 (2005).

Kroemer, G. & Levine, B. Autophagic cell death: the story of a misnomer. *Nat Rev Mol Cell Biol* **9**, 1004-1010 (2008).

Kuo, M.T., *et al*. The roles of copper transporters in cisplatin resistance. *Cancer Metastasis Rev* **26**, 71-83 (2007).

Kuo, Y.M., *et al.* Copper transport protein (Ctr1) levels in mice are tissue specific and dependent on copper status. *J Nutr* **136**, 21-26 (2006).

Lang, F., Vallon, V., Knipper, M. & Wangemann, P. Functional significance of channels and transporters expressed in the inner ear and kidney. *Am J Physiol Cell Physiol* **293**, 1187-1208 (2007).

Lange, S.S., Mitchell, D.L. & Vasquez, K.M. High mobility group protein B1 enhances DNA repair and chromatin modification after DNA damage*. Proc Natl Acad Sci USA* **105**, 10320-10325 (2008).

Laurell, G. & Jungnelius, U. High-dose cisplatin treatment: hearing loss and plasma concentrations. *Laryngoscope* **100**, 724-734 (1990).

Laurell, G., Ekborn, A., Viberg, A. & Canlon, B. Effects of a single high dose of cisplatin on the melanocytes of the stria vascularis in the guinea pig. *Audiol Neurootol* **12**, 170-178 (2007).

Lee, G.W., *et al*. Combination chemotherapy with gemcitabine and cisplatin as first-line treatment for immunohistochemically proven cholangiocarcinoma. *Am J Clin Oncol* **29**, 127-131 (2006).

Levresse, V., Marek, L., Blumberg, D. & Heasley, L.E. Regulation of platinum-compound cytotoxicity by the c- Jun N-terminal kinase and c-Jun signaling pathway in small-cell lung cancer cells. *Mol Pharmacol* **62**, 689-697 (2002).

Li, P., *et al.* Cytochrome c and dATP-dependent formation of Apaf-1/caspase-9 complex initiates an apoptotic protease cascade. *Cell* **91**, 479-489 (1997).

Li, Y., Womer, R.B. & Silber, J.H. Predicting cisplatin ototoxicity in children: the influence of age and the cumulative dose. *Eur J Cancer* **40**, 2445-2451 (2004).

Lieberthal, W. Macroautophagy: a mechanism for mediating cell death or for promoting cell survival. *Kidney Int* **74**, 555-557 (2008).

Lieberthal, W., Triaca, V. & Levine, J. Mechanisms of death induced by cisplatin in proximal tubular epithelial cells: apoptosis vs. necrosis. *Am J Physiol* **270**, 700-708 (1996).

Liedert, B., Pluim, D., Schellens, J. & Thomale, J. Adduct-specific monoclonal antibodies for the measurement of cisplatin-induced DNA lesions in individual cell nuclei. *Nucleic Acids Res* **34**, e47 (2006).

Ludwig, T., Riethmüller, C., Gekle, M., Schwerdt, G. & Oberleithner, H. Nephrotoxicity of platinum complexes is related to basolateral organic cation transport. *Kidney Int* **66**, 196-202 (2004).

Lynch, E.D., Gu, R., Pierce, C. & Kil, J. Reduction of acute cisplatin ototoxicity and nephrotoxicity in rats by oral administration of allopurinol and ebselen. *Hear Res* **201**, 81-89 (2005).

Machuy, N., Rajalingam, K. & Rudel, T. Requirement of caspase-mediated cleavage of c-Abl during stress-induced apoptosis. *Cell Death Differ* **11**, 290-300 (2004).

Madias, N.E. & Harrington, J.T. Platinum nephrotoxicity. *Am J Med* **65**, 307-314 (1978).

Mann, S.C., Andrews, P.A. & Howell, S.B. Short-term cis-diamminedichloroplatinum(II) accumulation in sensitive and resistant human ovarian carcinoma cells. *Cancer Chemother Pharmacol* **25**, 236-240 (1990).

Martin, L.P., Hamilton, T.C. & Schilder, R.J. Platinum resistance: the role of DNA repair pathways. *Clin Cancer Res* **14**, 1291-1295 (2008).

Masters, J.R. & Köberle, B. Curing metastatic cancer: lessons from testicular germ-cell tumours. *Nat Rev Cancer* **3**, 517-525 (2003).

Megyesi, J., *et al*. The p53-independent activation of transcription of p21 WAF1/CIP1/SDI1 after acute renal failure. *Am J Physiol Renal Physiol* **271**, 1211-1216 (1996).

Mello, J.A., Acharya, S., Fishel, R. & Essigmann, J.M. The mismatch-repair protein hMSH2 binds selectively to DNA adducts of the anticancer drug cisplatin. *Chem Biol* **3**, 579-589 (1996).

Motohashi, H., *et al.* Gene expression levels and immunolocalization of organic ion transporters in the human kidney. *J Am Soc Nephrol* **13**, 866-874 (2002).

Müller, J., Lips, K.S., Metzner, L., Neubert, R.H., Koepsell, H. & Brandsch, M. Drug specificity and intestinal membrane localization of human organic cation transporters (OCT). *Biochem Pharmacol* **70**, 1851-1860 (2005).

Nagatani, G., *et al.* Transcriptional activation of the human *HMG1* gene in cisplatin-resistant human cancer cells. *Cancer Res* **61**, 1592-1597 (2001).

Nagothu, K.K., Bhatt, R., Kaushal, G.P. & Portilla, D. Fibrate prevents cisplatin-induced proximal tubule cell death. *Kidney Int* **68**, 2680-2693 (2005).

Nakai, Y., *et al*. Ototoxicity of the anticancer drug cisplatin. An experimental study. *Acta Otolaryngol* **93**, 227-232 (1982).

Nakane, H., *et al.* High incidence of ultraviolet-B-or chemical-carcinogen-induced skin tumours in mice lacking the xeroderma pigmentosum group A gene. *Nature* **377**, 165-168 (1995).

Nies, A.T., *et al.* Expression of organic cation transporters OCT1 (SLC22A1) and OCT3 (SLC22A3) is affected by genetic factors and cholestasis in human liver. *Hepatology* **50**, 1227-1240 (2009).

O'Dwyer P.J., Stevenson J.P. & Johnson, S.W. Clinical pharmacokinetics and administration of established platinum drugs. *Drugs* **59**, 19-27 (2000).

Offner, F.F., Dallos, P. & Cheatham, M.A. Positive endocochlear potential: mechanism of production by marginal cells of stria vascularis. *Hear Res* **29**, 117-124 (1987).

Ogawa, M., Gale, G.R. & Keirn, S.S. Effects of cis-diamminedichloroplatinum (NSC 119875) on murine and human hemopoietic precursor cells. *Cancer Res* **35**, 1398-1401 (1975).

Olaussen, K.A., *et al*. DNA repair by ERCC1 in non-small-cell lung cancer and cisplatin-based adjuvant chemotherapy. *N Engl J Med* **355**, 983-991 (2006).

Oldenburg, J., *et al*. Cisplatin-induced longterm hearing impairment is associated with specific glutathione-S-transferase genotypes in testicular cancer survivors. *J Clin Oncol* **25**, 708-714 (2007).

Oliver, T. & Mead, G. Testicular cancer. *Curr Opin Oncol* **5**, 559-567 (1993).

Oliver, T.G., *et al.* Chronic cisplatin treatment promotes enhanced damage repair and tumor progression in a mouse model of lung cancer. *Genes Dev* **24**, 837-852 (2010).

Ott, R.J., Hui, A.C., Wong, F.M., Hsyu, P.H. & Giacomini, K.M. Interactions of quinidine and quinine and (+)- and (-)-pindolol with the organic cation/proton antiporter in renal brush border membrane vesicles. *Biochem Pharmacol* **41**, 142-145 (1991).

Pabla, N. & Dong, Z. Cisplatin nephrotoxicity: mechanisms and renoprotective strategies. *Kidney Int* **73**, 994-1007 (2008).

Perilongo, G., *et al*. Cisplatin versus cisplatin plus doxorubicin for standard-risk hepatoblastoma. *N Engl J Med* **361**, 1662-1670 (2009).

Periyasamy-Thandavan, S., Jiang, M., Wei, Q., Smith, R., Yin X.M. & Dong, Z. Autophagy is cytoprotective during cisplatin injury of renal proximal tubular cells. *Kidney Int* **74**, 631-640 (2008).

Peters, U., *et al*. Sequence variations of mitochondrial DNA and individual sensitivity to the ototoxic effect. *Anticancer Res* **23**, 1249-1255 (2003).

Peyrone, M. Über die Einwirkung des Ammoniaks auf Platinchlorür. *Ann Chemie Pharm* **51**, 1-29 (1844).

Pfaller, W. & Gstraunthaler, G. Nephrotoxicity testing *in vitro* - what we know and what we need to know. *Environ Health Perspect* **106**, 559-569 (1998).

Price, P.M., Safirstein, R.L. & Megyesi, J. Protection of renal cells from cisplatin toxicity by cell cycle inhibitors. *Am J Physiol Renal Physiol* **286**, 378-384 (2003).

Ramesh, G. & Reeves, W.B. Salicylate reduces cisplatin nephrotoxicity byinhibition of tumor necrosis factor-alpha. *Kidney Int* **65**, 490-499 (2004).

Reed, E. Platinum-DNA adduct, nucleotide excision repair and platinum based anti-cancer chemotherapy. *Cancer Treat Rev* **24**, 331-344 (1998).

Reed, E. ERCC1 and clinical resistance to platinumbased therapy. *Clin Cancer Res* **11**, 6100-6102 (2005).

Rosenberg, B. Noble metal complexes in cancer chemotherapy. *Adv Exp Med Biol* **91**, 129-150 (1977).

Rosenberg, B., VanCamp, L. & Krigas, T. Inhibition of cell division in *Escherichia coli* by electrolysis products from a platinum electrode. *Nature* **205**, 698-699 (1965).

Rosenberg, B., VanCamp, L., Trosko, J.E. & Mansour, V.H. Platinum compounds: a new class of potent antitumour agents. *Nature* **222**, 385-386 (1969).

Rosenfeldt, M.T. & Ryan, K.M. The role of autophagy in tumour development and cancer therapy. *Expert Rev Mol Med* **11**, e36 (2009).

Rossof, A.H., Slayton, R.E. & Perlia, C.P. Preliminary clinical experience with cis-diamminedichloroplatinum(II). *Cancer* **30**, 1451-1456 (1972).

Rybak, L.P., Whitworth, C. & Somani, S. Application of antioxidants and other agents to prevent cisplatin ototoxicity. *Laryngoscope* **109**, 1740-1744 (1999).

Rybak, L.P., Whitworth, C.A., Mukherjea, D. & Ramkumar V. Mechanisms of cisplatin induced ototoxicity and prevention. *Hear Res* **226**, 157-167 (2007).

Rybak, L.P. & Ramkumar, V. Ototoxicity. *Kidney Int* **72**, 931-935 (2007).

Saeter, G., *et al*. Chemotherapy in osteosarcoma. The Scandinavian Sarcoma Group experience. *Acta Orthop Scand Suppl* **285**, 74-82 (1999).

Samimi, G., Varki, N.M., Wilczynski, S., Safaei, R., Alberts, D.S. & Howell S.B. Increase in expression of the copper transporter ATP7A during platinum drug-

based treatment is associated with poor survival in ovarian cancer patients. *Clin Cancer Res* **9**, 5853-5859 (2003).

Santos, N.A., Catão, C.S., Martins, N.M., Curti, C., Bianchi, M.L. & Santos, A.C. Cisplatin-induced nephrotoxicity is associated with oxidative stress, redox state unbalance, impairment of energetic metabolism and apoptosis in rat kidney mitochondria. *Arch Toxicol* **81**, 495-504 (2007).

Santos, N.A., *et al*. Hydroxyl radical scavenger ameliorates cisplatin-induced nephrotoxicity by preventing oxidative stress, redox state unbalance, impairment of energetic metabolism and apoptosis in rat kidney mitochondria. *Cancer Chemother Pharmacol* **61**, 145-155 (2008).

Santoso, J.T., Lucci, J.A., Coleman, R.L., Schafer, I. & Hannigan, E.V. Saline, mannitol, and furosemide hydration in acute cisplatin nephrotoxicity: a randomized trial. *Cancer Chemother Pharmacol* **52**, 13-18 (2003).

Schiller, J.H., *et al*. Comparison of four chemotherapy regimens for advanced non-small-cell lung cancer. *N Engl J Med* **346**, 92-98 (2002).

Schweitzer, V.G., Rarey, K.E., Dolan, D.F., Abrams, G., Litterst, C.J. & Sheridan, C. Ototoxicity of cisplatin vs. platinum analogs CBDCA (JM-8) and CHIP (JM-9). *Otolaryngol Head Neck Surg* **94**, 458-470 (1986).

Schweitzer, V.G. Cisplatin-induced ototoxicity: the effect of pigmentation and inhibitory agents. *Laryngoscope* **103**, 1-52 (1993).

Screnci, D. & McKeage, M. Platinum neurotoxicity: clinical profiles, experimental models and neuroprotective approaches. *J Inorg Biochem* **77**, 105-110 (1999).

Sekiguchi, I., Suzuki, M., Tamada, T., Shinomiya, N., Tsuru, S. & Murata, M. Effects of cisplatin on cell cycle kinetics, morphological change, and cleavage pattern of DNA in two human ovarian carcinoma cell lines. *Oncology* **53**, 19-26 (1996).

Selvakumaran, M., Pisarcik, D.A., Bao, R., Yeung, A.T. & Hamilton, T.C. Enhanced cisplatin cytotoxicity by disturbing the nucleotide excision repair pathway in ovarian cancer cell lines. *Cancer Res* **63**, 1311-1316 (2003).

Seto, T., *et al*. Intrapleural hypotonic cisplatin treatment for malignant pleural effusion in 80 patients with non-small-cell lung cancer: a multi-institutional phase II trial. *Br J Cancer* **95**, 717-721 (2006).

Siddik, Z.H. Cisplatin: mode of cytotoxic action and molecular basis of resistance. *Oncogene* **22**, 7265-7279 (2003).

Simon, T., Hero, B., Dupuis, W., Selle, B. & Berthold, F. The incidence of hearing impairment after successful treatment of neuroblastoma. *Klin Padiatr* **214**, 149-152 (2002).

Sleijfer, D.T., Meijer, S. & Mulder, N.H. Cisplatin: a review of clinical applications and renal toxicity. *Pharm Weekbl Sci* **7**, 237-244 (1985).

Sluyter, S., Klis, S.F., de Groot, J.C. & Smoorenburg, G.F. Alterations in the stria vascularis in relation to cisplatin ototoxicity and recovery. *Hear Res* **185**, 49-56 (2003).

Sinani, D., Adle, D.J., Kim, H. & Lee, J. Distinct Mechanisms for Ctr1-mediated copper and cisplatin transport. *J Biol Chem* **282**, 26775-26785 (2007).

Song, I.S., *et al.* Role of human copper transporter Ctr1 in the transport of platinum-based antitumor agents in cisplatin-sensitive and cisplatin-resistant cells. *Mol Cancer Ther* **3**, 1543-1549 (2004).

Spano, A., Monaco, G., Barni, S. & Sciola, L. Cisplatin treatment of NIH/3T3 cultures induces a form of autophagic death in polyploid cells. *Histol Histopathol* **23**, 717-730 (2008).

Sweet-Cordero, A., *et al*. An oncogenic KRAS2 expression signature identified by cross-species gene-expression analysis. *Nat Genet* **37**, 48-55 (2004).

Takeuchi, S., Ando, M. & Kakigi, A. Mechanism generating endocochlear potential: role played by intermediate cells in stria vascularis. *Biophys J* **79**, 2572-2582 (2000).

Tang, D., *et al.* HMGB1 release and redox regulates autophagy and apoptosis in cancer cells. *Oncogene* **29**, 5299-5310 (2010).

Theis, S. & Roemer, K. c-Abl tyrosine kinase can mediate tumor cell apoptosis independently of the Rb and p53 tumor suppressors. *Oncogene* **17**, 557-564 (1998).

Thomas, M.C., *et al*. The role of advanced glycation in reduced organic cation transport associated with experimental diabetes. *J Pharmacol Exp Ther* **311**, 456-466 (2004).

Thomas, J.P., Lautermann, J., Liedert, B., Seiler, F. & Thomale, J. High accumulation of platinum-DNA adducts in strial marginal cells of the cochlea is an early event in cisplatin but not carboplatin ototoxicity. *Mol Pharmacol* **70**, 23-29 (2006).

Townsend, D.M., *et al*. Metabolism of cisplatin to a nephrotoxin in proximal tubule cells. *J Am Soc Nephrol* **14**, 1-10 (2003).

Treiber, D.K., Zhai, X., Jantzen, H.M. & Essigmann, J. M. Cisplatin-DNA adducts are molecular decoys for the ribosomal RNA transcription factor hUBF (human upstream binding factor). *Proc Natl Acad Sci USA* **91**, 5672-5676 (1994).

Troyano, A., Fernández, C., Sancho, P., De Blas E. & Aller. P. Effect of glutathione depletion on antitumor drug toxicity (apoptosis and necrosis) in U-937 human

promonocytic cells. The role of intracellular oxidation. *J Biol Chem* **276**, 47107-47115 (2001).

Tsuruya, K., *et al*. Antioxidant ameliorates cisplatin-induced renal tubular cell death through inhibition of death receptor-mediated pathways. *Am J Physiol Renal Physiol* **285**, 208-218 (2003).

Umapathi, T. & Chaudhry, V. Toxic neuropathy. *Curr Opin Neurol* **18**, 574-580 (2005).

van den Berg, J.H., Beijnen, J.H., Balm, A.J. & Schellens, J.H. Future opportunities in preventing cisplatin induced ototoxicity. *Cancer Treat Rev* **32**, 390-397(2006).

van Ruijven, M.W., de Groot, J.C., Klis, S.F. & Smoorenburg, G.F. The cochlear targets of cisplatin: an electrophysiological and morphological time-sequence study. *Hear Res* **205**, 241-248 (2005).

Visovsky, C. Chemotherapy-induced peripheral neuropathy. *Cancer Invest* **21**, 439-451 (2003).

Wang, D. & Lippard, S.J. Cellular processing of platinum anticancer drugs. *Nat Rev Drug Discov* **4**, 307-320 (2005).

Wang, X., Martindale, J.L. & Holbrook, N.J. Requirement for ERK activation in cisplatin-induced apoptosis. *J Biol Chem* **275**, 39435-39443 (2000).

Wangemann, P. Supporting sensory transduction: cochlear fluid homeostasis and the endocochlear potential. *J Physiol* **576**, 11-21 (2006).

Welsh, C., Day, R., McGurk, C., Masters, J.R., Wood, R.D. & Köberle, B. Reduced levels of XPA, ERCC1 and XPF DNA repair proteins in testis tumor cell lines. *Int J Cancer* **110**, 352-361 (2004).

Windebank, A.J. Drug-induced neuropathies. *Baillieres Clin Neurol* **5**, 529–573 (1996).

Windebank, A.J. & McDonald, E. Cell death in the peripheral nervous system: potential rescue strategies. *Neuroscientist* **8**, 62-72 (2002).

Wozniak, K. & Blasiak, J. Recognition and repair of DNA-cisplatin adducts. *Acta Biochim Pol* **49**, 583-596 (2002).

Yang, C., Kaushal, V., Shah, S.V. & Kaushal, G.P. Autophagy is associated with apoptosis in cisplatin injury to renal tubular epithelial cells. *Am J Physiol Renal Physiol* **294**, 777-787 (2008).

Yang, P., Ebbert, J.O., Sun, Z. & Weinshilboum, R.M. Role of the glutathione metabolic pathway in lung cancer treatment and prognosis: a review. *J Clin Oncol* **24**, 1761-1769 (2006).

Yang, Z., Schumaker, L.M., Egorin, M.J., Zuhowski, E.G., Guo, Z. & Cullen, K.J. Cisplatin preferentially binds mitochondrial DNA and voltage-dependent anion channel protein in the mitochondrial membrane of head and neck squamous cell carcinoma: possible role in apoptosis. *Clin Cancer Res* **12**, 5817-5825 (2006).

Yao, X., Panichpisal, K., Kurtzman, N. & Nugent, K. Cisplatin nephrotoxicity: a review. *Am J Med Sci* **334**, 115-124 (2007).

Yonezawa, A., *et al*. Association between tubular toxicity of cisplatin and expression of organic cation transporter rOCT2 (Slc22a2) in the rat. *Biochem Pharmacol* **70**, 1823-1831 (2005).

Yoon, M.S., *et al*. Erythropoietin overrides the triggering effect of DNA platination products in a mouse model of cisplatin-induced neuropathy. *BMC Neurosci* **10**, 77 (2009).

Yu, F., *et al*. Identification of the functional domain of p21(WAF1/CIP1) that protects cells from cisplatin cytotoxicity. *Am J Physiol Renal Physiol* **289**, 514-520 (2005).

Yu, L., *et al*. Autophagic programmed cell death by selective catalase degradation. *Proc Natl Acad Sci USA* **103**, 4952-4957 (2006).

Zamble, D.B., Mikata, Y., Eng, C.H., Sandman, K.E. & Lippard, S.J. Testis-specific HMG-domain protein alters the responses of cells to cisplatin. *J Inorg Biochem* **91**, 451-462 (2002).

Zdraveski, Z.Z., Mello, J.A., Marinus, M.G. & Essigmann, J.M. Multiple pathways of recombination define cellular responses to cisplatin. *Chem Biol* **7**, 39-50 (2000).

7. Appendix

7.1 Acknowledgment

My first and biggest thank to Dr. Jürgen Thomale, Institute for Cell Biology, Essen, the supervisor of this thesis and my mentor, who allowed me to do this wonderful project and during all this time helped me with many advises and discussions as well as found useful collaborations. I thank you, Jürgen, for that big credit you gave me and for your incredible kindness. I learn a lot of things about science during these years and your guidance allowed me came to the point where I am. I deeply appreciate all support you granted me all the time I spent in DNA Repair Laboratory.

I am happy that I met Dr. Trudy Oliver, Koch Institute for Integrative Cancer Research, MIT, Cambridge, USA, who is amazing women and awe-inspiring scientist. With all my zest I thank Trudy for her invaluable help she provided during this research was going.

I thank Dr. Daniel Manz, Head and Neck Clinic, Essen, for his help in measurement of hearing capacity in mice. Thank you Daniel for those long evenings after your main work you spent with me to get the results we have now.

I am grateful to Petra Altenhoff, Head and Neck Clinic, Essen, who introduced me to inner ear procedure and always answered my questions.

I would like to express my gratitude to Gabriele Ladwig, Institute of Pathology and Neuropathology, Essen, for her technical assistant with preparation of electron microscope samples.

Many thanks are also due to Michael Oepp and Wojciech Wegrzyn of the "Zentrales Tierlaboratorium", the Central Animal Facility of the University Hospital, Essen, for great cooperation in treatment and breeding of the mice.

I thank to all the people in DNA Repair Laboratory, especially, now already a Doctor Ann-Christin Nickel, for many scientific and non-scientific discussions and all that time we pass through together.

Special thanks go to Dr. Nicholas Wagner for critical reading this thesis and so helpful comments. Thank you, Nicki, for your patience.

Finally and most importantly, I thank my family in Ukraine for that they never gave up to love me and to believe in me and supported me during all these years.

The generous financial support of this doctoral thesis by a scholarship from the Jürgen Manchot-Stiftung, Düsseldorf, is gratefully acknowledged.

7.2 Curriculum Vitae

Name:	Diana Mendus
Address:	Nockwinkel 44 45277 Essen, Germany
E-mail:	di.mendus@gmail.com
Date of Birth:	October, 11 1982

EDUCATION

***2006 - 2010*:** Ph. D. student at DNA Repair Laboratory, Institute for Cell Biology (Tumor Research), Duisburg-Essen University, Essen, Germany

***2004 - 2006*:** Master of Science in biochemistry, biology and biology teaching at Department of Biochemistry and Molecular Biology of Kiev National Taras Shevchenko University, Kiev, Ukraine.

***2000 - 2004*:** Bachelor of Science in biology and molecular biology at Department of Biochemistry and Molecular Biology of Kiev National Taras Shevchenko University, Kiev, Ukraine.

RESEARCH EXPERIENCE

***Jun 2010 - Sep 2010*:** Visiting scientist at D.A.M.P. Laboratory, Department of Surgery, Hillman Cancer Center, University of Pittsburgh Medical School, Pittsburgh, PA, USA

***Nov 2006 - present*:** PhD student at Institute for Cell Biology (Tumor Research), Duisburg-Essen University, Essen, Germany.

***Feb 2006 - Apr 2006*:** Assistant practice in Kiev National University, Department of Biochemistry, subject: “Hormones and Neuroregulation”

***Jul 2002 – Oct 2006*:** Master student, bachelor student, research technician at Laboratory of Immunogenetics, Department of Hematology and Transplantology, Research Center for Radiation Medicine, Academy of Medical Sciences of Ukraine.

***May 2002 - Jul 2002*:** Summer-training, Department of Regulation Mechanisms of the Cell, Kavetsky Institute of Experimental Pathology, Oncology and Radiobiology of the National Academy of Sciences of Ukraine.

***May 2001 - Jun 2001*:** Summer-training, Department of Experimental Cell Systems, Kavetsky Institute of Experimental Pathology, Oncology and Radiobiology, National Academy of Sciences of Ukraine.

ARTICLES .

1. Oliver, T.G., Mercer, K.L., Sayles, L.C., Burke, J.R., Mendus, D., Lovejoy, K.S., Cheng, M.H., Subramanian, A., Mu, D., Powers, S., Crowley, D., Bronson, R.T., Whittaker, C.A., Bhutkar, A., Lippard, S.J., Golub, T., Thomale, J., Jacks, T. & Sweet-Cordero, E.A. Chronic cisplatin treatment promotes enhanced damage repair and tumor progression in a mouse model of lung cancer. *Genes Dev* **24**, 837-852 (2010).

Erklärung:

Hiermit erkläre ich, gem. § 6 Abs. 2, Nr. 7 der Promotionsordnung der Math.-Nat.-Fakultäten zur Erlangung der Dr. rer. nat., dass ich das Arbeitsgebiet, dem das Thema „Cisplatin-induced DNA damage in normal and malignant cells: Mechanisms of drug resistance and side effects and strategies for their prevention“ zuzuordnen ist, in Forschung und Lehre vertrete und den Antrag von Diana Mendus befürworte.

Essen, den _____

_____

Unterschrift d. wissenschaftl. Betreuers/Mitglieds

der Universität Duisburg-Essen

Erklärung:

Hiermit erkläre ich, gem. § 6 Abs. 2, Nr. 6 der Promotionsordnung der Math.-Nat.-Fakultäten zur Erlangung des Dr. rer. nat., dass ich die vorliegende Dissertation selbständig verfasst und mich keiner anderen als der angegebenen Hilfsmittel bedient habe.

Essen, den _____

_____

Unterschrift des/r Doktoranden/in

Erklärung:

Hiermit erkläre ich, gem. § 6 Abs. 2, Nr. 8 der Promotionsordnung der Math.-Nat.-Fakultäten zur Erlangung des Dr. rer. nat., dass ich keine anderen Promotionen bzw. Promotionsversuche in der Vergangenheit durchgeführt habe und dass diese Arbeit von keiner anderen Fakultät abgelehnt worden ist.

Essen, den _____

_____

Unterschrift des/r Doktoranden/in